UNIVERSIDADE FEDERAL DO RIO GRANDE DO SUL
INSTITUTO DE CIÊNCIAS BÁSICAS DA SAÚDE
PROGRAMA DE PÓS-GRADUAÇÃO EM
CIÊNCIAS BIOLÓGICAS: BIOQUÍMICA

AVALIAÇÃO DA DISTRIBUIÇÃO DE ZINCO REATIVO CEREBRAL EM PEIXES-ZEBRA (*Danio rerio*) E A SUA MODULAÇÃO POR DIETILDITIOCARBAMATO EM UM MODELO DE HIPÓXIA SEVERA

MARCOS MARTINS BRAGA

Orientador:
Prof. Dr. DIOGO ONOFRE GOMES DE SOUZA

Tese apresentada ao Programa de Pós-Graduação em Ciências Biológicas – Bioquímica da Universidade Federal do Rio Grande do Sul como requisito final para a obtenção de título de Doutor em Bioquímica

PORTO ALEGRE

2014

À minha família que soube enxergar a importância do conhecimento, prestando apoio e incentivo para realização deste trabalho.

Agradecimentos

Ao Professor Tuiskon Dick (*in memoriam*), por dar início a toda carreira profissional que venho construindo dentro do Departamento de Bioquímica da UFRGS.

Ao Professor Diogo Souza por me orientar e dar a oportunidade para trabalhar na linha de pesquisa desta Tese.

Ao colega e Professor Denis Rosemberg por incentivar a trabalhar com o tema desta tese e por todo auxílio prestado para a sua execução. Também a Professora Liziane Porciúncula pelos conselhos iniciais na definição dos objetivos desta pesquisa.

À Professora Maria Elisa Calcagnotto por dedicar todo o seu conhecimento e experiência para me ajudar na construção de muitos capítulos desta tese. Também à pós-doutoranda Leticia Pettenuzzo pela ajuda na execução e análise dos dados citométricos.

Ao Professor Renato Dias e ao pós-doutoranto Eduardo Rico pela ajuda inestimável prestadas nesta tese.

Ao aluno de iniciação científica Emerson Silva, pelo auxílio na execução deste trabalho.

A todos dos laboratórios 24, 26 e 28, pelo apoio científico e pelos momentos de descontração.

Ao laboratório 34 do professor Carlos Dutra por disponibilizar espaço e reagentes para a execução das técnicas de estresse oxidativo.

À minha família que me apoiou integralmente para a realização deste trabalho. Aos meus irmãos Lucas e Geovani, que de alguma forma ajudaram na execução deste estudo e aos meus pais Moizes e Eni, que sempre me apoiaram na conclusão deste trabalho.

A Tarsila Moraes, pelo carinho e apoio científico e por entender todos os momentos de dificuldade enfrentados ao longo desta tese. A toda sua família por também de alguma forma ter ajudado a concluir esta etapa.

Apresentação

Conforme as recomendações do Programa de Pós-Graduação em Ciências Biológicas: Bioquímica, esta tese está organizada em três partes principais:

Parte I – contém os resumos, a lista de abreviaturas, a introdução e os objetivos do trabalho;

Parte II – é constituída por materiais e métodos e os resultados do trabalho, sendo este apresentado na forma de capítulos, onde constam cinco artigos científicos;

Parte III – apresenta a discussão, as conclusões, as referências citadas nas partes I e III e os apêndices.

Sumário

PARTE I

RESUMO

O conteúdo de zinco (Zn) reativo cerebral é importante para o equilíbrio da sinaptofisiologia neural. A prova disto é que um aumento nos seus níveis, após evento hipóxico-isquêmico, resulta em neurotoxicidade, o que tem estimulado o tratamento desta disfunção cerebral com quelantes de Zn, tal como o dietilditiocarabamato (DEDTC). No caso do DEDTC, o uso deste composto sobre esta disfunção deve ser analisado com cuidado, pois ele também apresenta muitos efeitos colaterais sobre o sistema nervoso central. Desta forma, para atender este propósito, é necessário antes obter uma concentração de DEDTC com menores efeitos colaterais. Por esta razão, no presente trabalho, nós decidimos usar um modelo vertebrado mais simples, tal como o peixe-zebra, o qual permitiria a triagem, em larga escala, dos efeitos de DEDTC sobre o Zn reativo. Entretanto, jamais foi mostrada a presença de Zn reativo no cérebro de peixe-zebra. Com isto, através de marcações histológicas, nós conseguimos mostrar pela primeira vez a distribuição citoarquitectônica de Zn reativo em neurônios glutamatérgicos, bem como o número desses neurônios contendo Zn no cérebro de peixe-zebra. Isto nos permitiu avaliar o efeito de diferentes concentrações de DEDTC sobre o conteúdo de Zn cerebral do peixe-zebra, o qual foi intensamente quelado por elevadas quantidades do composto, induzindo comportamentos tipo-crise. Neste mesmo estudo nós obtemos também uma concentração de DEDTC com poucos efeitos colaterais que poderia exercer neuroproteção sobre o aumento de Zn reativo induzido pela hipóxia-isquemia. Assim, após a padronização de um modelo de hipóxia em peixe-zebra, que demonstra danos relacionados à isquemia, nós testamos se essa concentração de DEDTC poderia ser neuroprotetora sobre este modelo. Contudo, DEDTC apresentou efeitos pró-oxidantes, embora ele tenha atenuado o elevado conteúdo de Zn reativo induzido pela hipóxia. Portanto, mesmo que o DEDTC tenha falhado, este modelo, agora, está apto para a triagem de outros fármacos com potencial ação sobre o alterado conteúdo de Zn reativo que ocorre em eventos hipóxicos-isquêmicos.

Palavras-chave: Zn reativo, cérebro, hipóxia-isquemia, dietilditiocarbamato, peixe-zebra

ABSTRACT

The content of brain reactive zinc (Zn) is important for the synaptophysiology in the central nervous system (CNS). This is evidenced in hypoxic-ischemic events, when an increase in their levels results in neurotoxicity. Consequently, this has stimulated the treatment of cerebral ischemia with Zn chelators, such as diethyldithiocarbamate (DEDTC). In the case of DEDTC, the use of this compound in this dysfunction should be examined carefully, because it also has many side effects on the (CNS). Thus, to meet this, it is necessary first to obtain a concentration of DEDTC with negligible side effects. Here, we decided to use a simpler vertebrate model, such as zebrafish, which would allow large-scale screening of DEDTC effects on reactive Zn. However, the presence of reactive Zn has never been shown in zebrafish brain. Then, using histological markers, we were able to show for the first time the cytoarchitectonic distribution of reactive Zn in glutamatergic neurons as well as the number of these neurons containing Zn in the zebrafish brain. This allowed us to evaluate the effect of different DEDTC concentrations on the brain content of Zn in zebrafish. As a result, high levels of the compound did strongly chelate the metal, inducing seizure-like behaviors. In this study we also obtained a DEDTC concentration with few side effects that could exert neuroprotection on the increased reactive Zn induced by hypoxia-ischemia. Then, after the standardization of an ischemic-sensitive model of hypoxia in zebrafish, we tested if this DEDTC concentration could be neuroprotective on this model. Nevertheless, DEDTC showed pro-oxidant effects, though it had mitigated the elevated content of reactive Zn induced hypoxia. Therefore, despite the DEDTC have failed as neuroprotective drug, this model enables the screening of other chemical agents with potential action on the increased content of reactive Zn that occurs in hypoxic-ischemic events.

Keywords: reactive Zn, brain, hypoxia-ischemia, diethyldithiocarbamate, zebrafish

LISTA DE ABREVIATURAS

CAT – catalase

DEDTC – dietilditiocarbamato

δ-ALA-D – δ-aminolevulinato desidratase

EAAT1 – transportador de aminoácido excitatório tipo-1

GPx – glutationa peroxidase

hmga1 – proteína de alta mobilidade do grupo A1

HSF-1 – fator 1 de choque térmico

IGFBP-1 – fator de crescimento insulina tipo I ligado a proteína

P_{Crit} – pressão parcial de oxigênio crítico

PFA – paraformaldeído

PO_2 – pressão parcial de oxigênio

SNC – Sistema Nervoso Central

SOD – superóxido dismutase

TPEN – Tetrakis-(2-Piridilmetil)etilenodiamina

ZIP – transportador de zinco do meio extra-citoplasmático para o meio citoplasmático

ZnT – transportador de zinco do meio citoplasmático para o meio extra-citoplasmático

Zn – zinco divalente; Zn^{2+}

ZP1 – zinpyr-1, sonda fluorescente para Zn reativo, permeável a membranas

1. INTRODUÇÃO

O zinco (Zn) é o segundo metal traço mais abundante no organismo, sendo estimado um total de 2,3 g em todo o corpo humano, perdendo em quantidade apenas para o ferro (Coleman, 1992). Em sistemas biológicos, o Zn apresenta papel fundamental sobre um grande número de fatores de transcrição, proteínas estruturais e enzimas, sendo dividido em três categorias por conta das suas funções: regulatório, estrutural e catalítico (Cousins, 1994; Russel et al., 2002). Quando o Zn possui ação regulatória, ele apresenta papel importante em processos biológicos como, por exemplo, expressão do gene da proteína metalotioneína (Cousins, 1994; Dalton et al., 1997). Em funções constitutivas, o Zn coordena com domínios protéicos, provocando o dobramento observado nos *zinc-fingers*, e assim torna a molécula biologicamente ativa (Hartwig, 1994). Por último, como componente catalítico, o metal realiza funções como cofator em centenas de metaloenzimas, tais como, RNA polimerases, anidrase carbônica e δ-aminolevulinato desidratase (Cousins, 1994; Gibson et al., 1955).

Como micronutriente, o Zn é essencial para o funcionamento de diversas biomoléculas e processos celulares. Ele é fisiologicamente importante para os organismos, com papel na conservação da integridade celular e em funções biológicas, como o metabolismo de ácidos nucleicos, a síntese protéica, e o ciclo celular (Beyersmann & Haase, 2001; Favier & Hininger-Favier, 2005). Além disso, como fator de crescimento, o Zn é também um imunoregulador, e possui ação citoprotetora, com ação antiapoptótica e anti-inflamatória (Zalewski et al., 2005).

Para a manutenção dos seus níveis celulares existe uma família de transportadores do metal localizados na membrana plasmática e organelas intracelulares. Transportadores do tipo ZnTs têm a função de diminuir os níveis intracelulares de Zn, transportando-o do citoplasma para o espaço extracelular ou

para dentro de organelas. Entretanto, os transportadores do tipo ZIP agem de maneira oposta, aumentando os seus níveis intracelulares. Através de análises moleculares já foram identificados em mamíferos dez transportadores do tipo ZnT e quatorze transportadores do tipo ZIP, sendo que cada um apresenta características particulares relacionadas a expressão tecidual, localização e regulação celular (Lichten & Cousins, 2009). De fato, o papel destas moléculas é fundamental para a manutenção daqueles processos celulares envolvendo Zn, sendo isto reforçado através da observação de que a diminuição na expressão de alguns destes transportadores resulta na letalidade de embriões de roedores (Andrews et al., 2004).

1.1 Zinco reativo cerebral

Além das funções descritas acima, o Zn possui características particulares no sistema nervoso central (SNC). No cérebro, ele é encontrado tipicamente ligado a proteínas (Frederickson et al., 1983, 1992; Klitenick et al., 1983). Entretanto, em torno de 20% do Zn total do cérebro é livre ou fracamente ligado a biomoléculas (Cole et al., 1999), sendo esta fração correspondente ao conteúdo de Zn reativo[a] suscetível à ação de quelantes. Os primeiros indícios de que o Zn reativo poderia ter alguma importância para o cérebro vem de estudos da década de 70, onde a aplicação do método de Timm fez marcar, com prata, a região do hipocampo de roedores (Haug, 1973). Mais tarde, com o aprimoramento desta técnica na década de 80, foi possível verificar por microscopia eletrônica de transmissão que

[a]Zn reativo: Conforme definição em Paoletti et al. (2009), Zn reativo cerebral é a fração de Zn capaz de ser quelatável, sendo este conteúdo do metal considerado como tema de investigação desta Tese.

os grânulos de prata desenvolvidos pela marcação eram especificamente localizados em vesículas sinápticas dentro de botões, que estabeleciam sinapses assimétricas no hipocampo destes animais. Entretanto, somente com a utilização de técnicas adicionais é que foi possível confirmar a presença do elevado conteúdo de Zn reativo dentro dos terminais sinápticos revelados por Neo-Timm (Danscher et al., 1985). Desde então, a presença de Zn reativo foi detectada no cérebro de mamíferos (Chakravarty et al., 1997; Garcia-Cairasco et al., 1996), aves (Faber et al., 1989), répteis (Perez-Clausell, 1988) e peixes (Pinuela et al., 1992), o que reforça seu papel essencial na homeostasia cerebral de vertebrados.

No SNC diferentes células neurais podem conter Zn reativo. Em particular os neurônios glutamatérgicos são os principais tipos celulares contendo o metal (Paoletti et al., 2009). Nestes neurônios, Zn reativo é encontrado dentro de mitocôndrias (Dittmer et al., 2009) e associado à metalotioneínas no pericário (Frederickson et al., 2004b). Entretanto, algumas destas células apresentam alta concentração do metal (~1 mM) dentro de vesículas glutamatérgicas (Martinez-Guijarro et al., 1991). Esta captação de Zn reativo dentro de vesículas sinápticas somente é possível pela ação do transportador de Zn do tipo ZnT-3 (Cole et al., 1999; Palmiter et al., 1996). O Zn reativo é, portanto, passível de liberação sináptica, podendo agir tanto sobre alvos pós-sinápticos relacionados a sinapses inibitórias, quanto excitatórias, o que lhe concede o caráter integrador da neurotransmissão (Xie & Smart, 1991).

Quando associado a receptores GABAérgicos, este metal pode causar inibição do sistema, rendendo uma rede de transmissão neural hiperexcitada (Smart et al., 2004). Em maior detalhe, estudos têm observado que este efeito conduzido por Zn reativo é determinado pela ligação junto a certas subunidades do receptor $GABA_A$,

que possuem maior afinidade ao metal, indicando a plasticidade sináptica como fator determinante da ação moduladora de Zn (Brooks-Kayal et al., 2001).

Em sinapses glutamatérgicas, o Zn reativo tem adquirido maior importância neurofisiológica, por conta da sua co-localização com o neutransmissor excitatório. Após ser liberado na fenda sináptica, o metal pode se ligar a diversos alvos pós-sinápticos relacionados ao sistema glutamatérgico, como os receptores tipo-NMDA e tipo-AMPA, causando, respectivamente, inibição e ativação destes receptores (Paoletti et al., 2009). Similarmente aos receptores GABAérgicos, o metal promove ação diferencial sobre os receptores tipo-NMDA, induzindo inibição mais intensa de acordo com a sensibilidade das suas subunidades constituintes (Paoletti, et al., 1997; Williams, 1996).

Além de alvos neuronais, o metal liberado das vesículas pode agir sobre outras células circunvizinhas, como os astrócitos (Paoletti et al., 2009), que contêm menos Zn reativo do que os neurônios glutamatérgicos (Sekler and Silverman, 2012). Os astrócitos são capazes de captar Zn reativo extracelular (Varea et al., 2006), o qual pode regular a função do transportador astrocitário de glutamato, o transportador de aminoácido excitatório tipo-1 (EAAT1) (Vandenberg et al., 1998). Além disso, durante episódios de convulsão induzidos por ácido caínico, os astrócitos podem re-captar o Zn reativo liberado por neurônios glutamatérgicos (Revuelta et al., 2005), indicando um importante papel destas células gliais no controle dos níveis do metal.

Alguns estudos têm mostrado que o conteúdo de Zn reativo apresenta funções sobre atividades comportamentais dependentes do hipocampo e da amígdala. Por exemplo, com o uso de quelantes, foi demonstrado que o Zn reativo é fundamental para a memória espacial de roedores (Frederickson et al., 1990; Lassalle et al., 2000). Em outro teste comportamental foi reportado uma relação do Zn reativo com a aquisição e consolidação de memórias dependentes do hipocampo (Daumas et

al., 2004). Além disso, Takeda e colaboradores (2010) sugeriram que um aumento na liberação sináptica de Zn reativo é responsável pela potenciação de memórias aversivas relacionadas com a região da amígdala. Por fim, estudos utilizando dieta deficiente em Zn demontraram que uma deficiência de Zn reativo cerebral acarreta em aumento da ansiedade, e em prejuízos sobre a memória espacial e a extinção de aprendizagem (Keller et al., 2000; Takeda et al., 2007; Tassabehji et al., 2008; Whittle et al., 2010).

Embora muito já se tenha estudado a respeito do papel neural de Zn reativo, o número total de neurônios glutamatérgicos e astrócitos contendo Zn jamais foi quantificado em todo o cérebro. Desta maneira, ainda não se sabe quantos neurônios glutamatérgicos e astrócitos podem contribuir para o conteúdo de Zn reativo no SNC. De fato, uma melhor compreensão do número de células contendo Zn poderia ajudar na investigação de desordens cerebrais associadas com uma alteração nos níveis do metal (Paoletti et al., 2009). Assim, esta questão poderia ser solucionada com o desenvolvimento de métodos práticos para medir o número de células neurais contendo Zn, bem como seus níveis intracelulares de Zn reativo.

1.2 Zn reativo em injúrias cerebrais

A composição de uma sintonia fina na regulação de neurônios contendo Zn é justificada pelo fato de que o rompimento da homeostase deste íon pode resultar em algumas neuropatias, tais como crises convulsivas (Paoletti et al., 2009) e hipóxia-isquemia (Shuttleworth & Weiss, 2011). Nestas disfunções cerebrais, é perceptível que tanto a falta quanto o excesso nos níveis de Zn reativo cerebral podem conduzir a processos celulares neurotóxicos.

1.2.1 Crises epilépticas e Zn reativo

A epilepsia é uma desordem neurológica que afeta aproximadamente 1% da população mundial, da qual é caracterizada por crises epilépticas espontâneas e recorrentes. Tal disfunção pode ser acompanhada por distúrbios motores, sensoriais ou autonômicos, dependendo da região cerebral afetada. O desencadeamento desta disfunção cerebral resulta em crises epilépticas devido, principalmente, a um desequilíbrio entre excitação e inibição (Dichter and Ayala, 1987). Desta forma, as crises epilépticas podem ocorrer pelo aumento de mecanismos excitatórios, conduzindo alterações funcionais nos canais de iônicos. Por outro lado, uma deficiência da maquinaria sináptica inibitória é também capaz de gerar crises epilépticas, principalmente, devido a uma disfunção GABAérgica. Existem também outros fatores que contribuem para a ocorrência de crises como desequilíbrio energético celular, processos inflamatórios e a alteração da função de canais de cálcio, potássio, cloreto e sódio por conta de polimorfismos ou mudanças na expressão dessas moléculas (Lasoń et al., 2013).

Experimentalmente, os modelos animais mais comuns de crises epilépticas são induzidos por compostos químicos (pentilenotetrazol, ácido caínico e pilocarpina), por eletrochoque e por *"kindling"* químico ou elétrico (Lasoń et al., 2013). Nestes modelos é reportado com frequência um brotamento de fibras musgosas (Tauck & Nadler, 1985), que consiste na reorganização de terminais sinápticos contendo Zn reativo (Sutula et al., 1989). Este fenômeno envolvendo o conteúdo do metal, inicialmente, foi associado à suscetibilidade de animais a crises epilépticas, uma vez que a redistribuição destas fibras forma conexões sinápticas excitatórias. Entretanto, a observação de que algumas destas fibras também se associam com sinapses inibitórias de interneurônios reforçou a idéia de que o brotamento de fibras musgosas poderia ser uma resposta compensatória para prevenir as crises (Sutula & Dudek, 2007). Atualmente, ainda não se tem certeza

sobre o exato papel deste fenômeno, sendo apenas definido como um evento de plasticidade neuronal, que pode também ocorrer no exercício físico (Toscano-Silva et al., 2010).

A relação do Zn reativo com as crises se torna direta a medida que o bloqueio do metal pode alterar a suscetibilidade destas disfunções. É notável também que regiões cerebrais propensas a crises epilépticas são as mesmas áreas que fisiologicamente contêm Zn reativo. Baseado nisto, diversos estudos demonstraram um aumento na propensão de camundongos a manifestarem crises epilépticas após serem alimentados com dieta deficiente em Zn (Fukahori & Itoh, 1990; Feller et al., 1991; Takeda et al., 2003), e um efeito similar também foi observado em camundongos *"knockout"* para o transportador ZnT-3 (Cole et al., 2000). Além disso, a ação de quelantes de Zn tem também produzido um efeito pró-convulsivo em roedores (Mitchell and Barnes, 1993). Todos estes trabalhos mostram que o Zn vesicular pode ter funções anticonvulsivas, e a ação inibitória do metal sobre receptores tipo-NMDA poderia ser o mecanismo envolvido na sua proteção.

Em contraste com estes dados, um efeito próconvulsivo de Zn foi reportado após a administração do metal no hipocampo de coelhos (Pei & Koyama, 1986). Este efeito de Zn também foi determinado a partir da observação de que linhagens de ratos propensos a crises epilépticas apresentam maior conteúdo de Zn reativo do que ratos resistentes (Flynn et al., 2007). Estes trabalhos sugerem que o excesso de Zn poderia promover o desenvolvimento de crises epilépticas, o que seria explicado através da ação inibitória de Zn reativo sobre receptores tipo-$GABA_A$ (Smart et al., 2004). Portanto, a apresentação de propriedades ambíguas torna bastante difícil a definição do papel de Zn reativo como anti- ou pró-convulsivante.

1.2.2 Hipóxia-isquemia cerebral e Zn reativo

A hipóxia-isquemia é um fenômeno desenvolvido em patologias vasculares e distúrbios metabólicos, o qual pode desencadear infarto tecidual, principalmente, no cérebro devido a seu alto consumo de oxigênio (O_2) e de energia (Magistretti, 1999). Especificamente, a hipóxia-isquemia cerebral é uma das principais etiologias que desencadeia os acidentes vasculares cerebrais, que é a segunda maior causa de morte em todo mundo (10,64%), sendo responsável por cerca de 6,2 milhões de óbitos somente no ano de 2011 (World Health Organization, 2013). Entretanto, além do número expressivo de mortes, milhões de pessoas, após serem acometidas pela hipóxia-isquemia, apresentam incapacidade crônica devido ao dano sobre determinadas regiões cerebrais.

Já é bem conhecido que em episódios isquêmicos, as células neurais submetidas aos baixos níveis de O_2 e de energia exibem uma falha no metabolismo energético (Obrenovitch & Richards, 1995) que conduz à excitotoxicidade (Choi & Rothman, 1990), inflamação e hiper-ativação do sistema imune (Becker, 1998). Por consequência, isto resulta em apoptose e necrose celular (Besancon et al., 2008), gerando regiões cerebrais infartadas (Murphy et al., 2008), seguido pela perda de funções motoras e sensoriais (Hossmann, 2006). O dano cerebral causado pela hipóxia-isquemia pode ser devastador, mas ao considerar que muitos indivíduos sobrevivem a um evento inicial, torna-se bastante importante compreender melhor os mecanismos que envolvem a recuperação espontânea.

Neste sentido, a reperfusão do cérebro, que ocorre em indivíduos sobreviventes, ganha especial atenção, pois somado aos danos neurais gerados durante a hipóxia-isquemia, a subsequente reoxigenação cerebral acarreta em uma excessiva produção de espécies reativas, incluindo ânion superóxido ($O_2^{\bullet-}$), radical hidroxil ($^{\bullet}OH$), peróxido de hidrogênio (H_2O_2), óxido nítrico ($NO^{\bullet}$) e peroxinitrito ($ONOO^-$) (Collard & Gelman, 2001). Todavia, as células neurais conseguem, depois

de horas, atenuar os danos resultantes do episódio hipóxico-isquêmico, devido à ativação de mecanismos citoprotetores. Por exemplo, em resposta ao aumento de espécies reativas causados pela isquemia, ocorre uma indução de moléculas responsivas ao estresse, como proteínas de choque térmico (Dillmann, 1999) e enzimas antioxidantes, como a glutationa peroxidase (GPx), superóxido dismutase (SOD) e catalase (CAT) (Mahadik et al., 1993). Apesar disto, as nocivas condições intracelulares geradas no insulto cerebral geralmente superam os limites de defesa, podendo causar uma morte adicional de células. Desta maneira, uma maior compreensão dessas respostas celulares envolvidas na reperfusão poderia ajudar no desenvolvimento de terapias reabilitativas.

Sobre esta estratégia, a participação de neurônios contendo Zn na patologia da hipóxia-isquemia tem, recentemente, atraído a atenção de muitos pesquisadores. Isto se deve ao fato de que em um episódio hipóxico-isquêmico ocorre aumento na liberação de Zn reativo na fenda sináptica, da qual é postulado ser um mecanismo protetor devido à ação inibitória do metal sobre receptores excitatórios tipo-NMDA (Shuttleworth & Weiss, 2011). Entretanto, esta hipótese contraria a observação de que a hipóxia-isquemia induz um acúmulo deste íon dentro de neurônios pós-sinápticos, contribuindo para a morte dessas células neurais (Shuttleworth & Weiss, 2011). O acúmulo excitotóxico de Zn reativo nestes neurônios é determinado como uma consequência do aumento nos níveis de espécies reativas geradas pela isquemia, (principalmente de $NO^{\bullet}$), fazendo com que seja deslocado Zn de vários sítios pré- e pós-sinápticos (Frederickson et al., 2004b). Dado que a alteração na homeostasia de Zn reativo é capaz de gerar mais espécies reativas (Dineley et al., 2005), é também proposto que o próprio metal poderia amplificar este efeito. Assim, por apresentar papel importante em eventos hipóxicos-

isquêmicos, o conteúdo de Zn reativo destes neurônios pode ser considerado potencial alvo terapêutico para esta disfunção.

1.2.3 Dietilditiocarbamato

Com a habilidade para "sequestrar" Zn reativo, o uso de quelantes para o metal vem sendo considerado para mitigar o aumento nos níveis de Zn reativo, induzido pela hipóxia-isquemia cerebral. Em particular, o dietilditiocarbamato (DEDTC) é um quelante permeável à membrana plasmática altamente seletivo para Zn (Foresti et al., 2008; Paoletti et al., 2009), além de ter a capacidade de atravessar a barreira hemato-encefálica (Guillaumin et al., 1986). Embora o DEDTC tenha uma conhecida ação inibitória sobre a atividade da SOD (Heikkila et al. 1976), a aplicação do composto tem apresentado benefícios sobre várias desordens (Biagini et al., 1995; Cvek and Dvorak, 2007; Daocheng and Mingxi, 2010; Pang et al., 2007; Qazi et al., 1988). Portanto, as propriedades químicas de DEDTC o tornam um fármaco candidato para a investigação dos seus efeitos sobre parâmetros relacionados hipóxia-isquemia cerebral.

Por outro lado, a administração de DEDTC como uma substância neuroprotetora requer cuidados. Primeiramente, o DEDTC é um composto organosulfurado pertencente à classe de ditiocarbamatos, os quais são amplamente usados como pesticidas em plantas e sementes (Rath et al., 2011). Desta maneira, o DEDTC poderia apresentar os mesmos efeitos tóxicos causados por ditiocarbamatos em vertebrados (Cooper et al., 1999; Houeto et al., 1995; Tilton et al., 2006), os quais têm levado ao cancelamento destes compostos na agricultura (Agência Nacional de Vigilância Sanitária., 2005; United States Environmental Protection Agency, 2005). De fato, o DEDTC apresenta ação neurotóxica sobre SNC, sendo capaz de induzir dano a mielina (Tonkin et al., 2004), alterar a captação

de dopamina (Di Monte et al. 1989) e promover efeito pró-oxidante sobre células neurais (Viquez et al., 2009). Somado a estes efeitos, a administração de DEDTC também proporciona alterações comportamentais que vão desde alterações locomotoras (Domínguez et al., 2003; Foresti et al., 2008) a prejuízos sobre a memória de roedores (Daumas et al., 2004; Frederickson et al., 1990; Lassalle et al., 2000).

Além destes efeitos, a própria administração de DEDTC com o objetivo de diminuir os níveis de Zn reativo deve ser considerada com cuidado. Isto se justifica pelo fato de que a ação do composto pode aumentar a suscetibilidade de animais a desenvolverem crises convulsivas (Domínguez et al., 2003). Assim, mesmo que muitos estudos tenham contribuído para a aplicação terapêutica de DEDTC, é notável que pouca consideração foi dada para os efeitos colaterais, frequentemente, observados no tratamento com DEDTC. Isto faz com que antes mesmo de se avaliar os efeitos de DEDTC sobre condições de hipóxia-isquemia, seja determinada uma concentração que não proporcione estes efeitos adversos ou que ao menos apresente efeitos colaterais mínimos em relação aos possíveis benefícios.

1.3 Peixe-zebra

O objetivo de obter um nível de DEDTC adequado para o tratamento da hipóxia-isquemia, implica na execução de um estudo envolvendo a triagem de diferentes concentrações do composto sobre modelos animais. Conforme a grande maioria das investigações com DEDTC foi realizada em ratos e camundongos, a adoção destes modelos tradicionais poderia obter os efeitos dose-resposta desencadeados pelo composto. Todavia, a exequibilidade de estudos farmacológicos se torna bastante dispendiosa sobre estes animais, uma vez que

requerem uma quantidade considerável de substâncias candidatas, além de exigirem manutenção de condições ótimas que demandam espaço e custo elevado.

Baseado nestas limitações, o peixe-zebra (*Danio rerio*) vem sendo proposto como um modelo atrativo para este tipo de investigação. Estes animais apresentam algumas vantagens intrínsecas em relação a outros modelos vertebrados, tais como baixo custo, pequeno tamanho, fácil manutenção, produção abundante de prole (Goldsmith, 2004; Miller & Gerlai, 2011), além de compartilhar um alto grau de similaridade com os genes de mamíferos (Barbazuk et al., 2000; Woods et al., 2005). Juntamente com isto, eles apresentam embriões translúcidos, os quais são usados em estudos com foco no desenvolvimento animal (Becker & Rinkwitz, 2012), e a aplicação de técnicas de biologia molecular sobre estes peixes tem, facilmente, produzido indivíduos transgênicos para diversos genes-alvo (Moro et al., 2013).

Devido a estas características vantajosas o peixe-zebra vem ganhando cada vez mais espaço em estudos na área de neurociências. Destes trabalhos tem-se concluído que, em comparação a mamíferos, estes animais apresentam considerável conservação funcional de áreas cerebrais (Vargas et al., 2012), bem como dos sistemas de neurotransmissão (Rico et al., 2011). Isto tem suportado comportamentos semelhantes aos desempenhados por mamíferos, quando estes peixes são expostos a conhecidos fármacos psicoativos (Kalueff et al., 2014). De fato, todas estas características tornam o peixe-zebra um modelo com potencial para complementar o conhecimento neuroquímico adquirido em outros vertebrados. Desta mesma forma, a triagem, em ampla escala, de DEDTC em peixe-zebra adulto, além de possibilitar alta praticidade, permite com que os resultados obtidos possam ser ao menos parcialmente transladados para outros vertebrados.

1.3.1 Zn reativo em peixe-zebra

Para a investigação dos possíveis efeitos neurotóxicos de DEDTC, é imprescindível avaliar sua ação sobre os níveis cerebrais de Zn reativo, dado as suas propriedades químicas. Até certo ponto isto impõe um obstáculo para a adoção do peixe-zebra neste estudo, uma vez que jamais foi mostrada a presença de Zn reativo no cérebro desses animais. Atualmente, se sabe que a administração *in vitro* de Zn às células neurais desses peixes, causa um aumento nas atividades das ectonucleotidases (Senger et al., 2006), assim como o uso de quelantes de Zn proporciona um aumento na afinidade de receptores glicinérgicos (Suwa et al., 2001). De fato, estes dados suportam a presença de alvos moleculares sensíveis ao metal no cérebro desses animais e isto é reforçado ainda mais através da observação de que o SNC de peixe-zebra expressa os mesmos transportadores de Zn de outros vertebrados (Ho et al., 2013). Entretanto, mesmo que já se tenha mostrado o conteúdo de Zn reativo sendo liberado de fotoreceptores de peixe-zebra (Redenti et al., 2007), estes dados não comprovam a existência de Zn reativo em seu cérebro. Portanto, antes mesmo de ser executada uma triagem de DEDTC sobre peixe-zebra, é necessário determinar a presença e distribuição topográfica de Zn reativo em seu cérebro, bem como detectar suas células neurais que contêm Zn reativo.

1.3.2 Hipóxia como modelo de dano cerebral em peixe-zebra

Após a determinação de uma concentração de DEDTC que resulte em irrisórios efeitos colaterais, seria possível investigar seu efeito sobre o conteúdo cerebral de Zn reativo em um modelo de hipóxia-isquemia. Neste sentido, a aplicação de severas condições hipóxicas no próprio peixe-zebra poderia ser uma estratégia promissora para avaliar, ao menos em parte, os efeitos de DEDTC sobre a hipóxia-isquemia.

Neste modelo, os peixes são submetidos à hipóxia pela simples redução da pressão parcial de oxigênio (PO_2), fazendo diminuir a disponibilidade de O_2 aos animais de forma prática e não invasiva. Além disso, as potencialidades desse modelo são ainda mais evidenciadas a partir da observação de que o peixe-zebra contém genes induzidos por hipóxia altamente homólogos a outros vertebrados (Rojas et al., 2007). Assim, este modelo tem possibilitado a investigação de efeitos biológicos causados por distintos níveis de hipóxia por expor o peixe-zebra, em curto ou longo prazo, sob moderados (PO_2 ~8.7 KPa ou 65 mmHg) ou severos (PO_2 ~4.7 KPa ou 35 mmHg) níveis de O_2.

Os efeitos causados pela hipóxia em peixe-zebra vêm sendo investigados sobre estágios do desenvolvimento, simulando uma condição experimentada na fase inicial da vida. A submissão destes indivíduos a níveis severos de O_2 tem resultado em disfunções cerebrais, tais como alteração na formação de sinapses (Stevenson et al., 2012), e aumento nas expressões do fator de crescimento insulina tipo I ligado a proteína (IGFBP-1) (Maures and Duan, 2002), do proto-oncogene c-fos (Chen et al., 2013) e da proteína de alta mobilidade do grupo A1 (hmga1) (Moussavi Nik et al., 2011). Após a condição hipóxica, os efeitos cerebrais sobre a reperfusão também vêm sendo investigados em larvas de peixe-zebra, onde já foi reportado um papel neuroprotetor exercido pelo fator 1 de choque térmico (HSF-1) durante este período (Tucker et al., 2011). Adicionalmente, Chen e colegas (2013) demonstraram que a reperfusão em embriões de peixe-zebra causa apoptose de células neurais, um efeito associado ao aumento dos níveis de c-fos induzidos pela hipóxia.

Alguns dos prejuízos neurais causados por hipóxia também já foram investigados em peixe-zebra adulto. Nestes estudos foram mostrados que muitos dos genes do tecido cerebral relacionados à hipóxia são induzidos em peixe-zebra

depois da hipóxia severa, tais como o transportador 4 de monocarboxilatos, lactato desidrogenase A (Ngan and Wang, 2009), anidrase carbônica IX (Esbaugh et al., 2009) e hmga1 (Moussavi Nik et al., 2011). Também, depois de hipóxia severa, foi reportado um aumento nos níveis de mRNA e de proteína da neuroglobina em animais adultos, indicando um provável papel destas moléculas no suprimento de O_2 aos neurônios (Roesner et al., 2006).

Destes estudos iniciais têm se concluído que o modelo de hipóxia em peixe-zebra pode agregar conhecimento sobre os efeitos cerebrais da hipóxia-isquemia em vertebrados. Entretanto, atenção especial deve ser dada para a sua alta resistência e adaptação a ambientes com baixos níveis de O_2. Embora o peixe-zebra seja menos resistente a hipóxia do que outros peixes (Roesner et al. 2008), ele pertence a família Cyprinidae, que consiste de espécies hipóxia-tolerantes (Roesner et al., 2006). Comparado a outros vertebrados, os peixes tem uma baixa pressão parcial de oxigênio crítico (P_{Crit}), o que os faz manter o metabolismo aeróbico mesmo sob baixos níveis de O_2. Portanto, isto tem dificultado a completa translação dos resultados obtidos em modelos de hipóxia em peixe-zebra.

Em contraste, um modelo recente de hipóxia em peixe-zebra adulto tem produzido efeitos similares àqueles obtidos em roedores com isquemia cerebral. Este modelo consiste na submissão dos peixes a níveis críticos de O_2 dentro de uma câmara hipóxica, onde é induzido hipóxia severa em um sistema hermeticamente fechado (Yu and Li, 2011). Poucos minutos de hipóxia neste aparato pode conduzir o peixe-zebra a morte ou mesmo desencadear alta sensibilidade a infarto cerebral, tal como observado em roedores isquêmicos (Yu and Li, 2011). Além desses efeitos, os animais sujeitos a este modelo apresentam alterações locomotoras (Yu and Li, 2011) e um aumento nos níveis cerebrais de Zn reativo (Yu and Li, 2013).

Dado estas similaridades com os modelos tradicionais e as vantagens experimentais do peixe-zebra, é esperado que, no mínimo em uma fase pré-clínica, a indução de dano cerebral em câmara hipóxica possa suportar a triagem de compostos relacionados à hipóxia-isquemia. Isto dará apoio para avaliar os efeitos de DEDTC neste modelo, o que permitiria compreender melhor sua ação sobre a hipóxia-isquemia cerebral. Contudo, para que isto seja possível, é necessário, previamente, estabelecer a capacidade de recuperação espontânea de parâmetros comportamentais e neuroquímicos dos animais submetidos à câmara hipóxica. Certamente, isto se torna fundamental para obter uma janela de administração adequada de DEDTC sobre este modelo.

2. OBJETIVOS

Objetivo Geral: Determinar a distribuição fisiológica de Zn reativo no cérebro de peixes-zebra a fim de investigar sua modulação em animais submetidos à hipóxia, com ou sem o tratamento de DEDTC.

Objetivos Específicos:

Capítulo I – Determinar e Catalogar a distribuição topográfica e citoarquitectônica de Zn reativo em cérebro de peixe-zebra.

Capítulo II – Medir, no cérebro de peixe-zebra, a quantidade de astrócitos e neurônios glutamatérgicos contendo Zn reativo, assim como o conteúdo do metal dentro destas células neurais.

Capítulo III – Determinar o efeito de diferentes concentrações de DEDTC sobre o comportamento e a distribuição cerebral de Zn reativo.

Capítulo IV – Padronizar um modelo de hipóxia severa em peixe-zebra e investigar a capacidade de recuperação espontânea dos animais, considerando a atividade comportamental exploratória e o dano cerebral.

Capítulo V – Avaliar o efeito do DEDTC em animais submetidos a um episódio de hipóxia, considerando a atividade comportamental exploratória e parâmetros neuroquímicos como, a distribuição de Zn reativo, atividade das desidrogenases mitocondriais, níveis de espécies reativas e de tióis reduzidos e atividade da SOD.

PARTE II

CAPÍTULO I

Topographical analysis of reactive Zn in the central nervous system of adult zebrafish (*Danio rerio*)

Artigo publicado no periódico *Zebrafish*

ZEBRAFISH
Volume 10, Number 3, 2013

DOI: 10.1089/zeb.2013.0882

Topographical Analysis of Reactive Zinc in the Central Nervous System of Adult Zebrafish (*Danio Rerio*)

Marcos M. Braga,[1,2] Denis B. Rosemberg,[1,2] Diogo L. de Oliveira,[1,2] Cássio M. Loss,[1,2] Sandro D. Córdova,[1,2] Eduardo P. Rico,[1,2] Emerson S. Silva,[1,2] Renato D. Dias,[1,2] Diogo O. Souza,[1,2] and Maria Elisa Calcagnotto[1,2]

Abstract

Reactive zinc (Zn) is crucial for neuronal signaling and is largely distributed within presynaptic vesicles of some axon terminals of distinct vertebrates. However, the distribution of reactive Zn throughout the central nervous system (CNS) is not fully explored. We performed a topographical study of CNS structures containing reactive Zn in the adult zebrafish (*Danio rerio*). Slices of CNS from zebrafish were stained by Neo-Timm and/or cresyl violet. The Zn specificity of Neo-Timm was evaluated with Zn chelants, N,N,N′,N′-Tetrakis(2-pyridylmethyl)ethylenediamine (TPEN), sodium diethyldithiocarbamate (DEDTC), Zn sulfide washing solution, and hydrochloric acid (HCl). Unfixed slices were also immersed in the fluorescent Zn probe (zinpyr-1). Yellow-to-brown-to-black granules were revealed by Neo-Timm in the zebrafish CNS. Telencephalon exhibited slightly stained regions, while rhombencephalic structures showed high levels of staining. Although stained granules were found on the cell bodies, rhombencephalic structures showed a neuropil staining profile. The TPEN produced a mild reduction in Neo-Timm staining, while HCl and mainly DEDTC abolished the staining, indicating a large Zn content. This result was also confirmed by the application of a Zn probe. The present topographical study revealed reactive Zn throughout the CNS in adult zebrafish that should be considered in future investigation of Zn in the brain on a larger scale.

Introduction

Zinc (Zn) is the second most abundant trace metal in organisms and is essential for many metalloproteins.[1,2] As a micronutrient, Zn is crucial for several cellular processes, such as defense against free radicals, immune function, cell proliferation and reproduction. Zn is an important neuromodulator at synapses of specific brain regions, for example, the hippocampus and cortex,[3,4] and it is implicated in the memory formation process.[5] Alterations in Zn levels contribute to the imbalance in neurotransmission[6] and brain hypoxia[7] that is associated with brain disorders such as seizures and neuronal injury, respectively. Thus, the cellular control of Zn levels in the central nervous system (CNS) is critical for its homeostasis.

The reactive or chelatable Zn, a pool of Zn loosely bound to biomolecules, is implicated in neuronal signaling, and it is largely distributed within presynaptic vesicles in some axon terminals.[8] Zn-containing axon terminals are distributed throughout the telencephalon and are markedly colocalized with a subset of glutamatergic neurons.[9–11] There is robust evidence that links the glutamate receptor function and excitatory amino-acid transporter 1 to the neuromodulatory activity of Zn.[6] In contrast, the role of reactive Zn in the CNS, which is present in the synaptic reorganization of Zn-containing neurons in brain disorders[12–14] and following physical training,[15] is not clear. As a consequence, chelatable Zn has been detected in the brain of distinct vertebrate classes, such as mammals,[13,14] reptiles,[16–18] birds,[19] and fish,[20] using histochemical techniques (e.g., Neo-Timm staining). However, given its ubiquitous presence, phylogenetic conservation, and plasticity, a broader screening of reactive Zn could be a useful strategy to better understand its function in the CNS. While a topographical analysis of reactive Zn throughout the CNS in mammals can be quite complex, the use of small and simple animal models could be an interesting approach to easily perform this investigation.

Zebrafish (*Danio rerio*) is an attractive animal model for neuroscience studies.[21–24] In addition to its intrinsic advantages, such as low-cost, easy maintenance, abundant offspring production,[22,25] and highly conserved genes,[26] the adult zebrafish has a CNS with fewer neurons compared to other

[1]Departamento de Bioquímica, Universidade Federal do Rio Grande do Sul, Porto Alegre, Brazil.
[2]Instituto Nacional de Ciência e Tecnologia em Excitotoxicidade e Neuroproteção (INCT-EN), Porto Alegre, Brazil.

vertebrates. This feature makes it an appropriate animal model to investigate the pool of chelatable Zn throughout the CNS. A recent study performed by Ho and colleagues[27] reported the expression of Zn transporters in the brain during development, suggesting that Zn may play an important role in this species. Moreover, the zebrafish has also been used as an emergent organism for evaluating seizures[28,29] and hypoxia/ischemia-related phenotypes,[30] two brain disorders associated with Zn dyshomeostasis. Thus, for all these features, the distribution of the chelatable form of Zn in the CNS of adult zebrafish should be evaluated.

Therefore, the goal of the present study was to investigate the distribution of reactive Zn throughout the CNS of adult zebrafish. To address this issue, we used Zn-sensitive Neo-Timm staining and optical density quantification to perform a topographical study of Neo-Timm-positive regions/areas and a cytoarchitectonic location of stained granules in whole CNS structures. Zn specificity of the Neo-Timm was also examined using Zn chelants N,N,N′,N′-Tetrakis(2-pyridylmethyl)ethy lenediamine (TPEN) and sodium diethyldithiocarbamate (DEDTC), Zn sulfide washing solutions, and a membrane-permeable fluorescent Zn probe, zinpyr-1 (ZP1).

Materials and Methods

Zebrafish

Twenty-five wild-type male and female adult zebrafish (*Danio rerio*) were obtained from a specialized supplier (Delphis) and maintained under standard conditions. To neutralize ions that could be harmful to fish, we used tap water with Tetra's AquaSafe® (Tetra). The water was kept under continuous mechanical and chemical filtration at 26°C ± 2°C, and fish were housed for 2 weeks before the experiments under a 12-h light/12-h dark cycle photoperiod (lights on at 7:00 am). The animals were healthy and fed twice a day with a commercial flake fish food (Alcon Basic®). As a positive control, three Wistar rats were obtained from our animal facility.

The fish were cryoanesthetized and immediately euthanized by decapitation to remove the brain and spinal cord. The Wistar rats were euthanized by decapitation, and the brain was dissected. All animals were maintained according to the National Institute of Health Guide for the Care and Use of Laboratory Animals. The experiments were approved by the Ethics Committee of Universidade Federal do Rio Grande do Sul (number 19780–CEUA).

Neo-Timm staining

The protocol used for histochemical staining of reactive Zn was based on the traditional Neo-Timm method previously described for immersion autometallography.[31] Briefly, each zebrafish CNS was immersed in 2 mL of 3% glutaraldehyde solution in a 0.1 M phosphate buffer (pH 7.4) for 24 h, and then moved to 2 mL of a sodium sulfide solution (1% Na_2S) in a 0.12 M Millonig's buffer (97 mM NaOH, 138 mM NaH_2PO_4, and 0.18 mM $CaCl_2$) for 24 h. Later, each sample was embedded in 4% agarose (Invitrogen) and glued with cyanoacrylic adhesive to the stage of a vibroslicer (VTS-1000; Leica). Coronal (30-μm-thick) slices were cut in phosphate-buffered saline, mounted on gelatinized slides, and left to dry. For Neo-Timm staining, the CNS slices were incubated in a solution of 120 mL of 50% gum Arabic with 1.85 g of hydroquinone in 30 mL of H_2O, 5.12 g of citric acid, 4.72 g of sodium citrate in 20 mL of H_2O, and 0.17 g of silver nitrate in 1 mL of H_2O for 120 min. For topographical analysis of Neo-Timm staining in zebrafish, four adjacent series of slices were sampled from each CNS. Three series were processed using the Neo-Timm method, and the fourth was stained with cresyl violet (Nissl staining present in the cell bodies) (Supplementary Fig. S1; Supplementary Data are available online at www.liebertpub.com/zeb). For the cytoarchitectonic analysis of Neo-Timm staining, samples were cut and counterstained with both Neo-Timm and cresyl violet.[32] In addition, care was taken to verify the specificity of the Neo-Timm staining in zebrafish: (1) the CNSs were also immersed in 0.1% and 1% Na_2S, producing identical staining; (2) negative control slices (Na_2S-free) were also performed; (3) silver exposure time was also examined at 60 and 180 min, but 120 min exhibited specific staining without overexposure; (4) the rat brains were immersed in a 1% sulfide solution, similar to the method used for zebrafish, which resulted in an identical staining to that observed in perfused rodents (see Supplementary Fig. S2); (5) only ultrapure and metal-free reagents were used in the experiments.

Neo-Timm staining quantification

To define the Neo-Timm-positive regions/areas in the zebrafish CNS, we used the topographical description of zebrafish brain published by Rink and Wullimann[33] and Ullmann and colleagues.[34] The quantification of Neo-Timm staining was performed by analyzing the optical density of the total area for each CNS region in the slice under 10× magnification. The levels of optical densities were considered to determine each region according to all Neo-Timm-positive regions in the zebrafish CNS. Thus, regions with low (<17 arbitrary units), intermediate (≥17 and <34 a.u.), or high (≥34 a.u.) levels of staining were defined by the size, intensity, and number of Neo-Timm-positive granules. Regions that extended to more than one slice, received the correspondent slice number following the abbreviation (e.g., PGz_1, PGz_2). To minimize quantification error, the images were digitalized using the same parameters with a light microscope (Nikon Eclipse E-600) coupled with a camera (Nikon DXM 1200C CCD). The pictures were captured by NIS Elements AR 2.30 software (Nikon), and the images were equalized with the same contrast and brightness, and then converted to an 8-bit gray scale. The optical density was quantified using ImageJ 1.37v software. Specifically, the mean of three small squares with unspecific stain were determined for each slice as a background. This mean value was subtracted from the optical density of the total CNS areas for each slice.

Categorization of the whole Neo-Timm-positive structures

The whole CNS structures of adult zebrafish were categorized according to the level of Neo-Timm staining. The score for each structure (e.g., PGz) was determined by the mean of optical density of the correspondent CNS regions (e.g., PGz_1, PGz_2…PGz_5) in the same stained brain, considering three to six independent experiments. Fifty-nine anatomical structures were compared and categorized based upon high-, intermediate-, and low-level staining.

Determination of chelatable Zn specificity

To evaluate the Zn specificity in Neo-Timm staining, we used two membrane-permeable Zn chelants; TPEN (Sigma) was added in the glutaraldehyde fixative solution to a final concentration of 5 mM in 10% dimethyl sulfoxide (DMSO); and DEDTC (700 mg/kg) (Sigma) dissolved in the phosphate buffer 0.1 M (pH 7.4) was intraperitoneally injected 30 min before the Neo-Timm procedure as a previous study.[35] In parallel, we performed a pretreatment of some CNS slices with hydrochloric acid (HCl) 0.1 M for 30 min or 15% TCA for 5 min because both can dissolve Zn sulfide.[36–38] As controls, we performed three independent experiments using distinct vehicle solutions that did not alter the Neo-Timm staining pattern.

Zinpyr-1 staining procedure

The membrane-permeable fluorescent Zn probe, ZP1 (Sigma), was used as an additional technique to investigate the specificity and location of reactive Zn revealed by Neo-Timm, as previously described.[39] Briefly, adult zebrafish head were immediately frozen by burying them in dry ice for 3 min. Next, frozen samples were mounted on the chuck of a closed cabinet cryostat (Leica CM1850) and cut at −9°C to −11°C. The slices (60 μm thick) were allowed to dry on clean glass slides at room temperature for 1–2 h. The staining was achieved by applying ZP1 in DMSO dissolved in 0.9% NaCl to a final concentration of 20 μM at room temperature. After 3 min, the excess solution was removed, and the slides were viewed and photographed using a Nikon Eclipse E-600 coupled with a Nikon DXM 1200C CCD. Confocal imaging was performed using a LSM 710 Zeiss microscope, with illumination with a 488 ηm multiline argon laser and viewing through a 500 ηm long-pass filter.

Although ZP1 is considered a fluorescent probe highly specific for reactive Zn, we confirm this feature by adding TPEN on zebrafish CNS slice before ZP1 application. This approach did completely abolish ZP1 staining (see Supplementary Fig. S3).The effect of DEDTC application on the slices was similar to TPEN (data not shown). Therefore, as ZP1 is highly specific for reactive Zn, these data reinforce the strong affinity of these chelators to reactive Zn.

Results

Neo-Timm staining characterization

The Neo-Timm staining showed the presence of granules with a color variation from yellow-to-brown-to-black (bright gray-to-black in gray-scale images) and with diameters ranging from 0.5 to 4 μm thick. Overall, the granules exhibited a high staining intensity (black color) with sizes of approximately 2 μm thick, as observed in the periventricular gray zone (PGz) of the optic tectum (Fig. 1A,B).

Topographical CNS Neo-Timm staining

To evaluate the Neo-Timm staining, we divided the zebrafish CNS into three topographical sections.

Telencephalon. The most rostral section of the zebrafish brain exhibited a low level of staining, with the weakest staining and smallest number of Neo-Timm-positive granules (Fig. 2).

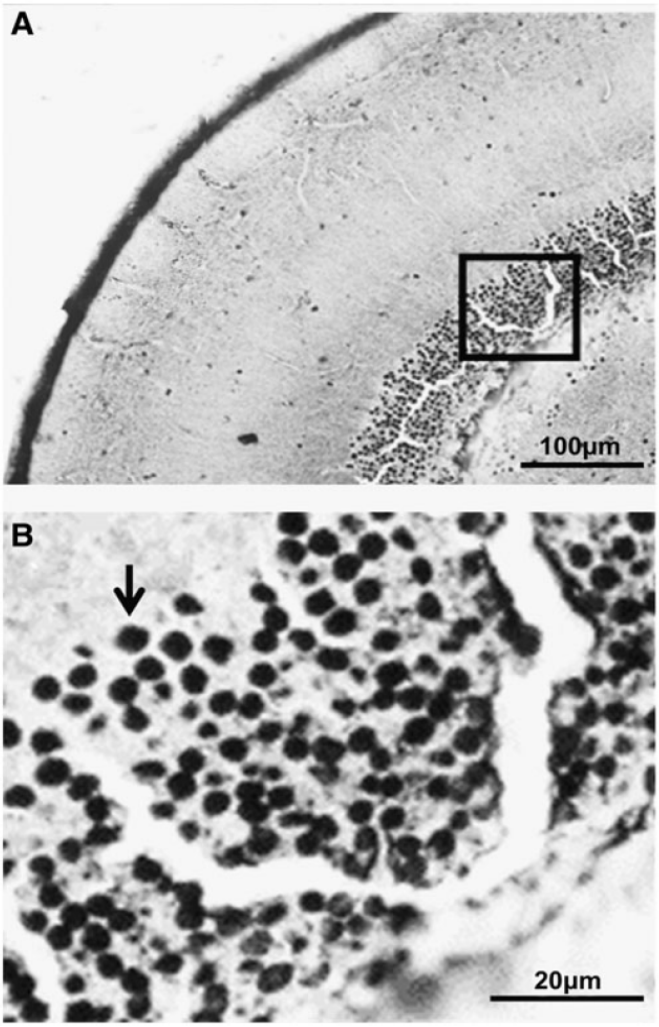

FIG. 1. Neo-Timm staining of adult zebrafish brain slice (30 μm thick). Low **(A)** and high **(B)** magnification of periventricular gray zone (PGz) of the optic tectum (OT) of adult zebrafish. The *black arrow* indicates a stained granule at higher magnification of the area denoted by the *square* in **(A)**.

Specifically, the olfactory bulb (Fig. 2A) showed small granules concentrated in the internal cellular layer (ICL) with an intermediate level of staining. Meanwhile, the glomerular layer (GL) and external cellular layer (ECL_1 and ECL_2) were weakly stained.

In the subsequent slice, we observed few widespread granules in the telencephalic hemispheres (Fig. 2B). Intermediate staining was observed in the posterior and dorsal nucleus (Dp_1 and Dd) of the dorsal area, in the anterior part of the parvocellular preoptic nucleus (PPa), and in the ventral part of the entopeduncular nucleus (NEv). Low-level staining was observed in the lateral nucleus of the dorsal telencephalic area (Dl), the dorsal part of the entopeduncular nucleus (NEd), the supracommissural nucleus of the ventral area (Vs), and the medial nucleus of the dorsal area (Dm). Additionally, the central nucleus of the dorsal area (Dc) was weakly stained, with an optical density close to the background.

In the preoptic slice (Fig. 2C), the magnocellular preoptic nucleus (PM) showed a high level of staining. The entopeduncular nucleus—ventral part (ENv), posterior part of

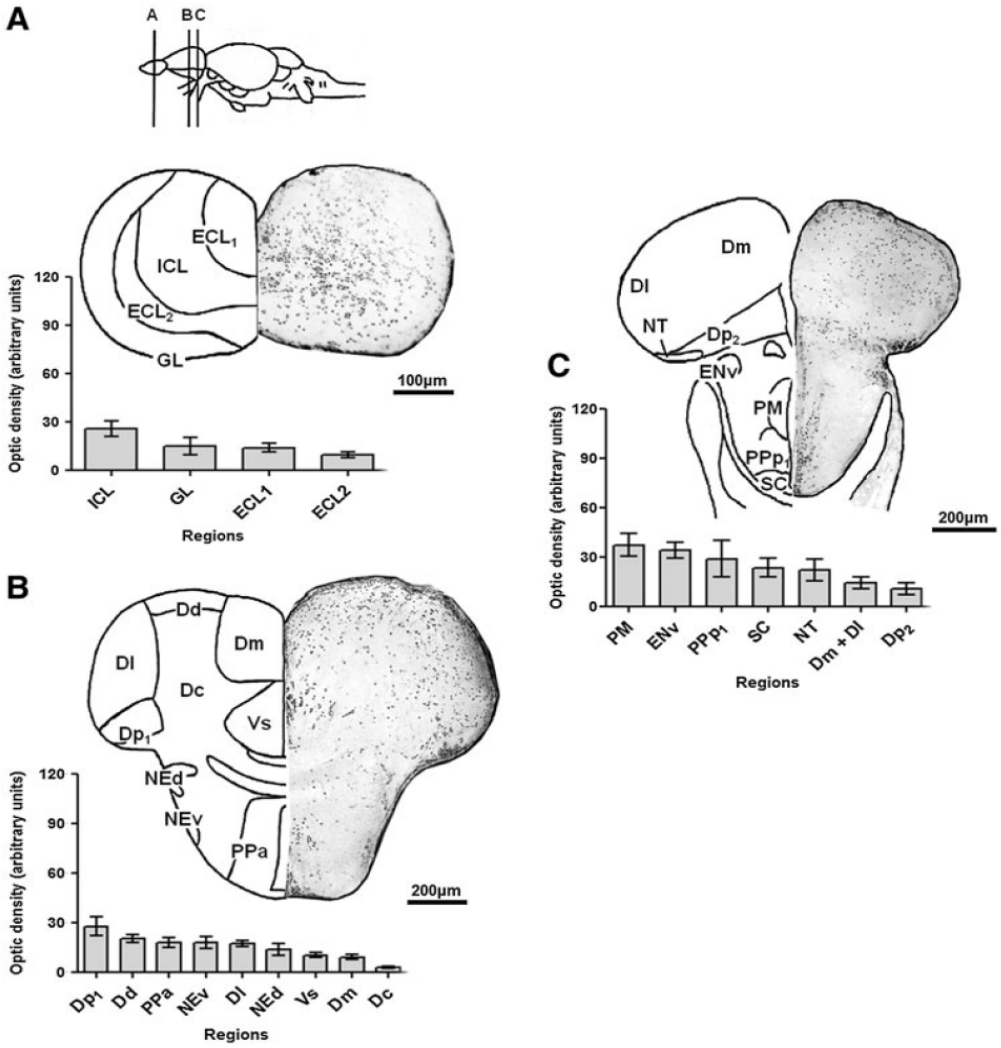

FIG. 2. Neo-Timm-positive regions: anterior central nervous system (CNS) section. Sequential representative slices (30 μm thick) showing the olfactory bulb **(A)**, telencephalon **(B)**, and preoptic **(C)** regions. The whole areas were delimited and measured in optic density. Values are presented as the mean ± SEM in arbitrary units ($n = 3$–6). For abbreviations, see Table 1. Schematic drawings adapted from a previous work.[40]

the parvocellular preoptic nucleus (PPp_1), suprachiasmatic nucleus (SC), and nucleus taeniae (NT) exhibited an intermediate staining profile. Finally, the posterior (Dp_2), medial, and lateral (Dm + Dl) nucleus of the dorsal telencephalic area exhibited a lower level of Neo-Timm staining.

Midbrain and diencephalon. At the initial portion of the diencephalon/mesencephalon (Fig. 3A), the PPp_2, anterior thalamic nucleus (A), ventromedial thalamic nucleus (VM), and ventral zone of the hypothalamic periventricular nucleus (Hv) displayed abundant Neo-Timm-positive cells. The habenula (H) and the ventrolateral optic tract (vot) exhibited an intermediate level of staining. The ventrolateral thalamus (VL) and optic tectum (OT_1) exhibited a low level of staining with few Neo-Timm granules.

In the subsequent slice (Fig. 3B), PGz_1 had markedly more Neo-Timm-positive granules (high optical density) than surrounding regions. The periventricular nucleus of the posterior tuberculum (PTp), torus longitudinalis (TL_1), and subcommissural nucleus (SCN) also had many Neo-Timm-positive granules, but exhibited an intermediate level of staining. The mesencephalic nucleus of the trigeminal nerve (MNV), ventral part of the periventricular pretectal nucleus (PPv), torus lateralis (TLa_1), and OT_2 had a lower level staining.

In the third slice (Fig. 3C), the granular layer in the lateral part of the valvula cerebelli (Val), the dorsal tegmental nucleus (DTN_1), PGz_2, and the central preglomerular nucleus (PGc) exhibited high levels of staining. An intermediate level of Neo-Timm staining was detected in the TL_2, dorsal zone of the hypothalamic periventricular nucleus (Hd_1), and OT_3. In contrast, a low level of staining was observed in the central and diffuse nucleus of the hypothalamic inferior lobe (CIL + DIL), corpus mamillare (CM_1), TLa_2, ventrolateral ($TSvl_1$), and central (TSc_1) nucleus of the torus semicircularis.

In the last representative slice of this segment (Fig. 3D), we observed a high optical density in the TL_3, PGz_3, Hd_2, granular layer of the lateral and medial part (Val + Vam) of the valvula cerebelli, CM_2, and perilemniscal nucleus (PL). The oculomotor nucleus (NIII), DTN_2, and OT_4 had intermediate levels of staining. Finally, few granules were found in the nucleus lateralis valvulae (NLV), nucleus of the lateral lemniscus (NLL), TSc_2, and $TSvl_2$, resulting in regions with a low level of staining.

Hindbrain: rostral part. This segment delimits the rhombencephalic region, which exhibited significant Neo-Timm staining.

In the first slice, the PGz_4, central gray (CG), and corpus cerebelli (CCe_1) (Fig. 4A) were highly stained regions. An

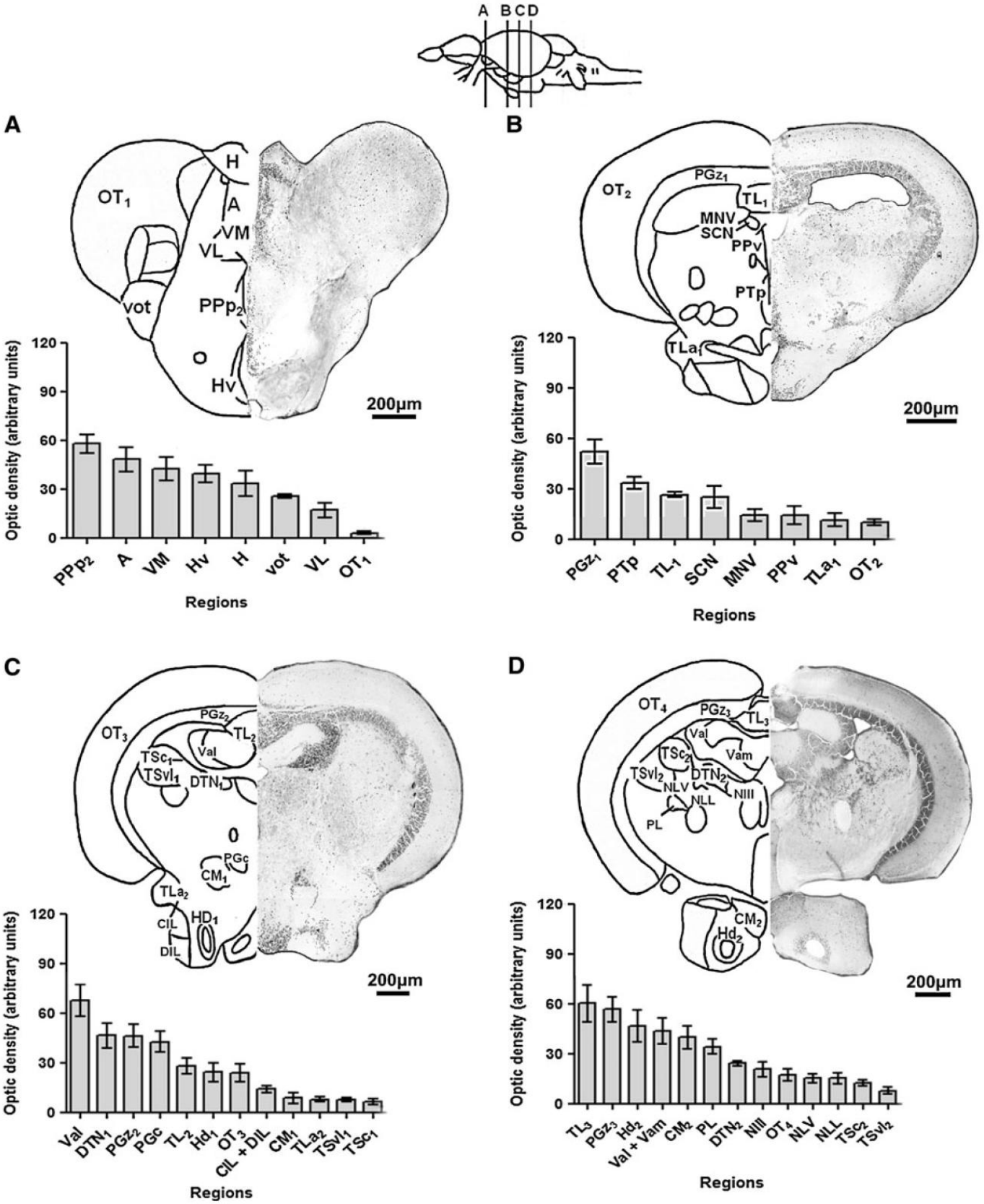

FIG. 3. Neo-Timm-positive regions: middle CNS section. Sequential representative slices (30 μm thick) showing the diencephalon/mesencephalon **(A–D)** regions. The whole areas were delimited and measured in optic density. Values are presented as the mean ± SEM in arbitrary units ($n = 3$–6). For abbreviations, see Table 1. Schematic drawings adapted from a previous work.[40]

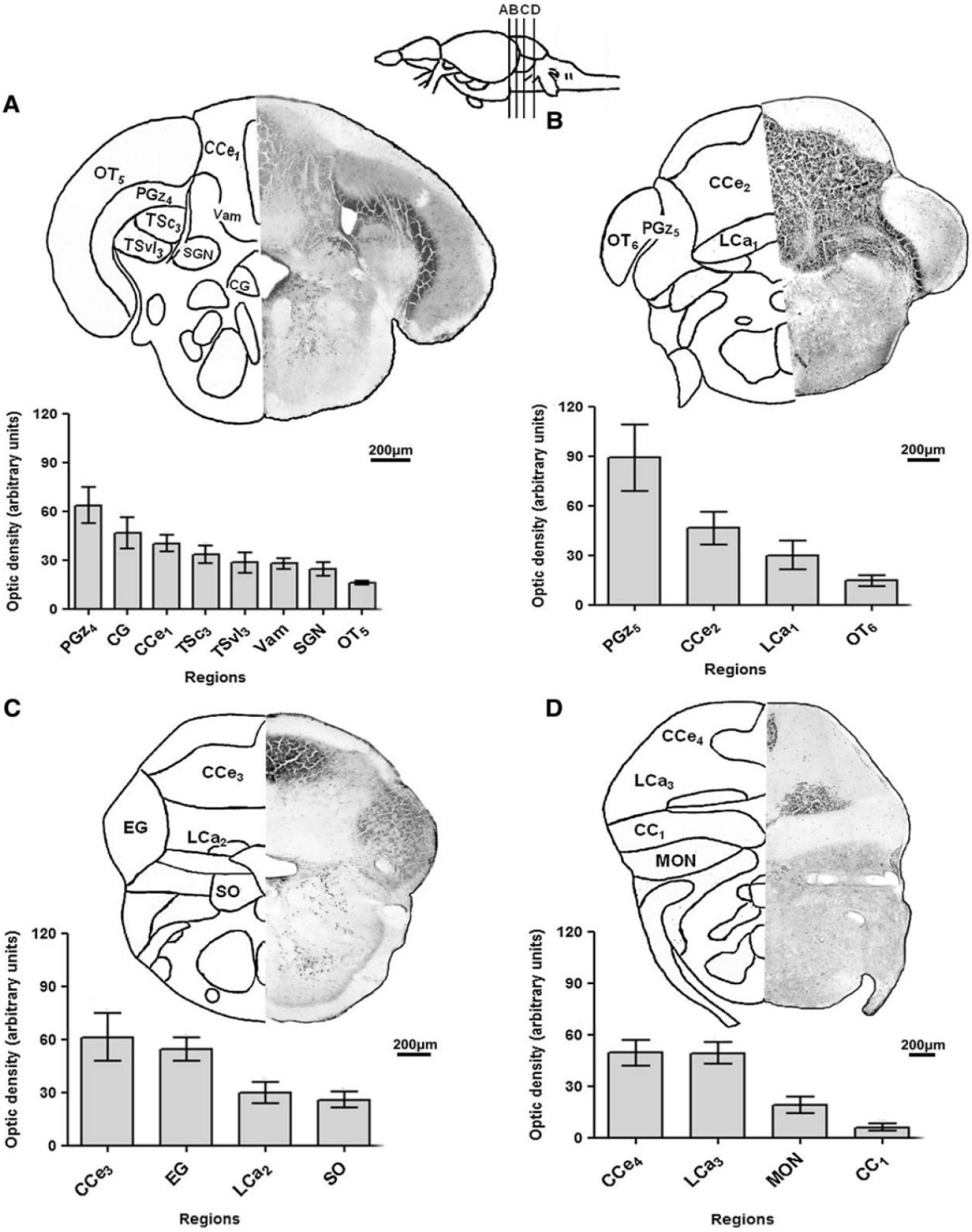

FIG. 4. Neo-Timm-positive regions: posterior CNS section—rostral rhombencephalon. Sequential representative slices (30 μm thick) showing rostral rhombencephalon **(A–D)** regions. The whole areas were delimited and measured by optic density. Values are presented as the mean ± SEM in arbitrary units (n = 3–6). For abbreviations, see Table 1. Schematic drawings adapted from a previous work.[40]

intermediate level of staining was observed in the TSc_3, $TSvl_3$, Vam, and secondary gustatory nucleus (SGN), while the OT_5 had a low level of staining.

In the subsequent topographical slice (Fig. 4B), we detected the highest level of Neo-Timm staining in the final portion of PGz_5 when compared with the other CNS regions. Likewise, the CCe_2 also exhibited a high level of staining. In parallel, intermediate and low levels of staining were observed in the lobus caudalis cerebelli (LCa_1) and the OT_6, respectively.

Positive staining was found in four specific regions on the next representative slice (Fig. 4C). A high level of staining was found in the CCe_3 and eminentia granularis (EG), while LCa_2 and the secondary octaval population (SO) had an intermediate level of staining.

In the next slice (Fig. 4D), a considerable number of Neo-Timm-positive granules were concentrated in the CCe_4 and LCa_3, representing highly stained regions. On the other hand, the medial octavolateral nucleus (MON) and the crista cerebellaris (CC_1) had intermediate and low levels of staining, respectively.

Hindbrain: caudal part. In the representative caudal slice of rhombencephalon (Fig. 5A), the glossopharyngeal lobe (LIX) exhibited a high level of staining. An intermediate level of staining was observed in the facial lobe (LVII), and low levels were observed in the CC_2.

In the spinal cord (Fig. 5B), few positive granules were observed. The ventral part of the lateral funiculus (Flv) and the ventral funiculus (Fv) exhibited only an intermediate optical density value. Additionally, low levels of staining were found in the ventral horn (VH) and the dorsal part of the lateral funiculus (Fld).

From this entire topographical analysis, we observed higher levels of Neo-Timm staining in the hindbrain (predominantly in the rhombencephalon) followed by midbrain/diencephalon and telencephalon sections of the zebrafish CNS.

The whole Neo-Timm-positive structures of adult zebrafish CNS

The rhombencephalic (Val, CG, EG, Vam, LIX, LCa, and CCe) and the diencephalic/mesencephalic structures (PGz, A, TL, Hv, PGc, VM, Hd, DTN, and PL) exhibited a high level of Neo-Timm staining. The preoptic zone displayed few structures with a high level of staining, and only PPp and PM had a substantial optical density (Table 1).

Throughout the zebrafish CNS, we observed structures with intermediate levels of staining such as in the diencephalon/mesencephalon (H, PTp, CM, vot, NIII, VL, and SCN) and in the rhombencephalon (SO, SGN, MON, LVII, and NLL). Similarly, the telencephalon exhibited a considerable number of structures with an intermediate optical density (ICL, Dp, NEv, Dd, PPa, and ECL). The preoptic zone represented by ENv, SC, and NT also had intermediate levels of Neo-Timm staining. In addition, the spinal cord exhibited structures with intermediate levels of staining, such as the Flv and Fv (Table 1).

The group with a low level of staining comprised mostly of telencephalic (Dl, GL, Dm, NEd, Vs, and Dc) and diencephalic/mesencephalic structures (TSvl, DIL, CIL, NLV, OT, MNV, PPv, TSc, and TLa). Moreover, lower levels of Neo-

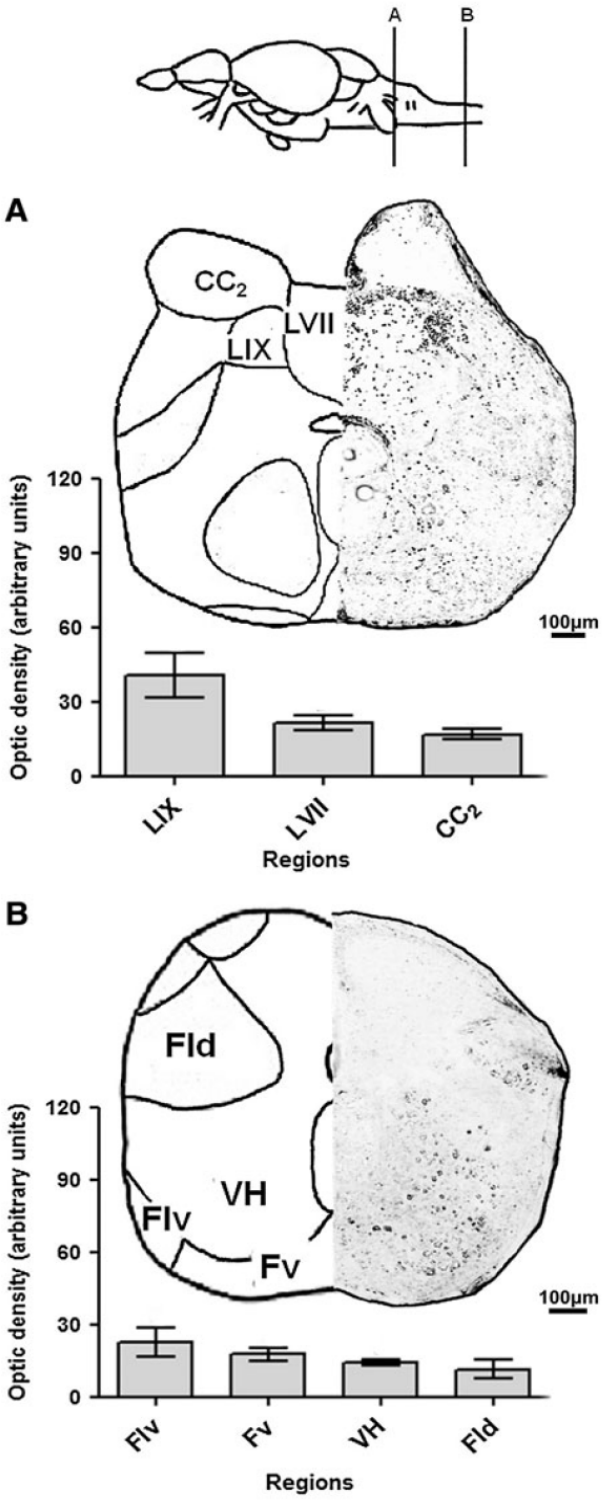

FIG. 5. Neo-Timm-positive regions: posterior CNS section—caudal rhombencephalon and spinal cord. Sequential representative slices (30 μm thick) showing caudal rhombencephalon **(A)** and spinal cord **(B)** regions. The whole areas were delimited and measured in optic density. Values are presented as the mean ± SEM in arbitrary units ($n = 3$–6). For abbreviations, see Table 1. Schematic drawings adapted from a previous work.[40]

Table 1. Neo-Timm Staining in Zebrafish Central Nervous System Structures

Staining level	*Structures*	*Abbreviations*	*Optic density*[a]
High	Valvula cerebelli, lateral part (granular layer)	Val	58.60 ± 6.14
	Central gray	CG	53.25 ± 9.26
	Periventricular gray zone of the optic tectum	PGz	50.80 ± 4.31
	Eminentia granularis	EG	48.79 ± 3.81
	Anterior thalamic nucleus	A	48.23 ± 7.54
	Torus longitudinalis	TL	45.57 ± 6.75
	Ventral zone of the hypothalamic periventricular nucleus	Hv	44.49 ± 2.91
	Central preglomerular nucleus	PGc	42.66 ± 6.08
	Ventromedial thalamic nucleus	VM	42.41 ± 7.13
	Dorsal zone of the hypothalamic periventricular nucleus	Hd	41.45 ± 4.87
	Valvula cerebelli, medial part (granular layer)	Vam	41.07 ± 2.60
	Glossopharyngeal lobe	LIX	40.62 ± 8.81
	Posterior part of the parvocellular preoptic nucleus	PPp	39.75 ± 3.38
	Dorsal tegmental nucleus	DTN	39.59 ± 3.20
	Perilemniscal nucleus	PL	38.38 ± 1.94
	Magnocellular preoptic nucleus	PM	37.20 ± 6.89
	Lobus caudalis cerebelli	Lca	37.11 ± 3.86
	Corpus cerebelli	Cce	35.62 ± 2.50
Intermediate	Entopeduncular nucleus, ventral part	Env	33.99 ± 4.68
	Habenula	H	33.22 ± 8.10
	Periventricular nucleus of the posterior tuberculum	PTp	30.19 ± 1.86
	Secondary octaval population	SO	29.56 ± 3.81
	Corpus mamillare	CM	28.23 ± 4.65
	Secondary gustatory nucleus	SGN	27.65 ± 3.93
	Medial octavolateral nucleus	MON	26.76 ± 1.75
	Ventrolateral optic tract	Vot	25.75 ± 1.07
	Internal cellular layer	ICL	25.53 ± 4.81
	Oculomotor nucleus	NIII	24.37 ± 2.85
	Suprachiasmatic nucleus	SC	23.38 ± 5.64
	Ventral part of the lateral funiculus	Flv	22.56 ± 6.02
	Nucleus taeniae	NT	22.09 ± 6.57
	Posterior nucleus of the dorsal Telencephalic area	Dp	21.89 ± 2.67
	Ventrolateral thalamic nucleus	VL	20.90 ± 2.33
	Ventral part of the entopeduncular nucleus	Nev	20.61 ± 2.48
	Dorsal nucleus of the dorsal telencephalic area	Dd	20.24 ± 2.43
	Anterior part of the parvocellular preoptic nucleus	Ppa	20.18 ± 2.38
	Subcommissural nucleus	SCN	19.09 ± 3.87
	Facial lobe	LVII	18.85 ± 1.45
	Nucleus of the lateral lemniscus	NLL	18.08 ± 2.54
	Ventral funiculus	Fv	17.56 ± 2.46
	External cellular layer	ECL	17.55 ± 2.18
Low	Ventrolateral nucleus of the torus semicircularis	TSvl	16.74 ± 2.72
	Diffuse nucleus of the hypothalamic inferior lobe	DIL	15.78 ± 2.02
	Central nucleus of the hypothalamic inferior lobe	CIL	15.78 ± 2.02
	Nucleus lateralis valvulae	NLV	15.33 ± 2.73
	Lateral nucleus of the dorsal telencephalic area	Dl	15.16 ± 2.11
	Glomerular layer	GL	14.90 ± 5.32
	Optic tectum	OT	14.94 ± 1.56
	Mesencephalic nucleus of the trigeminal nerve	MNV	14.22 ± 3.75
	Ventral horn	VH	14.21 ± 1.13
	Ventral part of the periventricular pretectal nucleus	PPv	14.02 ± 5.42
	Central nucleus of the torus semicircularis	TSc	12.36 ± 2.21
	Dorsal part of the lateral funiculus	Fld	11.38 ± 4.06
	Crista cerebellaris	CC	11.36 ± 1.83
	Medial nucleus of the dorsal telencephalic area	Dm	11.06 ± 2.14
	Dorsal part of the entopeduncular nucleus	Ned	10.50 ± 1.79
	Supracommissural nucleus of the telencephalic ventral area	Vs	10.18 ± 1.48
	Torus lateralis	Tla	7.05 ± 1.11
	Central nucleus of the dorsal telencephalic area	Dc	2.75 ± 0.51

Values are presented as mean ± SEM in arbitrary units ($n = 3–6$).

[a]Mean optical density of the correspondent CNS regions (e.g., PGz1, PGz2…PGz5) in the same stained brain, considering three to six independent experiments.

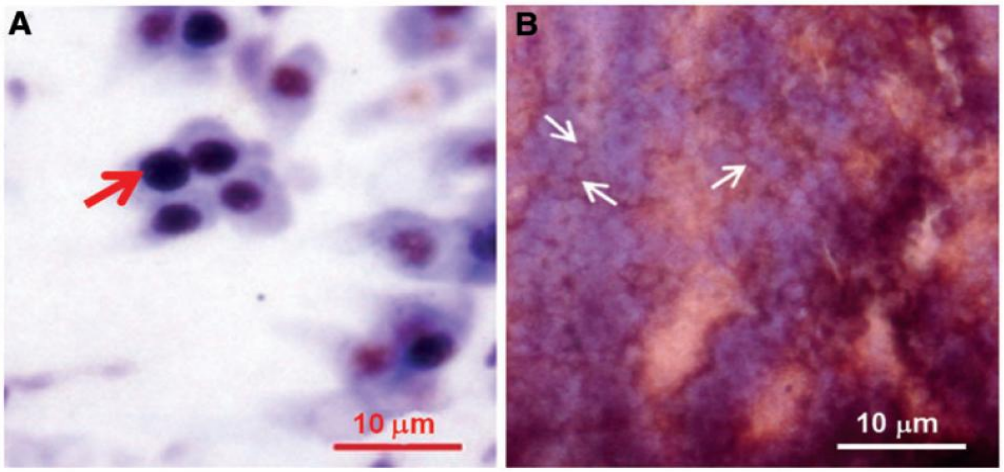

FIG. 6. Cytoarchitectonic distribution of Neo-Timm staining. Note that Neo-Timm staining is indicated by *arrows*. Counterstaining with cresyl violet and Neo-Timm revealed positive granules on the cell body **(A)** and in neuropil **(B)** as stained in central nucleus of the dorsal telencephalic area (Dc) and in torus longitudinalis (TL), respectively. Color images available online at www.liebertpub.com/zeb

Timm staining were found in structures of the rhombencephalon (CC) and spinal cord (VH and Fld) (Table 1).

Cytoarchitectonic distribution of Neo-Timm staining

To evaluate the cytoarchitectonic distribution of Neo-Timm granules, slices from zebrafish CNS were counterstained with Neo-Timm and cresyl violet. As a result, we observed two distinct Neo-Timm-positive areas, which were found on the cell bodies and in the neuropil of the zebrafish CNS.

Neo-Timm-stained granules were found on the cell bodies, mainly in the telencephalon. Structures with this pattern of staining were observed in the Dc (Fig. 6A), CG, PGz, A, Hv, PGc, VM, Hd, PPp, H, PL, PM, ENv, PTp, SO, SGN, MON, vot, ICL, NIII, SC, Flv, NT, Dp, VL, NEv, Dd, PPa, SCN, Fv, ECL, DIL, CIL, Dl, GL, VH, PPv, Fld, CC, Dm, NEd, Vs, TLa, Dc, LIX, DTN, LVII, TSvl, NLV, OT, MNV, and TSc.

Other structures exhibited Neo-Timm staining in the neuropil. In fact, this staining profile was mainly observed in rhombencephalic structures in the hindbrain, such as Val, EG, Vam, LIX, LCa, CCe, and LVII. Similar staining was also found in the TL (Fig. 6B), DTN, CM, NLL, TSvl, NLV, MNV, and TSc.

Neo-Timm staining attributed to chelatable Zn

To identify the contribution of chelatable Zn in Neo-Timm staining, we used, TPEN and DEDTC, two strong Zn chelants; HCl or TCA, which dissolve Zn sulfide (Fig. 7).

The pretreatment with TPEN produced a mild reduction in Neo-Timm staining in zebrafish CNS when compared with

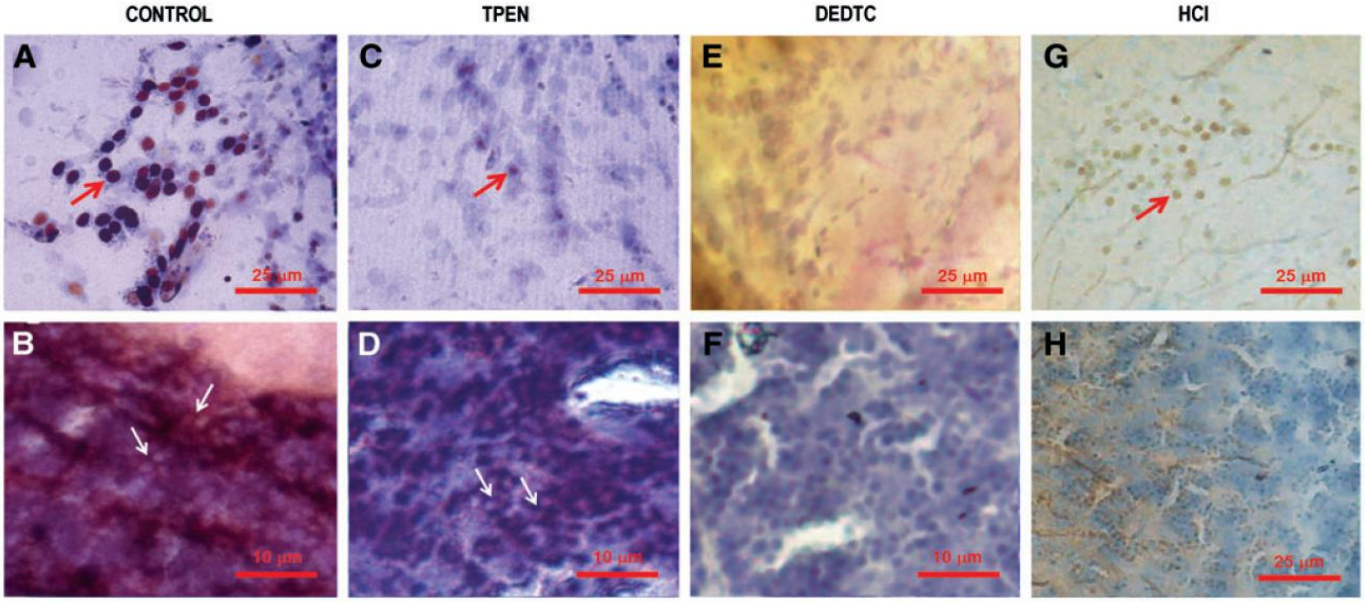

FIG. 7. Chelatable Zn present in Neo-Timm staining. The Neo-Timm staining is indicated by *arrows*. Neo-Timm and cresyl *violet* counterstaining of the central nucleus of the dorsal telencephalic area (Dc) **(A)** and valvula cerebelli, lateral part (Val) **(B)** of controls. Note that pretreatment with 5 mM TPEN decreased the Neo-Timm staining on the cell bodies in the Dc **(C)** and slightly reduced positive granules in neuropil regions, for example, in the Val **(D)**. Administration i.p. of DEDTC 700 mg/kg did completely abolish the *silver* staining on the cell bodies **(E)** and in neuropil regions **(F)**. The use of 0.1 M HCl in the preparation of the slices did significantly reduce Neo-Timm staining on the cell bodies and in neuropil regions, as observed in the Dc **(G)** and Val **(H)**, respectively. Color images available online at www.liebertpub.com/zeb

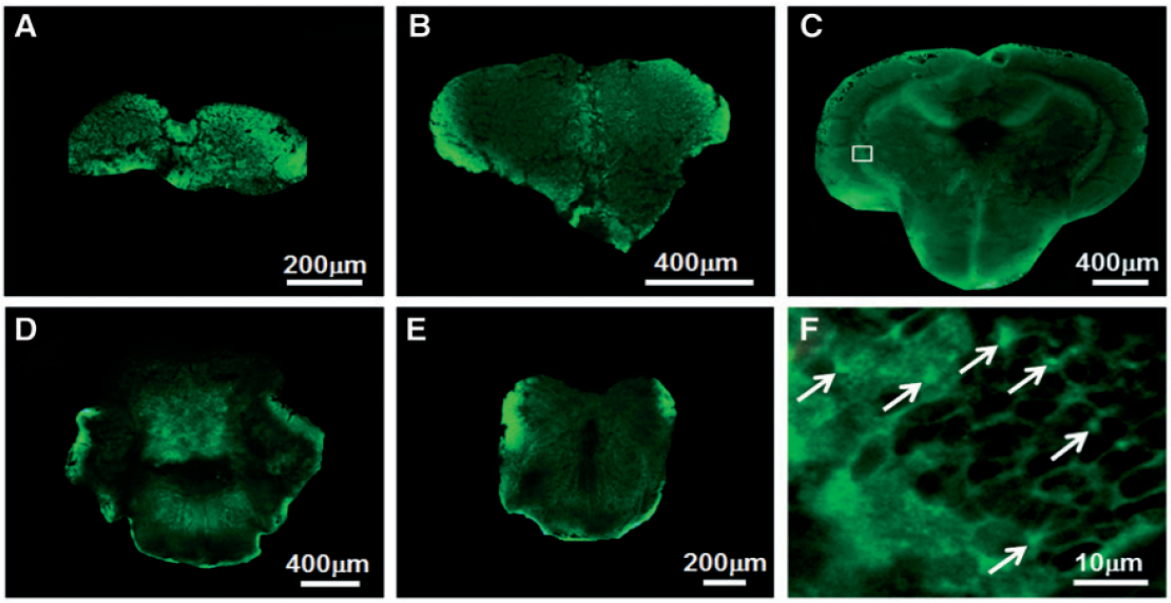

FIG. 8. Unfixed coronal slices (60 μm thick) of CNS stained by ZP1. ZP1 staining yielded widespread bright puncta in the same regions/areas of the zebrafish CNS stained by Neo-Timm. Fluorescence images of the olfactory bulb **(A)**, telencephalon **(B)**, optic tectum **(C)**, the cerebellum **(D)**, and spinal cord **(E)** showing the fluorescent staining in the representative slices. Confocal image of the periventricular gray zone (PGz) **(F)** depicted in the *box* in **(C)**. Note the distinct bright puncta (*arrows*) and the negative staining for somata, similar to those of rodents.[39] Unspecific staining is observed at the edge of the slices. Color images available online at www.liebertpub.com/zeb

the control (Fig. 7A, B). As observed in the central nucleus of the dorsal telencephalic area (Dc) in the telencephalon (Fig. 7C), TPEN decreased Neo-Timm granules located on the cell bodies. In addition, few modifications were detected in neuropil regions after TPEN administration, as seen in rhombencephalic structures, such as Val (Fig. 7D). In contrast, i.p. administration of DEDTC did completely abolish the staining on the cell bodies and in the neuropil, as showed in Dc (Fig. 7E) and Val (Fig. 7F), respectively.

The administration of TCA abolished Neo-Timm staining on the cell bodies in the telencephalon, and few alterations were observed in the staining pattern of the neuropil region in rhombencephalic structures (data not shown). Finally, HCl strikingly decreased Neo-Timm staining on the cell bodies and in neuropil regions, as indicated for the telencephalic (Fig. 7G) and rhombencephalic structures (Fig. 7H), respectively.

Zinpyr-1 staining

The ZP1 staining in the adult zebrafish CNS showed reactive Zn in all regions/areas (Fig. 8A–E) that were positive for Neo-Timm. The olfactory bulb (Fig. 8A) and spinal cord (Fig. 8E) exhibited few and widespread fluorescent staining. Similarly, the whole telencephalon was barely stained by ZP1, as in the central nucleus of the dorsal telencephalic area (Dc) (Fig. 8B). However, in the lateral nucleus of the dorsal telencephalic area (Dl), in the posterior nucleus of the dorsal telencephalic area (Dp_1), and in the supracommissural nucleus of the telencephalic ventral area (Vs), we observed some reactive Zn content. In contrast, representative slices from the optic tectum in the midbrain (Fig. 8C) and cerebellum in the hindbrain (Fig. 8D) showed regions with abundant reactive Zn content, coinciding with those obtained by Neo-Timm staining. Indeed, the periventricular gray zone of the optic tectum (PGz_3), the valvula cerebelli, lateral and medial part (Val + Vam), in the optic tectum, and corpus cerebelli (CCe_2) and lobus caudalis cerebelli (LCa_1), in the cerebellum, presented intensely fluorescent ZP1 staining.

The location of reactive Zn stained with ZP1 was determined by confocal analysis. Throughout the adult zebrafish CNS, ZP1 staining always appeared as bright puncta out of the perikarya in areas with Neo-Timm granules on the cell bodies (e.g., PGz_3 in Fig. 8F) and in regions with a neuropil staining pattern. Thus, we confirmed the result for the substantial reactive Zn content stained by Neo-Timm.

Discussion

The main finding of this study was the heterogeneous pattern of Neo-Timm staining detected for chelatable Zn in different regions and structures throughout the CNS of adult zebrafish. In distinct animal models, such as rodents, this method has been used to stain neuropil in hippocampal areas containing high levels of reactive Zn.[41] In the present study, we used Zn chelant treatments, Zn sulfide washing solutions, and a fluorescent Zn probe as approaches to support the highly specific avidity of Neo-Timm staining for reactive Zn. The use of these strategies allowed us to observe the presence of reactive Zn more predominantly in the rhombencephalon than in telencephalic structures.

As in zebrafish, the Neo-Timm method stained distinct CNS areas. We showed its specificity to reveal regions containing Zn by different approaches. In fact, the administration of TPEN, a specific Zn chelant,[42,43] produced a mild decrease of Neo-Timm-positive granules on the cell bodies and in the neuropil, suggesting the presence of reactive Zn in Neo-Timm-stained zebrafish CNS. Importantly, we cannot rule out that the residual Neo-Timm-positive granules left by TPEN

could be attributed to the nonsaturable chelant concentration or even to other metals. Indeed TPEN (5 mM) may have been insufficient to fully wash chelatable Zn from the tissue, similar to the results observed in rodents treated with the other Zn chelant.[35] Since copper and iron may be revealed by Neo-Timm,[44] these metals could also explain the residual staining observed in the zebrafish CNS. However, the marked absence of positive granules after the i.p. injection of DEDTC and the administration of Zn sulfide washing solutions,[36–38] suggests that other metals have a negligible contribution to Neo-Timm staining in the adult zebrafish CNS. Additionally, the presence of reactive Zn detected by Neo-Timm staining was reinforced by ZP1 application, which demonstrated that chelatable Zn was found at similar CNS regions and structures stained by Neo-Timm. Thus, as for other animal models,[39,45,46] the use of a fluorescent Zn probe in the zebrafish CNS confirmed the high specificity of Neo-Timm for the detection of reactive Zn.

The cytoarchitectonic distribution of reactive Zn in the zebrafish CNS detected by counterstaining of cresyl violet/Neo-Timm is consistent with the findings in other animal models.[13,14,20,47] Although we observed a pattern of staining in the neuropil that is usually seen in rodent hippocampi, the zebrafish CNS also exhibited Neo-Timm-positive granules located within the limits of the cell bodies, which could be either inside or surrounding the soma. Interestingly, Pinuela and colleagues[20] also found Neo-Timm staining on the cell bodies in the rainbow trout brain, possibly representing axosomatic terminals. However, it is also known that the presence of Neo-Timm granules in the healthy perikarya of mammals represents unspecific staining because chelating agents are unable to clean positive granules.[48] Surprisingly, when we pretreated the brains with Zn chelants before Neo-Timm staining, the granules on the cell bodies were also suppressed. It is difficult to know whether these granules correspond to those stained in the neuropil of mammals, which are correlated with the pool of reactive Zn located inside the vesicles of excitatory synapses. Future ultrastructural studies of Neo-Timm staining using zebrafish could be an interesting strategy to clarify the exact subcellular location of reactive Zn in regions with granules in the neuropil and areas on the cell bodies. Nevertheless, taking into account the confocal analysis of ZP1 staining, the reactive Zn was detected outside cell bodies throughout the zebrafish CNS, similar to rodents.[39]

Because our data support the presence of an abundant reactive Zn content in the adult zebrafish CNS, the whole structures were categorized according to the level of staining. As described, structures with a high level of Neo-Timm staining were predominantly found in the rhombencephalon in the hindbrain, similar to Zn-containing neurons in the hippocampal region of distinct vertebrate classes.[13,14,16–19] As in other teleosts, zebrafish also present the lateral nucleus of the dorsal telencephalic area (Dl), located in the pallium region of CNS, which structurally corresponds to the hippocampus.[49] Similar to a previous study using rainbow trout perfused with 1% sulfide,[20] our data showed less reactive Zn in the telencephalon when compared with other parts of the CNS of adult zebrafish. These results confirm the phylogenetic trend of the translocation of a high level of Neo-Timm from the rhombencephalon in zebrafish to telencephalic structures in mammals, reptiles, and birds. Although, further studies are required to elucidate this hypothesis, a small amount of reactive Zn in the zebrafish telencephalon could be sufficient to perform an allosteric modulation, like in mammals.[50,51]

It is well known that the abundant reactive Zn stained by Neo-Timm in the rodent hippocampus is associated with learning and memory formation[5] because Zn acts as a neuromodulator colocalized in vesicles with glutamate in Zn-containing neurons.[3] In fact, the corelease of reactive Zn and glutamate has been observed at the synaptic terminals of rod photoreceptors in zebrafish, modulating the synaptic activity.[52] Interestingly, we have observed a high level of Zn stained by Neo-Timm in the rhombencephalic structures (Val, CG, EG, Vam, LCa, and CCe), which are known to exhibit an abundant distribution of glutamatergic neurons.[53] These results lead us to hypothesize an important role of reactive Zn in the rhombencephalon of zebrafish as a neuromodulator in structures responsible for movement control.[54] As observed in rodents,[48] the substantial reactive Zn detected by Neo-Timm staining in the thalamic structures (A and VM) could also act in the control of the multifunctional thalamic and hypothalamic nucleus in the zebrafish CNS. Currently, we can only speculate on the neuromodulatory action of reactive Zn detected by Neo-Timm, and further studies must be performed to clarify the neurochemical function of reactive Zn in the CNS of zebrafish.

In summary, our data suggest that the zebrafish CNS contains a considerable amount of reactive Zn with a heterogenic distribution, as detected by Neo-Timm staining and a fluorescent Zn probe. Although, the rhombencephalic structures of zebrafish had higher levels of Neo-Timm staining than the telencephalon, the cytoarchitectonic location of the granules seemed to be similar to other vertebrates. Because this topographical investigation showed reactive Zn throughout the adult zebrafish CNS, additional studies could help to understand the exact function of the Zn content, mainly in those structures with high staining levels. Moreover, we described, for the first time, a protocol for assessing the chelatable Zn pool in the zebrafish CNS using ZP1 staining in unfixed brain slices. This protocol, together with Neo-Timm staining, could be a valuable tool for additional studies that aim to evaluate the functional roles of Zn. Therefore, considering the widespread distribution of reactive Zn and the possibility for testing the whole zebrafish CNS in topographical analyses, these techniques could be considered in future research to clarify the mechanisms underlying Zn homeostasis in the CNS of vertebrates on a larger scale.

Acknowledgments

We are grateful to Henrique Biehl from the Centro de Microscopia Eletrônica (CME) of the Universidade Federal do Rio Grande do Sul for the confocal technical assistance.

Disclosure Statement

No competing financial interests exist.

References

1. Vallee BL, Auld DS. Zinc coordination, function and structure of zinc enzymes and other proteins. Biochemistry 1990;29:5647–5659.

2. Braga MM, Dick T, de Oliveira DL, Guerra AS, Leite MC, Ardais AP, *et al.* Cd modifies hepatic Zn deposition and modulates δ-ALA-D activity and MT levels by distinct mechanisms. J Appl Toxicol 2012;32:20–25.
3. Qian J, Noebels JL. Exocytosis of vesicular zinc reveals persistent depression of neurotransmitter release during metabotropic glutamate receptor long-term depression at the hippocampal CA3-CA1 synapse. J Neurosci 2006;26: 6089–6095.
4. Cunningham MG, Ames HM, Christensen MK, Sorensen JC. Zincergic innervation of medial prefrontal cortex by basolateral projection neurons. Neuroreport 2007;18:531–535.
5. Sindreu C, Storm DR. Modulation of neuronal signal transduction and memory formation by synaptic zinc. Front Behav Neurosci 2011;5:68.
6. Paoletti P, Vergnano AM, Barbour B, Casado M. Zinc at glutamatergic synapses. Neuroscience 2009;158:126–136.
7. Stork CJ, Li YV. Rising zinc: a significant cause of ischemic neuronal death in the CA1 region of rat hippocampus. J Cereb Blood Flow Metab 2009;29:1399–1408.
8. Frederickson CJ, Suh SW, Silva D, Thompson RB. Importance of zinc in the central nervous system: the zinc-containing neurons. J Nutr 2000;130:1471–1483.
9. Martinez-Guijarro FJ, Soriano E, Del Rio JÁ, Lopez-Garcia C. Zinc-positive boutons in the cerebral cortex of lizards show glutamate immunoreactivity. J Neurocytol 1991;20:834–843.
10. Beaulieu C, Dyck R, Cynader M. Enrichment of glutamate in zinc-containing terminals of the cat visual cortex. Neuroreport 1992;3:861–864.
11. Sindreu CB, Varoqui H, Erickson JD, Perez-Clausell J. Boutons containing vesicular zinc define a subpopulation of synapses with low AMPAR content in rat hippocampus. Cereb Cortex 2003;13:823–829.
12. Penkowa M, Moos T. Disruption of the blood-brain interface in neonatal rat neocortex induces a transient expression of metallothionein in reactive astrocytes. Glia 1995;13:217–227.
13. Garcia-Cairasco N, Wakamatsu H, Oliveira JA, Gomes EL, Del Bel EA, Mello LE. Neuroethological and morphological (Neo-Timm staining) correlates of limbic recruitment during the development of audiogenic kindling in seizure susceptible Wistar rats. Epilepsy Res 1996;26:177–192.
14. Chakravarty DN, Babb TL, Chung CK, Mikuni N. Bilateral kainic acid lesions in the rat hilus induce non-linear additive mossy fiber neoinnervation. Neurosci Lett 1997;230:175–178.
15. Toscano-Silva M, Silva SG, Scorza FA, Bonvent JJ, Cavalheiro EA, Arida RM. Hippocampal mossy fiber sprouting induced by forced and voluntary physical exercise. Physiol Behav 2010;101:302–308.
16. Perez-Clausell J. The organization of zinc-containing terminal fields in the brain of the lizard Podarcis hispanica. A histochemical study. J Comp Neurol 1988;267:153–171.
17. Smeets WJAJ, Perez-Clausell J, Geneser FA. The distribution of zinc in the forebrain and midbrain of the lizard Gekko gecko. A histochemical study. Anat Embryol 1989;180:45–56.
18. Pimentel HC, dos Santos JR, Macedo-Lima M, de Almeida FT, Santos ML, Molowny A, *et al.* Structural organization of the cerebral córtex of the neotropical lizard Tropidurus hispidus. Cell Tissue Res 2011;343:319–330.
19. Faber H, Braun K, Zuschratter W, Scheich H. System specific distribution of zinc in the chick brain. A light- and electron-microscopic study using the Timm method. Cell Tissue Res 1989;258:247–257.
20. Pinuela C, Baatrup E, Geneser FA. Histochemical distribution of zinc in the brain of the rainbow trout, Oncorhynchos myciss. I. The telencephalon. Anat Embryol 1992;185:379–388.
21. Senger MR, Rosemberg DB, Rico EP, de Bem Arizi M, Dias RD, Bogo MR, *et al. In vitro* effect of zinc and cadmium on acetylcholinesterase and ectonucleotidase activities in zebrafish (Danio rerio) brain. Toxicol In Vitro 2006;20:954–958.
22. Egan RJ, Bergner CL, Hart PC, Cachat JM, Canavello PR, Elegante MF, *et al.* Understanding behavioral and physiological phenotypes of stress and anxiety in zebrafish. Behav Brain Res 2009;205:38–44.
23. Gerlai R. Using zebrafish to unravel the genetics of complex brain disorders. Curr Top Behav Neurosci 2012;12:3–24.
24. Rosemberg DB, Braga MM, Rico EP, Loss CM, Córdova SD, Mussulini BH, *et al.* Behavioral effects of taurine pretreatment in zebrafish acutely exposed to ethanol. Neuropharmacology 2012;63:613–623.
25. Gerlai R, Lee V, Blaser R. Effects of acute and chronic ethanol exposure on the behavior of adult zebrafish (Danio rerio). Pharmacol Biochem Behav 2006;85:752–761.
26. Barbazuk WB, Korf I, Kadavi C, Heyen J, Tate S, Wun E, *et al.* The syntenic relationship of the zebrafish and human genomes. Genome Res 2000;10:1351–1358.
27. Ho E, Dukovcic S, Hobson B, Wong CP, Miller G, Hardin K, *et al.* Zinc transporter expression in zebrafish (Danio rerio) during development. Comp Biochem Physiol C Toxicol Pharmacol 2012;155:26–32.
28. Baraban SC, Taylor MR, Castro PA, Baier H. Pentylenetetrazole induced changes in zebrafish behavior, neural activity and c-fos expression. Neuroscience 2005;131:759–768.
29. Alfaro JM, Ripoll-Gomez J, Burgos JS. Kainate administered to adult zebrafish causes seizures similar to those in rodent models. Eur J Neurosci 2011;33:1252–1255.
30. Zakhary SM, Ayubcha D, Ansari F, Kamran K, Karim M, Leheste JR, *et al.* A behavioral and molecular analysis of ketamine in zebrafish. Synapse 2011;65:160–167.
31. Danscher G, Stoltenberg M, Bruhn M, Sondergaard C, Jensen D. Immersion autometallography: histochemical *in situ* capturing of zinc ions in catalytic zinc–sulfur nanocrystals. J Histochem Cytochem 2004;52:1619–1625.
32. Wullimann MF, Puelles L. Postembryonic neural proliferation in the zebrafish forebrain and its relationship to prosomeric domains. Anat Embryol 1999;199:329–348.
33. Rink E, Wullimann MF. Connections of the ventral telencephalon (subpallium) in the zebrafish (Danio rerio). Brain Res 2004;1011:206–220.
34. Ullmann JFP, Cowin G, Kurniawan ND, Collin SP. A three-dimensional digital atlas of the zebrafish brain. Neuroimage 2010;51:76–82.
35. Foresti ML, Arisi GM, Fernandes A, Tilelli CQ, Garcia-Cairasco N. Chelatable zinc modulates excitability and seizure duration in the amygdale rapid kindling model. Epilepsy Res 2008;79:166–172.
36. Kozma M, Szerdahelyi P, Kasa P. Histochemical detection of zinc and copper in various neurons of the central nervous system. Acta Histochem 1981;69:12–17.
37. Szerdahelyi P, Kasa P. Histochemical demonstration of copper in normal rat brain and spinal cord. Evidence of localization in glial cells. Histochemistry 1986;85:341–347.
38. Danscher G. The autometallographic zinc-sulphide method. A new approach involving *in vivo* creation of nanometer-sized zinc sulphide crystal lattices in zinc-enriched synaptic and secretory vesicles. Histochem J 1996;28:361–373.
39. Frederickson CJ, Burdette SC, Frederickson CJ, Sensi SL, Weiss JH, Yin HZ, *et al.* Method for identifying cells

suffering toxicity by use of a novel fluorescent sensor. J Neurosci Methods 2004;139:79–89.
40. Clemente D, Porteros A, Weruaga E, Alonso JR, Arenzana FJ, Aijón J, *et al.* Cholinergic elements in the zebrafish central nervous system: histochemical and immunohistochemical analysis. J Comp Neurol 2004;474:75–107.
41. Perez-Clausell J, Danscher G. Intravesicular localization of zinc in rat telencephalic boutons. A histochemical study. Brain Res 1985;337:91–98.
42. Medvedeva YV, Lin B, Shuttleworth W, Weiss JH. Intracellular Zn2+ accumulation contributes to synaptic failure, mitochondrial depolarization, and cell death in acute slice oxygen-glucose deprivation model if ischemia. J Neurosci 2009;29:1105–1114.
43. Xu Z, Yoon J, Spring DR. Fluorescent chemosensors for Zn(2+). Chem Soc Rev 2010;39:1996–2006.
44. Danscher G. Histochemical demonstration of heavy metals. A revised version of the sulphide silver method suitable for both light and electron microscopy. Histochemistry 1981; 71:1–16.
45. Birinyi A, Parker D, Antal M, Shupliakov O. Zinc co-localizes with GABA and glycine in synapses in the lamprey spinal cord. J Comp Neurol 2001;433:208–221.
46. Varea E, Ponsoda X, Molowny A, Danscher G, Lopez-Garcia C. Imaging synaptic zinc release in living nervous tissue. J Neurosci Methods 2001;110:57–63.
47. Lopez-Garcia C, Varea J, Palop JJ, Nacher J, Ramirez C, Ponsoda X, *et al.* Cytochemical techniques for zinc and heavy metals localization in nerve cells. Micros Res Tech 2002;56:318–331.
48. Mengual E, Casanovas-Aguilar C, Perez-Clausell J, Gimenez-Amaya JM. Thalamic distribution of zinc-rich terminal fields and neurons of origin in the rat. Neuroscience 2001;102:863–884.
49. Mueller T, Dong Z, Berberoglu MA, Guo S. The dorsal pallium in zebrafish, *Danio rerio* (Cyprinidae, Teleostei). Brain Res 2011;1381:95–105.
50. Mony L, Kew JN, Gunthorpe MJ, Paoletti P. Allosteric modulators of NR2B-containing NMDA receptors: molecular mechanisms and therapeutic potential. Br J Pharmacol 2009;157:1301–1317.
51. Paoletti P. Molecular basis of NMDA receptor functional diversity. Eur J Neurosci 2011;33:1351–1365.
52. Redenti S, Ripps H, Chappell RL. Zinc release at the synaptic terminals of rod photoreceptors. Exp Eye Res 2007;85:580–584.
53. Bae YK, Kani S, Shimizu T, Tanabe K, Nojima H, Kimura Y, *et al.* Anatomy of zebrafish cerebellum and screen for mutations affecting its development. Dev Biol 2009;330: 406–426.
54. Ito M. Control of mental activities by internal models in the cerebellum. Nat Rev Neurosci 2008;9:304–313.

Address correspondence to:
Marcos Martins Braga, MSc
Departamento de Bioquímica
Instituto de Ciências Básicas da Saúde
Universidade Federal do Rio Grande do Sul
Rua Ramiro Barcelos 2600-Anexo
Porto Alegre 90035-000, RS
Brazil

E-mail: marcosmbraga@gmail.com

CAPÍTULO II

Quantification of astrocytes and glutamatergic neurons containing zinc in zebrafish brain

Artigo a ser submetido ao periódico *Cytometry, Part A*

Quantification of astrocytes and glutamatergic neurons containing zinc in zebrafish brain

Marcos Martins Braga,[a,b,(✉)] *Renato Dutra Dias,*[a,b] *Diogo Losch de Oliveira,*[a,b,c] *Maria Elisa Calcagnotto,*[a,b] *Diogo Onofre de Souza,*[a,b,c] *Leticia Ferreira Pettenuzzo* [a]

[a] *Programa de Pós-graduação em Bioquímica, Departamento de Bioquímica, Instituto de Ciências Básicas da Saúde, Universidade Federal do Rio Grande do Sul, Porto Alegre 90035-003, Brazil.*

[b] *Instituto Nacional de Ciência e Tecnologia em Excitotoxicidade e Neuroproteção (INCT-EN), Porto Alegre 90035-003, Brazil.*

[c] *Zebrafish Neuroscience Research Consortium (ZNRC).*

Running headline: Zn-containing cells in the brain

(✉) Marcos M. Braga

Departamento de Bioquímica, Instituto de Ciências Básicas da Saúde

Universidade Federal do Rio Grande do Sul

Rua Ramiro Barcelos, 2600-anexo

Zip code: 90035-003

Porto Alegre - RS - Brazil.

Phone: +55 (51) 33085555

Fax: +55 (51) 33085540

E-mail address: **marcosmbraga@gmail.com**

Abstract

Although reactive zinc (Zn) has an important role in synaptic physiology, the number of astrocytes and glutamatergic neurons containing Zn throughout the brain has never been quantified. Here, we developed a standardized method to determine the total number of astrocytes and glutamatergic neurons containing Zn as well as the intracellular levels of reactive Zn within these cells. We analyzed the zebrafish brain for double immunolabeling with cell-type specific markers and a membrane-permeant fluorescent Zn probe to detect astrocytes and glutamatergic neurons with or without reactive Zn, using flow cytometry. The application of this method to study zebrafish brain cells showed that ~50% of cells are astrocytes and ~30% are glutamatergic neurons. Moreover, ~14% of astrocytes and ~29% of glutamatergic neurons contain reactive Zn. We counted a total of 840,000 cells in the zebrafish brain; from this, we estimate that astrocytes and glutamatergic neurons containing Zn correspond to ~55,000 and ~70,000, respectively. Although the absolute number of these cell types is quite similar, an analysis by Zn probe fluorescence intensity indicates that glutamatergic neurons contain 2.3 more reactive Zn than astrocytes. With this technique we were able to demonstrate that the majority of reactive Zn content is concentrated in a subset of glutamatergic neurons in zebrafish brain. Thus, our data present a feasible quantitative method to measure the number of astrocytes and glutamatergic neurons containing Zn in the brain.

Key terms: reactive zinc; glutamatergic neurons; astrocytes; cytometry; zebrafish

INTRODUCTION

Zinc (Zn) is a metal found in the central nervous system (CNS) typically protein-bound (1-3). However, about 20% of total Zn in the brain is free or loosely bound to biomolecules (4), both corresponding to the reactive Zn pool susceptible to chelation. This reactive Zn in the brain has been investigated over decades (5). Furthermore, as the reactive Zn content is present in the brain of mammals (6,7), birds (8), reptiles (9) and fish (10,11), it is currently considered an essential component of brain homeostasis of vertebrates.

In the CNS, different neural cells may contain reactive Zn; in particular, glutamatergic neurons are the main cell type containing reactive Zn (12). The majority of this reactive Zn content is localized within the glutamatergic vesicles (13). Reactive Zn released by these vesicles may act on different excitatory postsynaptic receptors, mainly on glutamatergic NMDA-type receptors (12,14,15). Reactive zinc in glutamatergic neurons has also been found in mitochondria (16) and associated with metallothioneins in the perikaryon that can be released under excitotoxic conditions (17). Since reactive Zn is synaptically released, other cells are also susceptible to its effects, including astrocytes (12), which contain less reactive Zn than glutamatergic neurons (18). Astrocytes are able to uptake extracellular reactive Zn (19), which can regulate the function of astrocytic glutamate transporter, excitatory amino-acid transporter 1 (EAAT1) (20). During kainic acid-induced seizures, astrocytes may also uptake reactive Zn released by glutamatergic neurons (21), indicating an important role of these glial cells in controlling the reactive Zn pool.

Although investigations have been carried out to understand the neural role of reactive Zn, the total number of glutamatergic neurons and astrocytes containing Zn throughout the brain has never been quantified. Thus, it is not yet known how many

glutamatergic neurons and astrocytes may contribute to the pool of reactive Zn in the CNS. A better understanding of the number of Zn-containing cells could help the investigation of brain disorders associated with alteration in the reactive Zn levels (12). These issues could be addressed by developing a practical method to measure not only the total number of neural cells in the brain, but also the number of different cell types containing reactive Zn and its levels inside these cells.

Here, we describe a method by flow cytometry able to assess the total number of glutamatergic neurons and astrocytes in zebrafish (*Danio rerio*) brain, and their intracellular levels of reactive Zn, as a progression of a previous study from our group (11).

MATERIALS AND METHODS

Animals

Adult zebrafish (*Danio rerio*) of both sexes (4-7 months-old) were obtained from commercial distributor (Delphis, RS, Brazil). Animals were housed in an aquarium rack system (Zebtec, Tecniplast, Italy), at 14h light/10h dark cycle for at least 2 weeks prior to the experiments. Fish were fed twice a day with commercial flake fish food (alcon BASIC®, Alcon, Brazil) and once a day with *Arthemia sp*. Animal handling and experiments were approved by the Ethics Committee of Universidade Federal do Rio Grande do Sul (number 19780–CEUA). To dissect the whole brain, fish were cryoanesthetized and euthanatized by decapitation. Then, skin and skull were carefully removed to avoid any damage to the olfactory bulbs and telencephalon of zebrafish. Cranial nerves were then cut with a small scissors and brains were immediately transferred to tubes containing 0.3M phosphate-buffered saline (PBS, pH 7.4) with 1mM calcium ethylenediamine tetra acetic acid (Ca-EDTA) and kept at 4ºC for experimental proceedings.

Analysis of neural cells stained by fluorescent Zn probe using flow cytometry

Each brain was individually processed by mechanical dissociation (22) with a glass pasteur pipettes in PBS in order to obtain a suspension of neural cells from each individual animal. PBS with Ca-EDTA was used throughout the experiments to avoid the interference of free Zn in the medium or adsorbed to cell membranes. Each suspension of neural cells was filtered through a 40µm nylon mesh (Cell Filter Strainer-BD Biosciences) in order to retain particles bigger than dissociated cells. The cells were immediately bathed in PBS, with or without fixative solution (1% paraformaldehyde, PFA), for 20min at 4ºC. The samples were centrifuged at 1000g at 4°C for 10min. The pellets were suspended in permeabilization buffer containing 0.0001% Triton X-100 (Sigma, St. Louis, MO, USA) and 1% bovine serum albumin (BSA) in PBS for 20min at 22-24ºC. The specific immunostaining of astrocytes and glutamatergic neurons of zebrafish was performed by incubation with rabbit anti-glial fibrillary acidic protein (GFAP, Dako, Denmark A/S) or rabbit anti-vesicular glutamate transporter 1/2 (Vglut, Synaptic Systems, Germany), respectively. The primary antibodies were diluted (1:100) in permeabilization buffer and incubated for 1h at 22-24ºC. Samples were then rinsed with PBS and centrifuged as previously described. The supernatants were removed and pellets containing the cells were incubated in secondary fluorescent antibody Alexa fluor anti-rabbit 635 (Invitrogen Life Technologies; Carlsbad, CA) diluted in permeabilization buffer (1:200) at 22-24ºC. After 1h, the cells were washed in PBS and centrifuged at 1000g at 4°C for 10 min. The supernatants were discarded and the cells were incubated with the membrane-permeant fluorescent Zn probe, zinpyr-1 (ZP1, 20µM), diluted in PBS and 0.02% DMSO, for 30min at 22-24ºC. The cells were then washed in PBS and centrifuged at

1000g at 4°C for 10min. The cells in the pellet were suspended in PBS in order to evaluate, by a FACSCalibur flow cytometer (Becton-Dickinson, San Jose, CA), the percentage of cells stained by ZP1 (cell containing Zn), GFAP (astrocytes) and Vglut (glutamatergic neurons), as well as cells double labeled for GFAP and ZP1 (astrocytes containing Zn) or Vglut and ZP1 (glutamatergic neurons containing Zn). The mean fluorescence intensity (MFI) from ZP1 was also determined on each cell population. An aliquot of each sample was stained only with secondary antibody in order to set the negative region of the graph. The detection of ZP1 signals was obtained in FL1-H (530/30), and GFAP and Vglut signals were detected in FL4-H (661/16) band pass filters. Ten thousand events were acquired using Cell Quest software (Becton-Dickinson, San Jose, CA) and analyzed using FlowJo software (Tree Star, Inc).

In vivo exposure to membrane-permeant Zn chelator

To assess whether ZP1 retains sensitivity to stain reactive Zn in fixed cells, zebrafish were exposed to sodium diethyldithiocarbamate trihydrate (DEDTC) (Sigma, St. Louis, MO, USA) *in vivo*, which has been shown to be capable of chelating brain reactive Zn in this species (11). Animals were individually placed in beakers containing 5mM DEDTC in 400mL of reverse osmosis water supplemented with 0.018g/L of Instant Ocean® salt for 1h; control animals were kept in these same conditions, but without DEDTC. After, the brains were dissected and processed to analysis of ZP1 staining as described above.

Quantification of zebrafish brain total cells based on nuclear suspension

To determine the total number of cells in the zebrafish brain, each brain was individually prepared, based on Herculano-Houzel and Lent (23) for nuclear

quantification. Briefly, each whole brain was removed from skull and immediately immersed in 4% buffered PFA solution. After 24h post fixation, each fixed brain was weighed (3.87±0.46 mg tissue, *n* = 4) and homogenized mechanically with a 1 mL glass tissue homogenizer in PBS containing 0.0001% Triton X-100. This method allows the disruption of the plasmalemma, while maintaining intact the nuclear membrane (23,24). After total brain homogenization a centrifugation was performed at 4000g for 10min at 4°C in order to obtain the whole nuclei suspension. The supernatant was transferred into another tube, and pellet was suspended in homogenization buffer. Both fractions were incubated for 15min with 0.01% propidium iodide (Sigma, St. Louis, MO, USA), a fluorescent marker used to stain nucleus. The pellet and supernatant were separately stirred and 100µL aliquots were used for measure the number of nuclei in the flow cytometer. Fifty thousand events were analyzed and the PI signals were detected by flow cytometry in FL3-H (670LP).

Quantification of total cells and Zn-containing astrocytes, and Zn-containing glutamatergic neurons

The data from flow cytometry were used to calculate the total number of brain cells. The number of cells in each brain was estimated by the nuclear content in the pellet and in the supernatant obtained in the centrifugation (*n* = 4), using the following equations:

Pellet nuclear concentration X Total pellet volume = Total pellet nuclei *(p),*

Supernatant nuclear concentration X Total supernatant volume = Total supernatant nuclei *(s),*

Total number of brain cell = *p* + *s.*

To estimate the total number of astrocytes and glutamatergic neurons, with or without reactive Zn, the percentage of each cell population was multiplied by the mean of the total cells in the zebrafish brain.

Statistical analysis

The data were described as mean ± SEM. The effect of fixation on the number of neural populations was evaluated by independent samples Student's t-test. This same statistical test was applied to assess the Zn chelator effect on Zn probe signal. The effect of the fixative solution over time on MFI of ZP1 was evaluated by paired samples Student's *t*-test. The analysis on the percentage of positive cells and the MFI of ZP1 from cell populations was evaluated by one-way ANOVA followed by Tukey's *post hoc* test. All experiments were performed at least three times, and each brain was considered to $n = 1$. Statistical significance was determined at $p < 0.05$ level.

RESULTS

Standard conditions for analysis of Zn-containing cells from zebrafish brain

The quantification of the number of neural cells, with or without Zn, was performed as shown in the diagram in Fig. 1A. As reactive Zn could be exchanged among neural cells, this protocol was determined after obtaining the best conditions for analyzing the cells stained by intracellular Zn probe. As a first step, fresh and fixed (1% PFA) dissociated cells of the zebrafish brain were immunostained to identify astrocytes and glutamatergic neurons (Fig. 1B). Under both conditions, the astrocytes population was preserved, while a significant number of glutamatergic neurons were lost in the fresh preparation, compared to fixed condition. Therefore,

we performed the next experiments only in fixed cells. We also tested the ability of Zn probe MFI to remain stable in fixative solution for 6 hours (Fig. 1C), which was the time required to prepare the samples and to perform the incubations with the antibodies. As result, 1% PFA was able to keep the Zn signal bright for 6h. In addition, we tested the ZP1 sensitivity to reactive Zn in fixed cells using a membrane-permeant Zn chelating agent, DEDTC. The MFI of ZP1 signal significantly decreased (~45%) in neural cells from animals exposed to DEDTC compared to matched controls (Fig. 1D), indicating the ZP1 ability to detect changes in reactive Zn levels in cell fixed with 1% PFA. This protocol was subsequently used to evaluate the reactive Zn content of different cell populations in the brain.

Determination of cells containing reactive Zn in the zebrafish brain

The percentage of astrocytes and glutamatergic neurons, with or without ZP1 staining, are represented separately in the dot plots in Fig. 2A. From these analyses, 19.5% of the total brain cell population was ZP1 positive, 48% were astrocytes and 29.5% were glutamatergic neurons (Fig. 2B). When analyzing the double staining with ZP1 and specific cell-type markers, it was observed that the zebrafish brain had 6.5% of Zn-containing astrocytes and 8.5% Zn-containing glutamatergic neurons. ZP1 positive cells were more prevalent in glutamatergic neurons (28.5%) than astrocytes (13.5%) (Fig. 2B).

In order to estimate the absolute number of cells in the zebrafish brain, we used a suspension of cell nuclei (see Fig. 1A). We found that the zebrafish brain contains 841.68 ± 73.71 thousand cells (Table 1). Based on these total cell number and percentages of the two identified cell types, we estimated that the zebrafish brain contains 403.73 ± 32.76 thousand astrocytes and 247.87 ± 27.47 thousand glutamatergic neurons (Table 1). Furthermore, the number of astrocytes and

glutamatergic neurons containing reactive Zn were 54.42 ± 6.86 and 70.52 ± 10.01 thousand cells, respectively (Table 1).

Reactive Zn levels in different cell populations

The MFI of astrocytes (30.5 a.u.) was lower than the MFI of glutamatergic neurons (104.6 a.u.) (Fig. 3). Importantly, considering only the ZP1 positive cell population, the MFI of glutamatergic neurons was higher (333.2 a.u.) than the MFI of astrocytes (143.3 a.u.).

DISCUSSION

The identification of Zn-containing cells has previously been limited to the microscopic evaluation of histochemically stained brain regions. Accurate measurements of Zn levels were lacking (25). Here, we described a technique that enables the identification or specific sorting of Zn-containing cells in the zebrafish brain and the quantification of reactive Zn levels in astrocytes and neurons. We have validated and optimized this novel protocol to determine the Zn levels in both astrocytes and neurons. Our protocol worked best in cells fixed. Moreover, to prevent any artificial increment over the intracellular content of reactive Zn, membrane-impermeant Ca-EDTA based solutions were used. The addition of Ca-EDTA in physiological solutions is recommended in studies involving reactive Zn to minimize circumstantial Zn contamination (26), since it has a far higher affinity for transition metals (27). We show that our technique combined with the suspension of nuclei method to measure the total number of brain cells (23) provided a fast method to determine the number of cells containing Zn. Moreover, another important advantage is the small amount of samples, like the zebrafish brain, required for an accurate measurement of different cell types.

To test the applicability of this technique, we used the adult zebrafish brain. Our data show that these animals have more astrocytes than glutamatergic neurons in the brain. In contrast, the absolute number of Zn containing astrocytes and glutamatergic neurons were quite similar. Based on our data, we estimated that 2 every 7 glutamatergic neurons contain reactive Zn in the zebrafish brain, indicating that zebrafish has only a subset of glutamatergic neurons containing Zn, similar to other vertebrates (28). It has been published recently in other models that reactive Zn is present also in astrocytes, playing a role in glial-neuron signaling (18). Similarly, we found Zn-containing astrocytes in zebrafish brain, where 2 every 15 astrocytes contain reactive Zn. Interestingly, ~4% of all Zn-containing cells could not be identified as astrocytes or glutamatergic neurons. These could be other cells, such as GABAergic and glycinergic neurons, as seen in spinal cord of lamprey (29).

By measuring the intracellular levels of Zn in zebrafish brain we observed that glutamatergic neurons have more reactive Zn content in the brain than astrocytes. Accordingly, in previous study, we shown, by histochemical staining, high levels of reactive Zn in zebrafish brain regions containing glutamatergic neurons (11). However, here we were able to show for the first time the colocalization of glutamatergic neurons with substantial reactive Zn content in the zebrafish brain. Glutamatergic neurons of other vertebrates are known to contain also high level of reactive Zn stored in synaptic vesicles (30). Indeed, in the present study, we cannot determine the exact subcellular localization of the reactive Zn in these neurons, but the application of our protocol on different cellular fractions (e.g., synaptosomes) could meet this goal.

The samples prepared by this method may contain blood cells. We found that ~23% of the total cells were not identified as astrocytes or glutamatergic neurons; these remaining cells could be blood cells, other glial cells (e.g., oligodendrocytes,

microglia) or other neuronal types (e.g., GABAergic, serotonergic neurons). Future work could be performed to determine the incidence of blood cells in this preparation. Nevertheless, as this unidentified cell population was also considered in the measurement of total number cells in the brain, it is conceivable that the estimated Zn containing cells was not affected.

This study presents a novel method to accurately quantify astrocytes and glutamatergic neurons containing Zn in the zebrafish brain. This technique can be applied to other species to quantify the distribution of reactive Zn in glial and neuronal cells under physiological circumstances - physical exercise - and pathological conditions - ischemia and seizures -, where reactive Zn levels in neural cells are altered or even synaptically translocated (12, 31). Therefore, this is a fast method that can be used to measure not only the number of specific cells containing Zn, but also the intracellular levels of Zn.

ACKNOWLEDGEMENTS

This work was supported by Coordenação de Aperfeiçoamento de Pessoal de Nível Superior (CAPES), Conselho Nacional de Desenvolvimento Científico e Tecnológico (CNPq), INCT-Excitoxicidade e Neuroproteção and by FINEP research grant “Rede Instituto Brasileiro de Neurociência (IBN-Net)” # 01.06.0842-00. The authors declare no competing financial interests.

LITERATURE CITED

1. Frederickson CJ, Klitenick MA, Manton WI, Kirkpatrick JB. Cytoarchitectonic distribution of zinc in the hippocampus of man and the rat. Brain Res 1983;273:335-339.

2. Frederickson CJ, Rampy BA, Reamy-Rampy S, Howell GA. Distribution of histochemically reactive zinc in the forebrain of the rat. J Chem Neuroanat 1992;5:521-530.

3. Klitenick MA, Frederickson CJ, Manton WI. Acid-vapor decomposition for determination of zinc in brain tissue by isotope dilution mass spectrometry. Anal Chem 1983;55:921-923.

4. Cole TB, Wenzel HJ, Kafer KE, Schwartzkroin PA, Palmiter RD. Elimination of zinc from synaptic vesicles in the intact mouse brain by disruption of the ZnT3 gene. Proc Natl Acad Sci USA 1999;96:1716-1721.

5. Perez-Clausell J, Danscher G. Intravesicular localization of zinc in rat telencephalic boutons. A histochemical study. Brain Res 1985;337:91-98.

6. Garcia-Cairasco N, Wakamatsu H, Oliveira JA, Gomes EL, Del Bel EA, Mello LE. Neuroethological and morphological (Neo-Timm staining) correlates of limbic recruitment during the development of audiogenic kindling in seizure susceptible Wistar rats. Epilepsy Res 1996;26:177-192.

7. Chakravarty DN, Babb TL, Chung CK, Mikuni N. Bilateral kainic acid lesions in the rat hilus induce non-linear additive mossy fiber neoinnervation. Neurosci Lett 1997;230:175-178.

8. Faber H, Braun K, Zuschratter W, Scheich H. System specific distribution of zinc in the chick brain. A light- and electronmicroscopic study using the Timm method. Cell Tissue Res 1989;258:247-257.

9. Perez-Clausell J. The organization of zinc-containing terminal fields in the brain of the lizard Podarcis hispanica. A histochemical study. J Comp Neurol 1988;267:153-171.

10. Pinuela C, Baatrup E, Geneser FA. Histochemical distribution of zinc in the brain of the rainbow trout, Oncorhynchos myciss. I. The telencephalon. Anat Embryol 1992;185:379-388.

11. Braga MM, Rosemberg DB, de Oliveira DL, Loss CM, Córdova SD, Rico EP, Silva ES, Dias RD, Souza DO, Calcagnotto ME. Topographical analysis of reactive zinc in the central nervous system of adult zebrafish (Danio rerio). Zebrafish 2013;10:376-388.

12. Paoletti P, Vergnano AM, Barbour B, Casado M. Zinc at glutamatergic synapses. Neuroscience 2009;158:126-136.

13. Martinez-Guijarro FJ, Soriano E, Del Rio JA, Lopez-Garcia C. Zinc-positive boutons in the cerebral cortex of lizards show glutamate immunoreactivity. J Neurocytol 1991;20:834-843.

14. Peters S, Koh J, Choi DW. Zinc selectively blocks the action of N-methyl-D-aspartate on cortical neurons. Science 1987;236:589-593.

15. Westbrook GL, Mayer ML. Micromolar concentrations of Zn2+ antagonize NMDA and GABA responses of hippocampal neurons. Nature 1987;328:640-643.

16. Dittmer PJ, Miranda JG, Gorski JA, Palmer AE. Genetically encoded sensors to elucidate spatial distribution of cellular zinc. J Biol Chem 2009;284:16289-16297.

17. Frederickson CJ, Maret W, Cuajungco MP. Zinc and excitotoxic brain injury: a new model. Neuroscientist 2004;10:18-25.

18. Sekler I, Silverman WF. Zinc homeostasis and signaling in glia. Glia 2012;60:843-850.

19. Varea E, Alonso-Llosa G, Molowny A, Lopez-Garcia C, Ponsoda X Capture of extracellular zinc ions by astrocytes. Glia 2006;54:304-315.

20. Vandenberg RJ, Mitrovic AD, Johnston GA. Molecular basis for differential inhibition of glutamate transporter subtypes by zincions. Mol Pharmacol 1998;54:189-196.

21. Revuelta M, Castaño A, Machado A, Cano J, Venero JL. Kainate-induced zinc translocation from presynaptic terminals causes neuronal and astroglial cell death and mRNA loss of BDNF receptors in the hippocampal formation and amygdala. J Neurosci Res 2005;82:184-195.

22. Weiss SN, Pettenuzzo LF, Krolow R, Valentim LM, Mota CS, Dalmaz C, Wyse AT, Netto CA. Neonatal hypoxia-ischemia induces sex-related changes in rat brain mitochondria. Mitochondrion 2012;12:271-279.

23. Herculano-Houzel S, Lent R. Isotropic fractionator: a simple, rapid method for the quantification of total cell and neuron numbers in the brain. J Neurosci 2005;25:2518-2521.

24. Lee GM, Thornthwait JT, Rasch EM. Picogram per cell determination of DNA by flow cytofluorometry. Anal Biochem 1984;137:221-226.

25. Sindreu C, Storm DR. Modulation of neuronal signal transduction and memory formation by synaptic zinc. Front Behav Neurosci 2011;5:68.

26. Kay AR. Detecting and minimizing zinc contamination in physiological solutions, BMC Physiol 2004;4:4.

27. Smith RM, Martell AE. NIST Critically Selected Stability Constants of Metal Complexes Database. 7.0th edition. *Gaithersburg, MD, NIST*; 2003.

28. Sindreu CB, Varoqui H, Erickson JD, Pérez-Clausell J. Boutons containing vesicular zinc define a subpopulation of synapses with low AMPAR content in rat hippocampus. Cereb Cortex 2003;13:823-829.

29. Birinyi A, Parker D, Antal M, Shupliakov O. Zinc co-localizes with GABA and glycine in synapses in the lamprey spinal cord. J Comp Neurol 2001;433:208-221.

30. Frederickson CJ, Bush AI. Synaptically released zinc:physiological functions and pathological effects. Biometals 2001;14:353-366.

31. Toscano-Silva M, Gomes da Silva S, Scorza FA, Bonvent JJ, Cavalheiro EA, Arida RM. Hippocampal mossy fiber sprouting induced by forced and voluntary physical exercise. Physiol Behav 2010;101:302-308.

Figure Legends

Figure 1. (**A**)**,** Schematic representation of protocol steps performed to obtain the percentage of cells labeled with GFAP, Vglut, and ZP1, as well as the number of total cells of zebrafish brain. Bars in images represent 1 mm. (**B**)**,** Effect of the cell fixation on the percentage of astrocytes and glutamatergic neurons. A: total astrocytes; GN: total glutamatergic neurons (*n* = 6 - 8). (**C**)**,** Effect of fixative solution on the MFI of ZP1 in all dissociated cells of zebrafish brain. The samples were analyzed at 0 and 6h after cells dissociation (*n* = 4). (**D**)**,** Effect of 5mM DEDTC on the MFI of ZP1 in all dissociated cells of zebrafish brain (*n* = 8). * *p* = 0.0045; # *p* = 0.0316.

Figure 2. (**A**)**,** Representative dot plots from astrocyte marker GFAP (FL4-H) vs. Zn probe ZP1 (FL1-H) (I) and glutamatergic neuron marker Vglut (FL4-H) vs. Zn probe ZP1 (FL1-H) (II). (**B**)**,** Percentage of cells (*n* = 6 - 8) stained by Zn probe (ZP1), total astrocytes (A), total glutamatergic neurons (GN), and cells double stained for astrocytes and Zn probe (A+ZP1) and glutamatergic neurons and Zn probe (GN+ZP1). Distinct letters indicate statistical differences. ZP1 x A, A x A+ZP1, A x GN+ZP1 and A+ZP1 x GN, *p* = 0.0001; GN x GN+ZP1, *p* = 0.0002; A x GN, *p* = 0.0007; ZP1 x A+ZP1, *p* = 0.0209.

Figure 3. Mean fluorescence intensity (MFI) from ZP1 (*n* = 6 - 8) in dissociated cells (total cells), ZP1 positive cells (ZP1), total astrocytes (A), total astrocytes ZP1 positive cells (A+ZP1), total glutamatergic neurons (GN), and total glutamatergic neurons ZP1 positive cells (GN+ZP1). Distinct letters indicate statistical differences. Total cell x ZP1, Tota cells x GN+ZP1, ZP1 x A, ZP1 x GN, A x A+ZP1, A x GN+ZP1, A + ZP1 x GN+ZP1 and GN x GN+ZP1, *p* = 0.0001; ZP1 x A+ZP1, *p* =

0.0002; Total cell x A+ZP1, p = 0.0005; ZP1 x GN+ZP1, p = 0.0040; A x GN, p = 0.0192.

Table 1. Cell populations of zebrafish brain, with or without reactive Zn

	Mean ± SEM
n cells ($x10^3$)	841.68 ± 73.71
Cells ($x10^3$)/mg	230.39 ± 34.92
Percentage of $ZP1^+$ cells	19.48 ± 2.94
n cells containing reactive Zn ($x10^3$)	163.96 ± 24.77
Cells containing reactive Zn (10^3)/mg	42.37 ± 6.40
Percentage of $GFAP^+$ cells	47.97 ± 3.89
n astrocytes ($x10^3$)	403.73 ± 32.76
Astrocytes ($x10^3$)/mg	105.55 ± 8.56
Percentage of $GFAP^+$ and $ZP1^+$ cells	6.47 ± 0.82
n astrocytes containing reactive Zn ($x10^3$)	54.42 ± 6.86
Astrocytes containing reactive Zn (10^3)/mg	14.23 ± 1.79
Percentage of $Vglut^+$ cells	29.45 ± 3.26
n glutamatergic neurons ($x10^3$)	247.87 ± 27.47
Glutamatergic neurons (10^3)/mg	64.80 ± 7.18
Percentage of $Vglut^+$ and $ZP1^+$ cells	8.38 ± 1.19
n glutamatergic neurons containing reactive Zn ($x10^3$)	70.52 ± 10.01
Glutamatergic neurons containing reactive Zn (10^3)/mg	18.44 ± 2.62

The data were obtained by analysis of 4-6 individual brains.

FIGURE 1

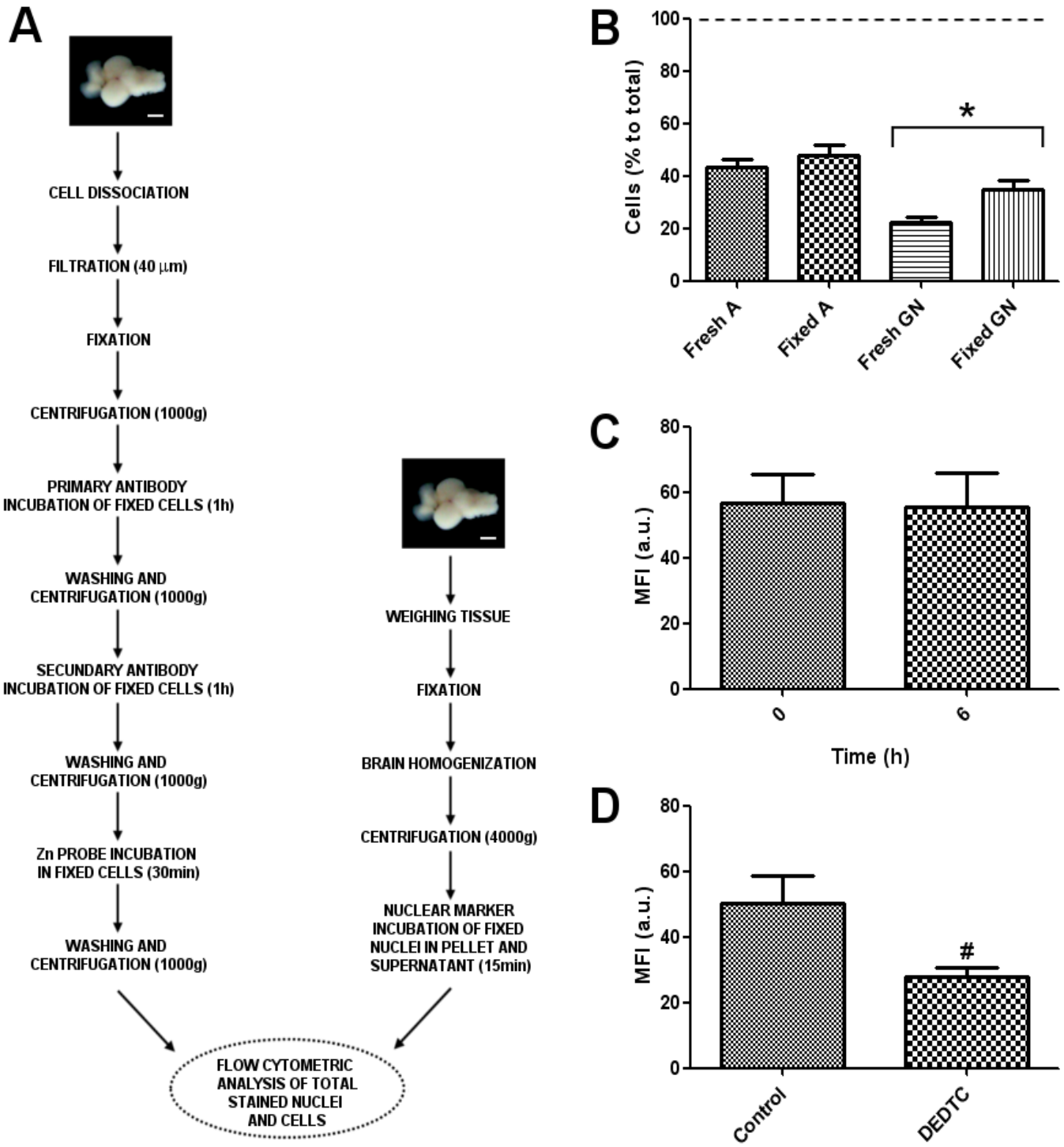
A
CELL DISSOCIATION
FILTRATION (40 μm)
FIXATION
CENTRIFUGATION (1000g)
PRIMARY ANTIBODY INCUBATION OF FIXED CELLS (1h)
WASHING AND CENTRIFUGATION (1000g)
SECUNDARY ANTIBODY INCUBATION OF FIXED CELLS (1h)
WASHING AND CENTRIFUGATION (1000g)
Zn PROBE INCUBATION IN FIXED CELLS (30min)
WASHING AND CENTRIFUGATION (1000g)
WEIGHING TISSUE
FIXATION
BRAIN HOMOGENIZATION
CENTRIFUGATION (4000g)
NUCLEAR MARKER INCUBATION OF FIXED NUCLEI IN PELLET AND SUPERNATANT (15min)
FLOW CYTOMETRIC ANALYSIS OF TOTAL STAINED NUCLEI AND CELLS
B
Cells (% to total)
100
80
60
40
20
0
*
Fresh A
Fixed A
Fresh GN
Fixed GN
C
MFI (a.u.)
80
60
40
20
0
0
6
Time (h)
D
MFI (a.u.)
80
60
40
20
0
#
Control
DEDTC

FIGURE 2

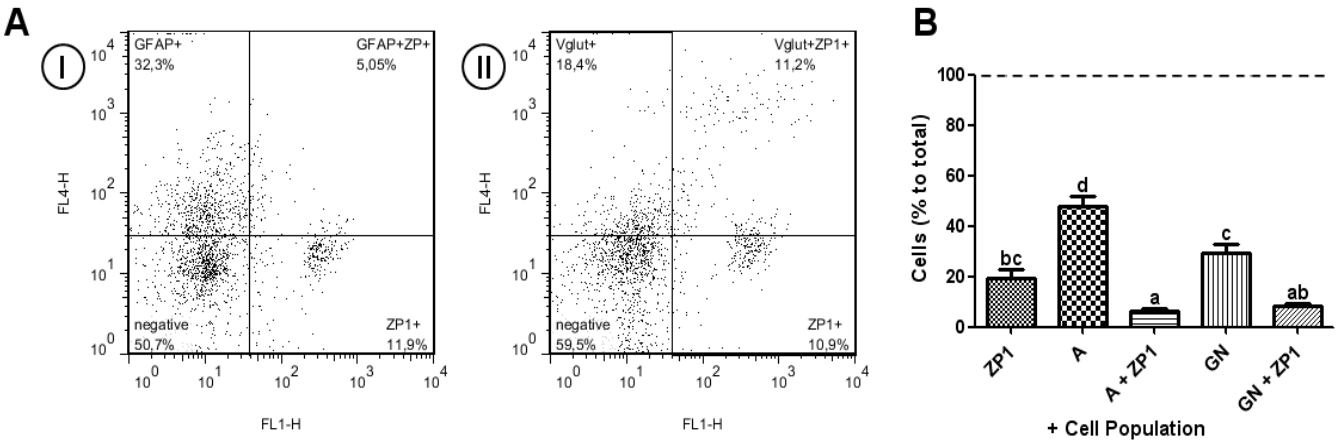
A
I
GFAP+
32,3%
GFAP+ZP+
5,05%
negative
50,7%
ZP1+
11,9%
FL4-H
FL1-H
II
Vglut+
18,4%
Vglut+ZP1+
11,2%
negative
59,5%
ZP1+
10,9%
FL4-H
FL1-H
B
Cells (% to total)
100
80
60
40
20
0
bc
d
a
c
ab
ZP1
A
A + ZP1
GN
GN + ZP1
+ Cell Population

FIGURE 3

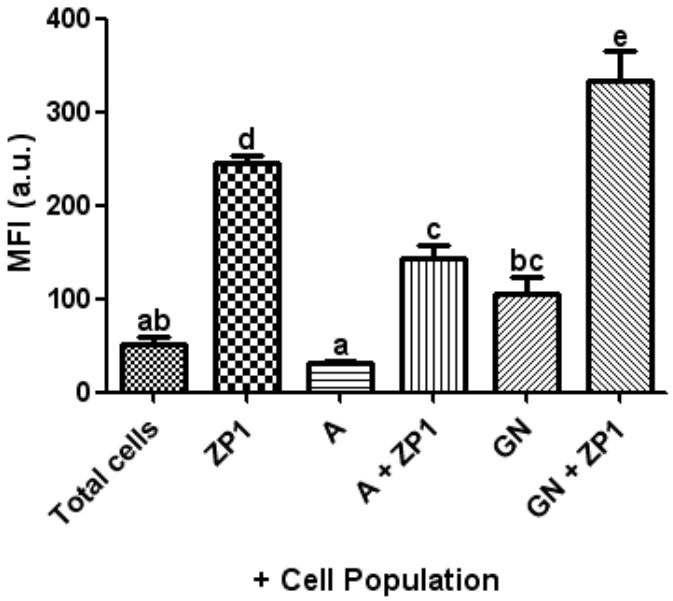
400
300
200
100
0
MFI (a.u.)
ab
d
a
c
bc
e
Total cells
ZP1
A
A + ZP1
GN
GN + ZP1
+ Cell Population

CAPÍTULO III

Diethyldithiocarbamate induces behavioral impairment and chelation of brain reactive Zn in adult zebrafish

Artigo a ser submetido ao periódico *Toxicology*

Diethyldithiocarbamate induces behavioral impairment and chelation of brain reactive Zn in adult zebrafish

Marcos M. Braga,[a,b,] Emerson S. Silva,[a,b] Eduardo P. Rico,[a,b] Leticia F. Pettenuzzo,[a] Diogo L. Oliveira,[a,b,c] Renato D. Dias,[a,b] Maria Elisa Calcagnotto,[a,b] Robert L. Tanguay,[d] Diogo O. Souza,[a,b,c] Denis B. Rosemberg [b,c,e]*

[a] *Programa de Pós-graduação em Bioquímica, Departamento de Bioquímica, Instituto de Ciências Básicas da Saúde, Universidade Federal do Rio Grande do Sul, Porto Alegre 90035-003,Brazil.*

[b] *Instituto Nacional de Ciência e Tecnologia em Excitotoxicidade e Neuroproteção (INCT-EN), Porto Alegre 90035-003,Brazil.*

[c] *Zebrafish Neuroscience Research Consortium (ZNRC).*

[d] *Department of Environmental and Molecular Toxicology, the Environmental Health Sciences Center, Oregon State University, Corvallis 97331, USA.*

[e] *Laboratório de Genética e Ecotoxicologia Molecular, Programa de Pós-graduação em Ciências Ambientais, Área de Ciências Exatas e Ambientais, Universidade Comunitária da Região de Chapecó, Chapecó 89809-000,Brazil.*

* Marcos M. Braga

Departamento de Bioquímica, Instituto de Ciências Básicas da Saúde

Universidade Federal do Rio Grande do Sul

Rua Ramiro Barcelos, 2600-anexo

Zip code: 90035-003

Porto Alegre - RS - Brazil.

Phone: (55-51) 33085555

Fax: (55-51) 33085540

E-mail address: **marcosmbraga@gmail.com**

Abstract

Diethyldithiocarbamate (DEDTC) is a controlled compound used in clinical trials for cancer therapy and experimental studies of hypoxia. However, high DEDTC concentrations can affect different cellular mechanisms in the brain, inducing potential neurotoxic effects. In this concern, little is known about the contribution of the chelation of zinc (Zn) in DEDTC-induced neurotoxicity. Here we evaluate the effects of high DEDTC concentrations on behavior and brain Zn content in adult zebrafish. Animals were acutely exposed to DEDTC (0.2, 1, 5 mM in home tank water) for 1h and their behaviors were evaluated during the exposure period. Afterwards, the brains were excised to measure the levels of DEDTC and the content of reactive Zn in total brain, glutamatergic neurons and astrocytes. Moreover, we also measured the Zn-dependent activity of δ-aminolevulinate dehydratase (δ-ALA-D). Seizure-like behavior was observed at 1 and 5 mM DEDTC and mortality occurred only when fish were exposed to 5 mM DEDTC. Brain content of DEDTC was detectable at 1 and 5 mM (above 100 $mg.kg^{-1}$ tissue). The amount of reactive Zn was reduced after exposure to 1 and 5 mM DEDTC. Analysis of glutamatergic neurons indicated a decrease of reactive Zn at 1 and 5 mM, while 0.2 and 5 mM reduced Zn content in astrocytes. Additionally, DEDTC did not change brain δ-ALA-D activity. In conclusion, our results showed that high concentrations of DEDTC induce behavioral impairment in zebrafish, which could be related to the reactive Zn chelation in the brain.

Keywords: brain; δ-aminolevulinate-dehydratase; diethyldithiocarbamate; reactive Zn; zebrafish

1. Introduction

Dithiocarbamates are organosulfur compounds widely used in agriculture as pesticides to treat crops and seeds (Rath et al., 2011). However, they are also toxic to vertebrates, leading to body axis abnormalities (Tilton et al., 2006) and hormonal dysfunctions (Houeto et al., 1995; Cooper et al., 1999). Due to the prominent toxicity, the use of dithiocarbamates has been regulated in several countries by limiting the tolerable levels detected in crops (ANVISA, 2005; EU, 2001; U.S. EPA, 2004). As a result, the agricultural use of some dithiocarbamates have been canceled (ANVISA, 2005; U.S. EPA, 2005). However, despite all the precautions, these substances can be significantly detected in diet and blood samples of humans (Brugnone et al., 1993; Caldas et al., 2006).

In particular, the diethyldithiocarbamate (DEDTC) is important in agriculture, but studies have drawn the attention to its protective properties to treat diseases such as, HIV (Pang et al., 2007) and cancer (Qazi et al., 1988; Cvek and Dvorak, 2007). Although these reports have substantially contributed to the clinical application of DEDTC, little consideration has been taken to its side effects frequently observed at high DEDTC concentrations.

Similar to other dithiocarbamates, DEDTC has a neurotoxic action in the central nervous system (CNS), inducing myelin injury (Tonkin et al., 2004), and changes on dopamine uptake (Di Monte et al. 1989). However, with the ability to chelate divalent metals (Rigas et al., 1979), DEDTC can affect the pool of reactive zinc (chelatable Zn) co-localized in a subset of glutamatergic neurons (Paoletti et al., 2009). This reactive Zn can be released at synaptic cleft, acting as a neuromodulator of excitatory receptors (Paoletti et al., 2009) in distinct vertebrate classes. Consequently, the effects of DEDTC on reactive Zn content can trigger important changes on behavior and brain homeostasis.

An interesting strategy to study the neurotoxicity of DEDTC is the use of zebrafish (*Danio rerio*) as experimental model. As an emergent model system, zebrafish presents attractive features for toxicological research such as low cost, easy maintenance, and abundant offspring (Kalueff et al., 2014). In particular, the cellular Zn transporters have been recently characterized, showing a high degree of similarity with their mammalian counterparts (Ho et al., 2012). Moreover, the topographical characterization of reactive Zn in zebrafish have shown the presence of this metal throughout the CNS (Braga et al., 2013), suggesting that Zn could play a role for brain homeostasis in this species. These features make the zebrafish an appropriate model system to investigate the acute effect of DEDTC on behavior and also on the pool of reactive Zn in the CNS.

In the present study, we evaluated the behavioral profile and brain Zn content in adult zebrafish after acute DEDTC exposure at high concentrations. In order to associate the behavioral findings with potential changes of the levels of reactive Zn, we performed the measurement of DEDTC amounts in brain and detected the presence of reactive Zn in brain regions and its location in glutamatergic neurons and astrocytes. Finally, we also measured the Zn-dependent activity of δ-aminolevulinate dehydratase (δ-ALA-D) in zebrafish brain.

2. Materials and Methods

2.1. Zebrafish

Male and female (50:50 ratio) wild-type adult zebrafish (4–7 months-old) of short-fin phenotype were obtained from commercial distributor (Delphis, RS, Brazil). Fish were kept in an aquarium rack system (Zebtec, Tecniplast, Italy) at 27 ± 1ºC under a light/dark cycle of 14/10 h (lights on at 7:00 am) for at least 2 weeks prior to

the experiments. Animals were fed twice a day with commercial flake fish food (alcon BASIC®, Alcon, Brazil). All experiments were performed using reverse osmosis water supplemented with 0.018mg/L Instant Ocean® salt. Experimental procedures were conducted in accordance with National Institute of Health Guide for Care and Use of Laboratory Animals. The experimental protocols were approved by the Ethics Committee of Universidade Federal do Rio Grande do Sul (number 19780 – CEUA).

2.2. DEDTC exposure

Animals were individually placed in beakers containing 400 mL of sodium DEDTC trihydrate (Sigma, St. Louis, MO, USA) solution for 1 h at 28ºC. Experimental groups consisted in (i) Control (home tank water), (ii) DEDTC 0.2 mM, (iii) DEDTC 1 mM, and (iv) DEDTC 5 mM. Both DEDTC concentrations and exposure period were based on recent studies that evaluated the potential protective effects of this compound in zebrafish (Knockaert et al., 2012; Skovgaard and Olson, 2012). Matched controls were simultaneously performed with DEDTC exposure groups. DEDTC was prepared daily, dissolved in home system water.

2.3. Behavior evaluation

The main zebrafish behaviors were recorded using a video camera (Sony Handycam DCR-SX22 SD) and further analyzed by two independent trained blind observers during the DEDTC exposure period. The behavioral manifestations were expressed at 1 min intervals, which were determined by the main behaviors of the animal. According the zebrafish behavioral catalog (Kalueff et al., 2013), each behavior was determined as follows: 0, normal behavior (regular exploration of the apparatus); 1, burst movements (rapid changes of swimming direction); 2, seizure-

like behavior (or corkscrew-like swimming); 3, loss of posture; 4, death (see **Supplementary video S1**). After each exposure, the fish were cryoanestethized and euthanatized by decapitation in order to remove the whole brain for further analyses. Throughout the experiments, care was taken to move fish gently between home tanks and beakers and the solutions were replaced after each trial. All fish were handled and tested in a similar way and the behaviors were recorded in the same room, which kept the manipulation, water quality, and illumination uniform and constant between trials. Fish that died during the exposure period were not used for further biochemical experiments.

2.4. Measurement of DEDTC levels in the brain

The levels of DEDTC were measured using a spectrophotometric method to quantify Zn (Uddin et al., 2013), in which the reaction of DEDTC with Zn yields a white complex. As the $Zn(DEDTC)_2$ complex is somewhat stable, a displacement reaction was performed by addition of Cu, yielding a yellow complex measured colorimetrically. The calibration curve consisted of 1.2 mM $CuSO_4$ added at the DEDTC concentrations, both dissolved in dimethyl sulfoxide (DMSO, Sigma, St. Louis, MO, USA). The linear calibration range was 6.6 - 99µg/mL of DEDTC with the regression coefficient (*r*) 0.993 (see **Supplementary fig. S1**). For this protocol, we used a pool of 6 whole brains for each independent sample, which were weighed and homogenized in DMSO containing 1.2 mM $CuSO_4$. In order to isolate the $Cu(DEDTC)_2$ complex, samples were centrifuged at 15.000g at 20°C for 10 min. Then, the yellow supernatants were transferred to 96-well microplates and the absorbance was read at 435 nm. The blank samples were from unexposed animals and the results were expressed in mg of DEDTC per kg of brain tissue.

2.5. Histochemical and quantification of reactive Zn

Histochemical staining of reactive Zn was performed using the Neo-Timm method previously described for zebrafish brain (Braga et al., 2013). After the exposure period, brains were excised and immersed in 3% glutaraldehyde mixed to 0.1M phosphate buffer (pH 7.4) for 24 h, and then transferred to sodium sulfide solution (1% Na_2S) in 0.12M Millonig's buffer for 24 h. Coronal (30-µm-thick) slices were cut in a vibroslicer (VTS-1000;Leica), and mounted on slides. For histochemical staining of reactive Zn, the slices were incubated in a solution containing silver. The reaction was carried out in the dark, and only ultrapure and metal-free reagents were used. Images were captured by NIS Elements AR 2.30 software (Nikon) using the same parameters with a light microscope (Nikon Eclipse E-600) coupled with a camera (Nikon DXM1200C CCD). Quantification of Neo-Timm was performed by analyzing the total area stained for each CNS region under 10x magnification. Images were converted to 8-bit gray scale and the optic density was quantified using ImageJ 1.37v software.

2.6. Flow cytometric analysis of reactive Zn in neural cells

Zinc content analysis in nervous tissue was based in Malavolta et al. (2006). Brain cell suspensions (**Fig. 4A**) were obtained by mechanical dissociation with phosphate-buffered saline (PBS, pH 7.4) containing 1 mM ethylenediamine tetraacetic acid (EDTA). To avoid possible interferences due to free Zn in the medium and adsorbed to the cell membrane, EDTA was used throughout the experiment. Cells were filtered through a 40 µm nylon mesh (Cell Filter Strainer-BD Biosciences) and incubated with PBS containing 1% paraformaldehyde at 4°C for 20 min. Samples were centrifuged at 1.000g at 4°C for 10 min. The supernatants were discarded and the cells were suspended in permeabilization buffer containing 1%

bovine serum albumin (BSA) and 0.0001% triton X-100 (Sigma, St. Louis, MO, USA) in PBS for 20 min at room temperature. Cells were processed for specific immunostaining of glutamatergic neurons and astrocytes using rabbit anti-vesicular glutamate transporter 1/2 (Vglut, 1:100, Synaptic Systems, Germany) and rabbit anti-glial fibrillary acidic protein (GFAP, 1:100, Dako, Denmark A/S), respectively. Antibodies were diluted in permeabilization buffer and incubated for 1h at room temperature. Cells were then washed (1x) with PBS and centrifuged as above. The supernatants were removed and the cells were bathed in secondary fluorescent antibody Alexa fluor anti-rabbit 635 (1:200, Invitrogen Life Technologies; Carlsbad, CA) diluted in permeabilization buffer, being further incubated for 1h at room temperature. The cells were rinsed (1x) with PBS and centrifuged as mentioned above. The supernatants were removed and the cells were incubated with 20 μM of the membrane permeable Zn fluorescent probe, Zinpyr-1 (ZP1), diluted in 0.02% DMSO and PBS. After 30 min, the cells were rinsed (1x) in PBS and centrifuged as previously described. The cells were suspended in PBS for analysis of the relative fluorescence using a FACSCalibur flow cytometer (Becton-Dickinson, San Jose, CA). Controls stained only with secondary antibody were used to set the negative region of the graph. Signals from ZP1 were detected in FL1 (530/30) and Vglut, and GFAP were detected in FL4 (661/16) band pass filters. The events (10.000) were collected using Cell Quest software (Becton-Dickinson, San Jose, CA) and data were analyzed using FlowJo software (Tree Star, Inc).

2.7. *δ-ALA-D activity*

The enzyme activity was determined as previously described by Sassa (1982) and Braga et al. (2012). Briefly, a pool of 5 whole brains was used for each sample, which was homogenized in 0.9% NaCl (1:5). The homogenate was centrifuged

(4.000g at 4°C for 10 min) and the supernatant (100ug per assay) was used for enzyme assay. The δ-ALA-D activity was measured in a medium containing 3 mM δ-aminolevulinic acid (Sigma, St. Louis, MO, USA) and 80 mM potassium phosphate buffer, pH 6.8, at 37 °C for 2 h. The product of reaction, porfobilinogen (PBG), was determined using Ehrlich's reagent at 555 nm, with molar absorption coefficient of 6.1×10^4 M^{-1}. The experimental conditions for measuring the δ-ALA-D activity in zebrafish brain were previously investigated. Protein concentration and time of incubation were chosen in order to maintain the linearity of reaction and saturating amounts of substrate were used (data not shown). Protein content was measured according to Lowry et al. (1951) using BSA as standard. Results were expressed in ηmol of PBG per mg of protein per h.

2.8. Statistical analysis

Non-parametric data of observed phenotypes were expressed as median ± interquartile range and the analysis of variance across time was performed by Friedman test followed by Dunn's Multiple Comparison test. The correlation between the main phenotype and DEDTC concentrations was assessed with the non-parametric Spearman's rank correlation test. All other data were described as means ± S.E.M., and statistical comparisons were performed using one-way ANOVA followed by Tukey's test as post hoc. The relationship between these parametric data and DEDTC concentrations was evaluated by linear regression analysis. Statistical significance was set at $p < 0.05$ level.

3. Results

3.1. Effect of DEDTC on behavior

The quantitative analysis of behaviors showed that DEDTC exposure induced significant behavioral impairments during 60 min ($p < 0.0001$), which were strongly correlated to DEDTC concentration ($r = 0.949$, $p = 0.042$) (**Fig. 1A**). The representative analysis showed that control fish exhibited normal behavior consisted by spontaneous short swims during the test (**Fig. 1B**). Fish immersed in 0.2 mM DEDTC also showed no significant changes on behavior (**Fig. 1C**). In contrast, 1 mM DEDTC (**Fig. 1D**) produced behavioral changes after ~4 min of exposure, in which animals displayed burst movements up to the ~16th min. After this period, the fish reestablished normal swimming up to ~39 min of exposure, when they exhibited seizure-like behavior in alternation with erratic movements, maintaining these effects up to 60 min. The behavioral effects of DEDTC were more pronounced at 5 mM (**Fig. 1E**). At this concentration, after ~2 min, we observed burst movements that extended up to the 5th min. After normal behavior, fish performed seizure-like behavior along with burst movements from the 17th to the 37th min. In ~49 min, the animal exhibited a persistent loss of body posture, leading to death in the end of the trial.

3.2. DEDTC brain accumulation

Animals exposed to 0.2 mM presented brain DEDTC levels below the detection limit (**Table 1**). However, animals immersed into 1 and 5 mM DEDTC solutions presented substantial brain accumulation of the compound that reached values of 113.8 and 960.2 mg.kg^{-1} tissue, respectively. In addition, brain amounts of DEDTC were strongly correlated to the exposure concentrations ($r = 0.987$, $p = 0.001$).

3.3. Effects of DEDTC on reactive Zn distribution in the brain

DEDTC exposure substantially affected the levels of reactive Zn in zebrafish brain (**Fig. 2**). In the midbrain, fish exposed to 0.2 mM DEDTC exhibited a slight change in the content of reactive Zn in the optic tectum (**Fig. 2B, 2F and 2J**). In contrast, 1 mM (**Fig. 2C, 2G and 2K**) and 5 mM (**Fig. 2D, 2H and 2L**) DEDTC induced a prominent decrease in the amount of reactive Zn throughout the brain. These results were further confirmed by optic density quantification (**Fig. 3**) and the periventricular gray zone (PGz) (showed in **Figs. 2I-2L**) had its abundant reactive Zn content significantly decreased after 1 and 5 mM DEDTC exposure. A moderate association between PGz optic density and DEDTC concentrations was confirmed by linear regression (r = - 0.566, p = 0.045). Moreover, Neo-Timm analysis showed a normal staining pattern throughout the brain excluding the possibility of cytoarchitectonic re-distribution of reactive Zn after DEDTC exposure.

3.4. Reactive Zn in glutamatergic neurons and astrocytes

As shown in the **Fig. 4B** a significant decrease in the mean fluorescence intensity (MFI) of neural cells from animals exposed to 1 and 5 mM DEDTC was detected, which were moderately associated (r = - 0.407, p = 0.032). To determine the neural cell types affected by DEDTC, we assessed the reactive Zn content in glutamatergic neurons and astrocytes (immunostaining with Vglut and GFAP, respectively). Flow cytometry analysis showed a moderately strong association between reactive Zn of glutamatergic neurons and DEDTC concentrations (r = - 0.649, p = 0.001). Both 1 mM and 5 mM DEDTC decrease Zn content of these cells at 28 and 40%, respectively (**Fig. 4C**). The astrocytes had lower content of reactive Zn in comparison to glutamatergic neurons (data not shown), but they also presented sensitivity to DEDTC. DEDTC (at 0.2 and 5 mM) decreased the astrocyte levels of reactive Zn (35 and 32%, respectively), whereas exposure to 1 mM

presented similar results to control group (**Fig. 4D**). In addition, there was a trend for a mild association between reactive Zn of astrocytes and DEDTC concentrations (r = - 0.325, p = 0.085).

3.5. Evaluation of δ-ALA-D activity

In order to investigate a possible additional effect of DEDTC on the fraction of Zn strongly bound to biomolecules, we evaluated the Zn-dependent activity δ-ALA-D in zebrafish brain. As shown in **Table 2**, DEDTC did not significantly change the enzyme activity, indicating no association between these variables (r = 0.157, p = 0.463).

4. Discussion

The restriction to the use of dithiocarbamates has been increased due its toxic effects to vertebrates. Their clinical application has called the attention since the adverse effects have been quite neglected. In particular, the use of high DEDTC concentrations as neuroprotective drug has rarely addressed its strong chelating action, which could affect the pool of Zn in the brain that is crucial for the CNS homeostasis (Paoletti et al., 2009). Indeed, the exposure of zebrafish to high DEDTC concentrations induced behavioral changes and alterations in brain Zn content, more specifically in its reactive fraction in glutamatergic neurons (**Fig. 5**). Moreover, the severity of these effects was significantly correlated to the DEDTC concentrations. These findings allow us to establish future DEDTC concentrations with lower side effects for zebrafish.

It is remarkable that only few clinical studies have evaluated the behavioral effects of high DEDTC concentrations. Here, we observed that 5 mM DEDTC induced loss of posture and death, while 1 mM DEDTC caused burst movements

and seizure-like behaviors. Studies have reported a decrease of locomotor activity (Domínguez et al., 2003; Foresti et al., 2008) and the occurrence of seizure-like behavior (Blasco-Ibáñez et al., 2004) in rodents, suggesting that high DEDTC concentrations may act as a proconvulsant (Mitchell and Barnes, 1993; Domínguez et al., 2003). Interestingly, Haycock et al. (1978) have demonstrated an electrographic recording of seizures induced by high DEDTC concentration in rat, which also suggest a convulsant effect. Thus, as we observed seizure-like behavior, similar to that induced by common convulsant agents in zebrafish (Baraban et al., 2005; Tiedeken and Ramsdell, 2010; Alfaro et al., 2011; Mussulini et al., 2013), more precaution should be taken with the use of high DEDTC concentrations.

The abnormal behavior is a prominent consequence of DEDTC exposure, since it is able to cross the blood-brain barrier affecting the CNS (Guillaumin et al., 1986). In fact, we showed, for the first time, that behavioral changes caused by exposure to high DEDTC concentrations were associated with its accumulation in the zebrafish brain. Moreover, histochemical and flow cytometry analyses revealed that these effects were associated to a reduction (~40%) in the brain reactive Zn content. Given the ability of DEDTC to chelate the pool of reactive Zn in the brain (Foresti et al., 2008), our data strongly suggests that this action can have been played in the neurotoxic effects observed. Interestingly, brain clearance of reactive Zn by DEDTC has been associated with behavioral impairment in rodents, attributed the proconvulsant effect (Mitchell and Barnes, 1993; Domínguez et al., 2003; Blasco-Ibáñez et al., 2004). Accordingly, our results showed that DEDTC had the chelating effect over Zn only in concentrations that induced behavioral changes, such as seizure-like behavior.

Since a subset of glutamatergic neurons have high reactive Zn content (Paoletti et al., 2009), these cells are possibly the most affected by DEDTC. According to our

data, the glutamatergic neurons showed a significant reduction of intracellular content of reactive Zn after exposure to 1 mM and 5 mM DEDTC. The decrease of reactive Zn levels in glutamatergic neurons has been associated to seizure susceptibility in rats treated with a Zn-deficient diet (Takeda et al., 2003) and in vesicular Zn transporter knockout mice (Cole et al., 2000). Our results also support an important role of the Zn content in glutamatergic neurons on the behavioral manifestations induced by high concentrations of DEDTC. Thus, the effects of DEDTC could have implication on the dyshomeostasis of neural network, since reactive Zn released from glutamatergic neurons can modulate neighboring neural cells, including astrocytes (Paoletti et al., 2009). Although astrocytes have substantially lower reactive Zn content than the glutamatergic neurons (Sekler and Silverman, 2012), we have observed that glial cells had a reduction of ~35% in the pool of reactive Zn after exposure to 0.2 mM and 5 mM DEDTC. Another study has also shown that DEDTC decreases the levels of intracellular reactive Zn in these cells (Sekler and Silverman, 2012). In contrast, the astrocyte content of reactive Zn after exposure to 1 mM DEDTC was similar to control. Because these cells can capture extracellular Zn ions (Varea et al., 2006), this result suggests a possible metal uptake from other sources. In fact, the Zn uptake of astrocytes from glutamatergic neurons could be the reason for the increased amount of reactive Zn in glial cells at 1 mM DEDTC, as occurs in seizures induced by kainic acid (Revuelta et al., 2005). Therefore, our data demonstrate that high DEDTC concentrations cause a distinct neurotoxic effect on the reactive Zn content in both cell types.

Considering that DEDTC altered the pool of reactive Zn in the brain, we sought to investigate whether other fractions of Zn could also be affected. The δ-ALA-D is a highly conserved enzyme containing Zn rigidly associated to the molecular structure, but high concentrations of Zn chelator may inactivate its activity (Emanuelli et al.,

1998). Although the effect of DEDTC on the CNS Zn-dependent activity of δ-ALA-D is still unknown, our data showed no changes in the enzyme activity of zebrafish brain after DEDTC exposure. Studies in rats showed that DEDTC did not alter δ-ALA-D activity in other tissues, such as blood and hepatic tissue (Khandelwal et al., 1987). Further investigation is necessary to clarify whether high concentrations of DEDTC are unable to mobilize the pool of tightly bond metals in the CNS. Importantly, it is reasonable to affirm that the neurotoxic effects of DEDTC described here are associated with the chelation of reactive Zn rather than chelation of Zn strongly associated with biomolecules.

Our data showed the toxicological effects of high DEDTC concentrations. A clinical study performed by Qazi and colleagues (1988) determined 150 $mg.kg^{-1}$ as the limit for toxic effects of DEDTC. In our study, DEDTC showed to have few neurotoxic effects only at 0.2 mM (or < $100mg.kg^{-1}$ brain tissue). In this same line, previous studies have shown that this concentration of DEDTC can be beneficial against several disorders (Pang et al., 2007; Daocheng and Mingxi, 2010). Moreover, neuroprotective effects of 0.25 mM DEDTC have been reported in an experimental model of hypoxia in zebrafish (Yu and Li, 2013). However, we emphasize that further studies are required in order to indicate an appropriate protective concentration of DEDTC in CNS. In summary, our results provide the first evidence of the relationship between the potential Zn chelating action in the brain with the mechanisms underlying the neurotoxicity of high DEDTC concentrations in zebrafish. Since DEDTC may chelate other metals (e.g., copper) or even impair function of other molecular targets and non-brain structures, additional studies may be required to better elucidate its toxicological effects. However, in future pharmacological studies, it is crucial to consider the high concentration-side effects of DEDTC.

Acknowledgements

This work was supported by Coordenação de Aperfeiçoamento de Pessoal de Nível Superior (CAPES), Conselho Nacional de Desenvolvimento Científico e Tecnológico (CNPq), INCT-Excitoxicidade e Neuroproteção and by FINEP research grant “Rede Instituto Brasileiro de Neurociência (IBN-Net)” # 01.06.0842-00.

Conflict of Interest Statement

There are no conflict of interest.

References

Alfaro, J.M., Ripoll-Gómez, J., Burgos, J.S., 2011. Kainate administered to adult zebrafish causes seizures similar to those in rodent models. Eur. J. Neurosci. 33, 1252-1255.

ANVISA, 2005. Agencia Nacional de Vigilância Sanitária. Ministério da Saúde. Monografias Autorizadas de Agrotóxicos. Available: http://portal.anvisa.gov.br/wps/content/Anvisa+Portal/Anvisa/Inicio/Agrotoxicos+e+Toxicologia/Assuntos+de+Interesse/Monografias+de+Agrotoxicos/Monografias [accessed 01 October 2013].

Baraban, S.C., Taylor, M.R., Castro, P.A., Baier, H., 2005. Pentylenetetrazole induced changes in zebrafish behavior, neural activity and c-fos expression. Neuroscience 131, 759-768.

Barbazuk, W.B., Korf, I., Kadavi, C., Heyen, J., Tate, S., Wun, E., Bedell, J.A., McPherson, J.D., Johnson, S.L., 2000. The syntenic relationship of the zebrafish and human genomes. Genome Res. 10, 1351-1358.

Blasco-Ibáñez, J.M., Poza-Aznar, J., Crespo, C., Marques-Mari, A.I., Gracia-Llanes, F.J., Martinez-Guijarro, F.J., 2004. Chelation of synaptic zinc induces overexcitation in the hilar mossy cells of the rat hippocampus. Neurosci. Lett. 355, 101-104.

Braga, M.M., Dick, T., de Oliveira, D.L., Guerra, A.S., Leite, M.C., Ardais, A.P., Souza, D.O., Rocha, J.B., 2012. Cd modifies hepatic Zn deposition and modulates δ-ALA-D activity and MT levels by distinct mechanisms. J. Appl. Toxicol. 32, 20-25.

Braga, M.M., Rosemberg, D.B., de Oliveira, D.L., Loss, C.M., Córdova, S.D., Rico, E.P., Silva, E.S., Dias, R.D., Souza, D.O., Calcagnotto, M.E., 2013. Topographical analysis of reactive zinc in the central nervous system of adult zebrafish (Danio rerio). Zebrafish 10, 376-388.

Brugnone, F., Maranelli, G., Guglielmi, G., Ayyad, K., Soleo, L., Elia, G., 1993. Blood concentrations of carbon disulphide in dithiocarbamate exposure and in the general population. Int. Arch. Occup. Environ. Health 64, 503-507.

Caldas, E.D., Tressou, J., Boon, P.E., 2006. Dietary exposure of Brazilian consumers to dithiocarbamate pesticides—A probabilistic approach. Food Chem. Toxicol. 44, 1562-1571.

Cole, T.B., Robbins, C.A., Wenzel, H.J., Schwartzkroin, P.A., Palmiter, R.D., 2000. Seizures and neuronal damage in mice lacking vesicular zinc. Epilepsy Res. 39, 153-169.

Cooper, R.L., Goldman, J.M., Stoker, T.E., 1999. Neuroendocrine and reproductive effects of contemporary-use pesticides. Toxicol. Ind. Health 15, 26-36.

Cvek, B., Dvorak, Z., 2007. Targeting of nuclear factor-kappaB and proteasome by dithiocarbamate complexes with metals. Curr. Pharm. Des. 13, 3155-3167.

Daocheng, W., Mingxi, W., 2010. Preparation of the core-shell structure adriamycin lipiodol microemulsions and their synergistic anti-tumor effects with diethyldithiocarbamate in vivo. Biomed. Pharmacother 64, 615-623.

Di Monte, D., Irwin, I., Kupsch, A., Cooper, S., DeLanney, L.E., Langston, J.W., 1989. Diethyldithiocarbamate and disulfiram inhibit MPP+ and dopamine uptake by striatal synaptosomes. Eur. J. Pharmacol. 166, 23-29.

Domínguez, M.I., Blasco-Ibáñez, J.M., Crespo, C., Marqués-Marí, A.I., Martínez-Guijarro, F.J., 2003. Zinc chelation during non-lesioning overexcitation results in neuronal death in the mouse hippocampus. Neuroscience 116, 791-806.

Emanuelli, T., Rocha, J.B., Pereira, M.E., Nascimento, P.C., Souza, D.O., Beber, F.A., 1998. delta-Aminolevulinate dehydratase inhibition by 2,3-dimercaptopropanol is mediated by chelation of zinc from a site involved in maintaining cysteinyl residues in a reduced state. Pharmacol. Toxicol. 83, 95-103.

EU., 2001. Monitoring of Pesticide Residues in Products of Plant Origin in the European Union, Norway, Iceland and Liechtenstein, 2001 Report. European Commission, Health and Consumer Protection Directorate. Available: http://ec.europa.eu/food/fvo/specialreports/pesticide_residues/report_2001_en.pdf [accessed 01 October 2013].

Foresti, M.L., Arisi, G.M., Fernandes, A., Tilelli, C.Q., Garcia-Cairasco, N., 2008. Chelatable zinc modulates excitability and seizure duration in the amygdala rapid kindling model. Epilepsy Res. 79, 166-172.

Guillaumin, J.M., Lepape, A., Renoux, G., 1986. Fate and distribution of radioactive sodium diethyldithiocarbamate (imuthiol) in the mouse. Int. J. Immunopharmacol. 8, 859-865.

Haycock, J.W., van Buskirk, R., Gold, P.E., McGaugh, J.L., 1978. Effects of diethyldithiocarbamate and fusaric acid upon memory storage processes in rats. Eur. J. Pharmacol. 51, 261-273.

Ho, E., Dukovcic, S., Hobson, B., Wong, C.P., Miller, G., Hardin, K., Traber, M.G., Tanguay, R.L., 2012. Zinc transporter expression in zebrafish (Danio rerio) during development. Comp. Biochem. Physiol. C Toxicol. Pharmacol. 155, 26–32.

Houeto, P., Bindoula, G., Hoffman, J.R., 1995. Ethylenebisdithiocarbamates and ethylenethiourea: possible human health hazards. Environ. Health. Perspect. 103, 568-573.

Johansson, B., 1992. A review of the pharmacokinetics and pharmacodynamics of disulfiram and its metabolites. Acta Psychiatr. Scand. 86, 15-26.

Kalueff, A.V., Gebhardt, M., Stewart, A.M., Cachat, J.M., Brimmer, M., Chawla, J.S., Craddock, C., Kyzar, E.J., Roth, A., Landsman, S., et al., 2013. Towards a comprehensive catalog of zebrafish behavior 1.0 and beyond. Zebrafish 10, 70-86.

Kalueff , A.V., Stewart, A.M., Gerlai R., 2014. Zebrafish as an emerging model for studying complex brain disorders. Trends Pharmacol. Sci. 35, 63-75.

Khandelwal, S., Kachru, D.N., Tandon, S.K., 1987. Influence of metal chelators on metalloenzymes. Toxicol. Lett. 37, 213-219.

Knockaert, L., Berson, A., Ribault, C., Prost, P.E., Fautrel, A., Pajaud, J., Lepage, S., Lucas-Clerc, C., Bégué, J.M., Fromenty, B., et al., 2012. Carbon tetrachloride-mediated lipid peroxidation induces early mitochondrial alterations in mouse liver. Lab. Invest. 92, 396-410.

Lowry, O.H., Rosebrough, N.J., Lewis Farr, A., Randall, R.J., 1951. Protein measurement with Folin phenol reagent. J. Biol. Chem. 193, 265-275.

Malavolta, M., Costarelli, L., Giacconi, R., Muti, E., Bernardini, G., Tesei, S., Cipriano, C., Mocchegiani, E., 2006. Single and three-color flow cytometry assay for intracellular zinc ion availability in human lymphocytes with Zinpyr-1 and double immunofluorescence: relationship with metallothioneins. Cytometry A 69, 1043-1053.

Mitchell, C.L., Barnes, M.I., 1993. Proconvulsant action of diethyldithiocarbamate in stimulation of the perforant path. Neurotoxicol. Teratol. 15, 165-171.

Mussulini, B.H., Leite, C.E., Zenki, K.C., Moro, L., Baggio, S., Rico, E.P., Rosemberg, D.B., Dias, R.D., Souza, T.M., Calcagnotto, M.E., et al., 2013. Seizures induced by pentylenetetrazole in the adult zebrafish: a detailed behavioral characterization. PLoS One 8, e54515.

Pang, H., Chen, D., Cui, Q.C., Dou, Q.P., 2007. Sodium diethyldithiocarbamate, an AIDS progression inhibitor and a copper-binding compound, has proteasome-inhibitory and apoptosis-inducing activities in cancer cells. Int. J. Mol. Med. 19, 809-816.

Paoletti, P., Vergnano, A.M., Barbour, B., Casado, M., 2009. Zinc at glutamatergic synapses. Neuroscience 158, 126-136.

Qazi, R., Chang, A.Y., Borch, R.F., Montine, T., Dedon, P., Loughner, J., Bennett, J.M., 1988. Phase I clinical and pharmacokinetic study of diethyldithiocarbamate as a chemoprotector from toxic effects of cisplatin. J. Natl. Cancer Inst. 80, 1486-1488.

Rath, N.C., Rasaputra, K.S., Liyanage, R., Huff, G.R., Huff, W.E., 2011. Dithiocarbamate toxicity-An appraisal. In: Stoytcheva M, editor. Pesticides in the Modern World-Effects of Pesticides Exposure. New York: InTech Publishing Online. pp323-340.

Revuelta, M., Castaño, A., Machado, A., Cano, J., Venero, J.L., 2005. Kainate-induced zinc translocation from presynaptic terminals causes neuronal and astroglial cell death and mRNA loss of BDNF receptors in the hippocampal formation and amygdala. J. Neurosci. Res. 82, 184-195.

Rigas, D.A., Eginitis-Rigas, C., Head, C., 1979. Biphasic toxicity of diethyldithiocarbamate, a metal chelator, to T lymphocytes and polymorphonuclear granulocytes: reversal by zinc and copper. Biochem. Biophys. Res. Commun. 88, 373-379.

Sassa, S., 1982. Delta-Aminolevulinic acid dehydratase assay. Enzyme 28, 133-145.

Sekler, I., Silverman, W.F., 2012. Zinc homeostasis and signaling in glia. Glia 60, 843-850.

Skovgaard, N., Olson, K.R., 2012. Hydrogen sulfide mediates hypoxic vasoconstriction through a production of mitochondrial ROS in trout gills. Am. J. Physiol. Regul. Integr. Comp. Physiol. 303, R487-494.

Takeda, A., Hirate, M., Tamano, H., Nisibaba, D., Oku, N., 2003. Susceptibility to kainate-induced seizures under dietary zinc deficiency. J. Neurochem. 85, 1575-1580.

Tiedeken, J.A., Ramsdell, J.S., 2010. Zebrafish seizure model identifies p,p -DDE as the dominant contaminant of fetal California sea lions that accounts for synergistic activity with domoic acid. Environ. Health Perspect. 118, 545-551.

Tilton, F., La Du, J.K., Vue, M., Alzarban, N., Tanguay, R.L., 2004. Dithiocarbamates have a common toxic effect on zebrafish body axis formation. Toxicol. Appl. Pharmacol. 216, 55-68.

Tonkin, E.G., Valentine, H.L., Milatovic, D.M., Valentine, W.M., 2004. N,N-diethyldithiocarbamate produces copper accumulation, lipid peroxidation, and myelin injury in rat peripheral nerve. Toxicol. Sci. 81, 160-171.

Uddin, M.N., Salam, M.A., Hossain, M.A., 2013. Spectrophotometric measurement of Cu(DDTC)2 for the simultaneous determination of zinc and copper. Chemosphere 90, 366-373.

U.S. EPA., 2004. Reregistration eligibility decision for thiram. Prevention, pesticides and toxic substances. EPA-738-F-04-012. Available: http://www.epa.gov/oppsrrd1/REDs/0122red_thiram.pdf [accessed 01 October 2013].

U.S. EPA., 2005. EBDC fungicides mancozeb, maneb, and metiram; notice of receipt of requests to voluntarily cancel, amend, or terminate uses of certain pesticide registrations. Available: http://www.epa.gov/fedrgstr/EPA-PEST/2005/June/Day-01/p10577.htm [accessed 01 October 2013].

Varea, E., Alonso-Llosa, G., Molowny, A., Lopez-Garcia, C., Ponsoda, X., 2006. Capture of extracellular zinc ions by astrocytes. Glia 54, 304-315.

Yu, X., Li, Y.V., 2013. Neuroprotective effect of zinc chelator DEDTC in a zebrafish (Danio rerio) Model of Hypoxic Brain Injury. Zebrafish 10, 30-35.

Highlights

1. Therapeutic levels of DEDTC induced behavior impairment in zebrafish.
2. Behavior impairment was associated to brain accumulation of DEDTC.
3. DEDTC chelated reactive Zn in glutamatergic neurons and astrocytes.
4. DEDTC did not change Zn-dependent activity of δ-ALA-D.

Figure Captions

Fig. 1. Effects of DEDTC on behavioral phenotypes during the 60 min of exposure. Scheme of behavior phenotypes (only the highest phenotype was considered in each interval) was designed for the representative profiles of the control (A), 0.2 mM (B), 1 mM (C) and 5 mM DEDTC groups (D). Exposure to lower concentration of DEDTC (0.2 mM) showed normal behavior across time (B). Exposure to 1 mM DEDTC produced seizure-like behavior at the end of the test (C). Administration of 5 mM DEDTC caused several seizure-like episodes up to death (D). Quantitative analysis of behavioral phenotypes performed by each experimental group (n = 8) did confirm the behavioral effects performed by DEDTC concentrations (E). Values were expressed as median ± interquartile range of observed phenotypes, which were numbered as 0 (normal behavior), 1 (burst movements), 2 (seizure-like behavior), 3, (loss of posture), and 4 (death). Data were analyzed by Friedman test followed by Dunn's Multiple Comparison test. Spearman correlation between the highest observed phenotype, after exposure period, and DEDTC concentrations was obtained and plotted in the graphic.

Fig. 2. Histochemical staining of reactive Zn in the optic tectum after DEDTC exposure. In comparison to the control (A and E) 0.2 mM DEDTC caused little change on the content of reactive Zn (B and F), while 1 mM (C and G) and 5 mM (D and H) DEDTC produced a reduction in the levels of reactive Zn. At higher magnification of the area represented by the red square in E, F, G and H, the abundant content of reactive Zn of the periventricular gray zone (I) was unaltered at 0.2 mM DEDTC (J), while it was substantially decreased at 1 mM (K) and 5 mM (L). The images were obtained by analyzing four brains for each group (n = 4). Bars represent 60 µm in A-D panels, 200 µm in E-H panels, and 400 µm in I-L panels.

Fig. 3. Optic density quantification of reactive Zn in the periventricular gray zone. Results confirmed the substantial decrease in the levels of reactive Zn at 1 mM and 5 mM DEDTC (*n* = 4). Values were expressed as the mean ± S.E.M of arbitrary units (a.u.). Data were analyzed by one-way ANOVA followed by Tukey's test as post hoc. Distinct letters indicate statistical differences. The linear regression between optic density and DEDTC concentrations was obtained and plotted in the graphic.

Fig. 4. Flow cytometry measurement of intracellular reactive Zn content of glutamatergic neurons and astrocytes. Representative plots of side scatter (SSC) and forward scatter (FSC) of neural cells isolated from each zebrafish brain (*n* = 6 - 8) are shown. (A). Percentage of mean fluorescence intensity (MFI) of reactive Zn obtained for all the neural cells of zebrafish brain after exposure to DEDTC concentrations (B). Percentage of MFI of reactive Zn in glutamatergic neurons of zebrafish in different DEDTC concentrations (C). Percentage of MFI of reactive Zn in astrocytes of zebrafish caused by exposure to DEDTC (D). Values were expressed as the mean ± S.E.M. in percentage of MFI related to the control. Data were analyzed by one-way ANOVA followed by Tukey's test as post hoc. Distinct letters indicate statistical differences. The linear regression between cellular reactive Zn and DEDTC concentrations was obtained and plotted in each graphic.

Fig. 5. Schematic representation of the effects caused by DEDTC in zebrafish. Each numbered strip represents one unique parameter and the colors in the stripes represent changes in the parameter. In general, increased DEDTC concentrations generate most significant changes in the parameters.

Supplementary Figure Caption

Supplementary fig. S1. Calibration curve constructed by plotting absorbance against corresponding concentrations of DEDTC ($mg.mL^{-1}$).

Table 1. Level of DEDTC in the brain after acute exposure.

[DEDTC] in the water	[DEDTC] in the brain ($mg.kg^{-1}$)	*r**
0.2 mM	< 100	
1 mM	113.8 ± 19.6^{a}	0.987 $p = 0.001$
5 mM	960.2 ± 72.6^{b}	

The experiments were performed at least three times, and a pool of 6 whole brains was used for each independent sample (each group was $n = 3$). Values were expressed as means ± S.E.M. Distinct letters indicate statistical differences.

* Linear regression was performed without 0.2 mM DEDTC group.

Table 2. δ-ALA-D activity in the zebrafish brain after DEDTC exposure.

[DEDTC]	δ-ALA-D activity (nmol PBG.mg protein^{-1}.h)	*r**
Control	0.62 ± 0.05[a]	0.157 *p* = 0.463
0.2 mM	0.64 ± 0.04[a]	
1 mM	0.59 ± 0.03[a]	
5 mM	0.66 ± 0.04[a]	

The experiments were performed at least five times, and a pool of 5 whole brains was considered to $n = 1$ (each group was $n = 5$). Values were expressed as means ± SEM. Distinct letters indicate statistical differences.
* Linear regression

FIGURE 1

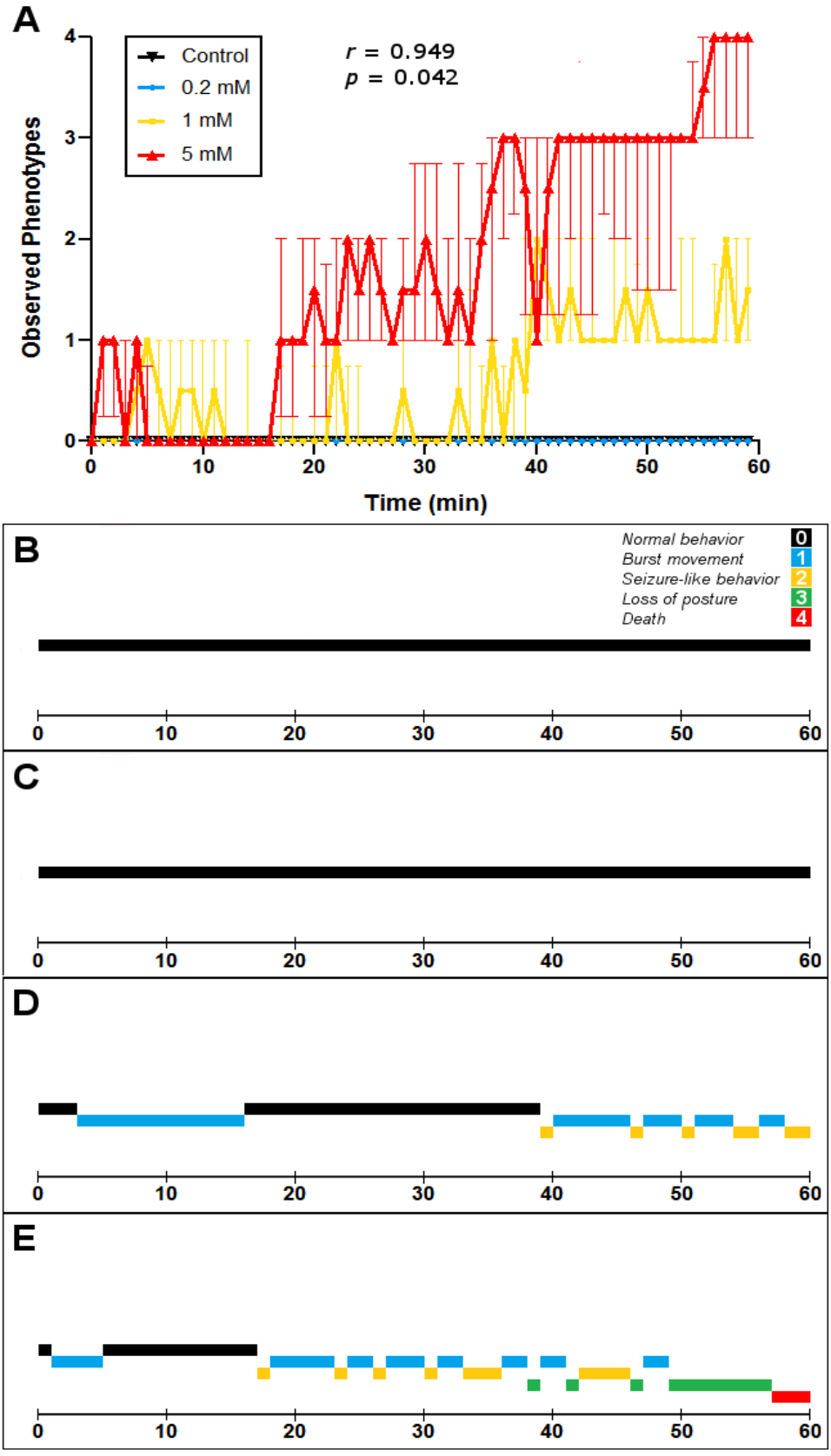
A
Control
0.2 mM
1 mM
5 mM
r = 0.949
p = 0.042
Observed Phenotypes
Time (min)
B
Normal behavior
Burst movement
Seizure-like behavior
Loss of posture
Death
0
1
2
3
4
C
D
E

FIGURE 2

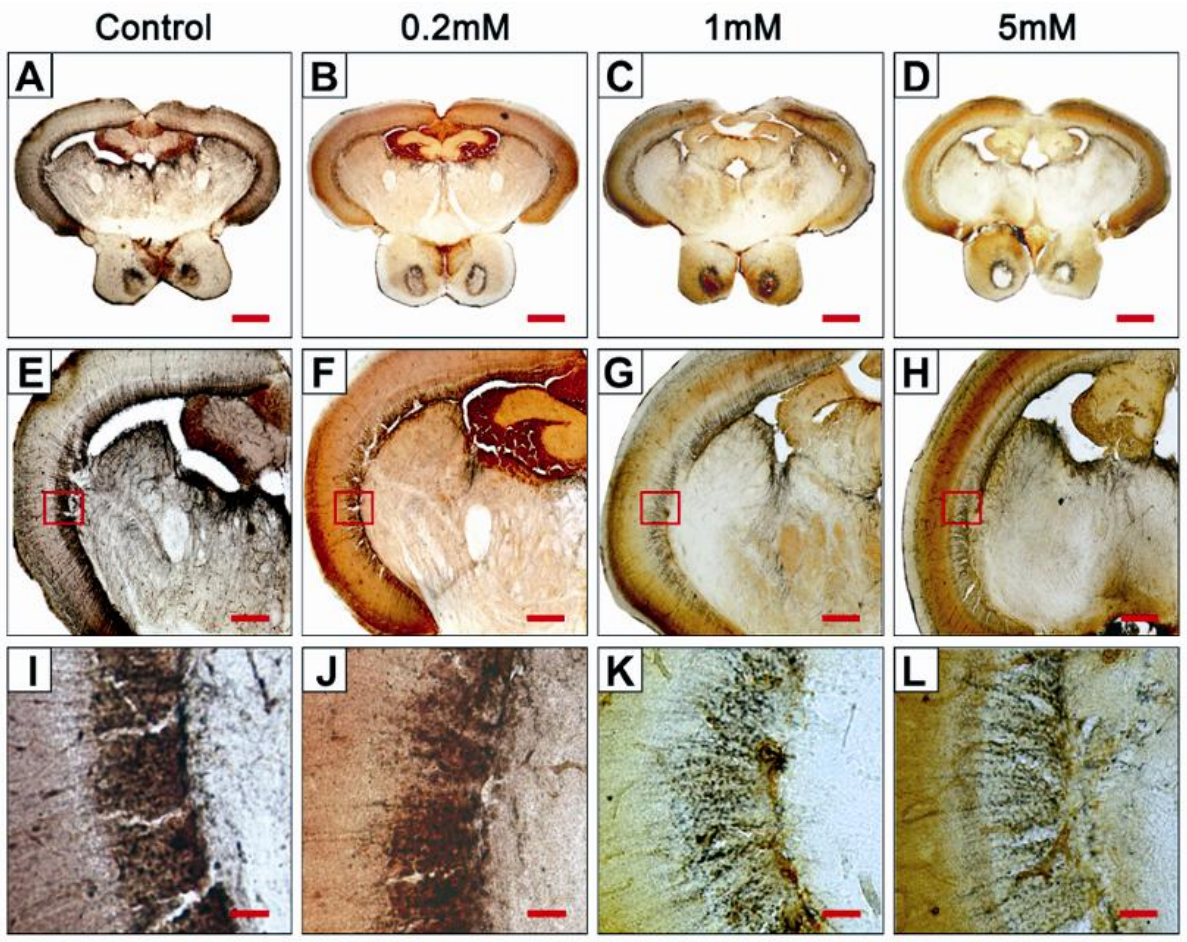

FIGURE 3

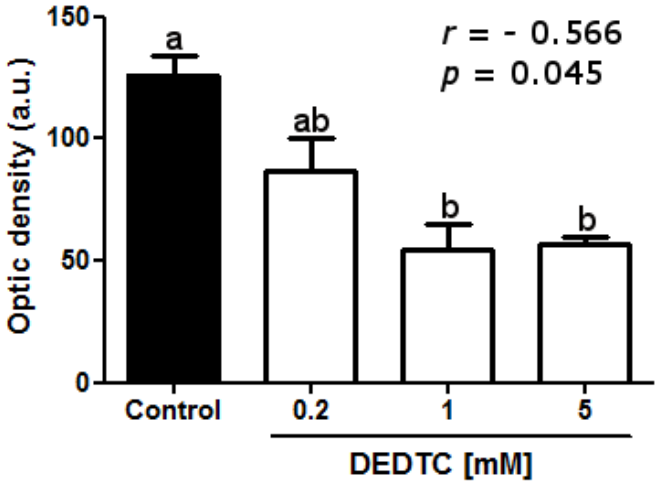
r = - 0.566
p = 0.045
Optic density (a.u.)
150
100
50
0
a
ab
b
b
Control
0.2
1
5
DEDTC [mM]

FIGURE 4

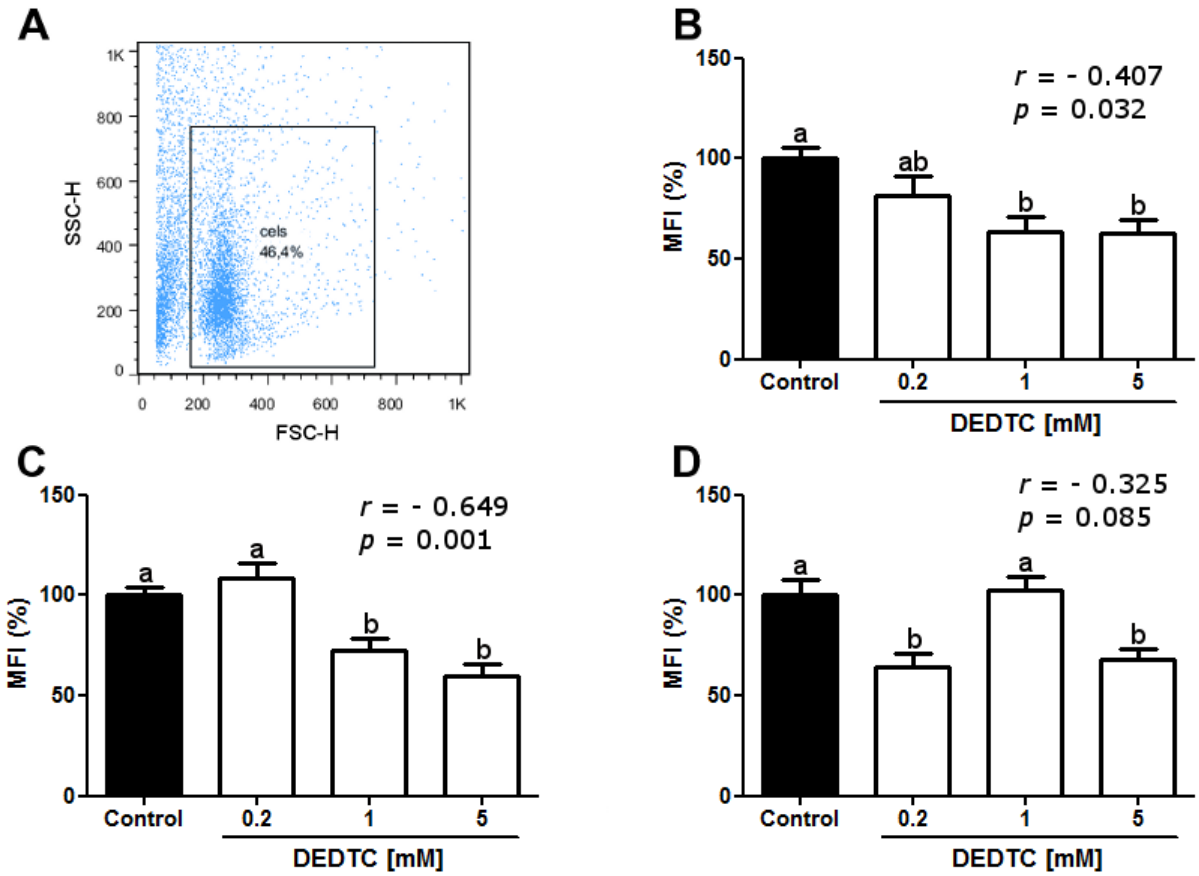
A
SSC-H
FSC-H
cels
46,4%
B
MFI (%)
r = - 0.407
p = 0.032
a
ab
b
b
Control
0.2
1
5
DEDTC [mM]
C
MFI (%)
r = - 0.649
p = 0.001
a
a
b
b
Control
0.2
1
5
DEDTC [mM]
D
MFI (%)
r = - 0.325
p = 0.085
a
b
a
b
Control
0.2
1
5
DEDTC [mM]

FIGURE 5

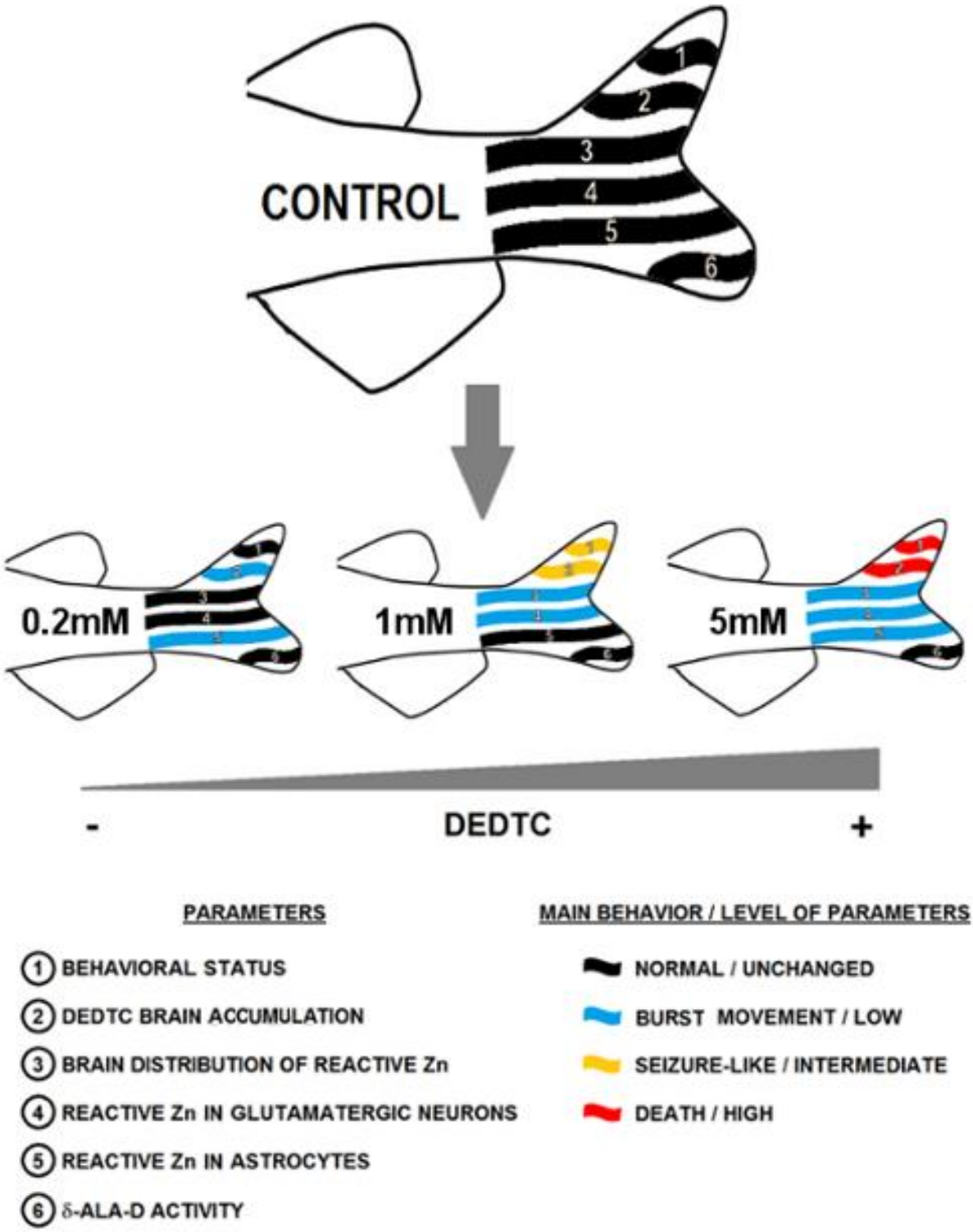
CONTROL
1
2
3
4
5
6
0.2mM
1mM
5mM
-
DEDTC
+
PARAMETERS
1 BEHAVIORAL STATUS
2 DEDTC BRAIN ACCUMULATION
3 BRAIN DISTRIBUTION OF REACTIVE Zn
4 REACTIVE Zn IN GLUTAMATERGIC NEURONS
5 REACTIVE Zn IN ASTROCYTES
6 δ-ALA-D ACTIVITY
MAIN BEHAVIOR / LEVEL OF PARAMETERS
NORMAL / UNCHANGED
BURST MOVEMENT / LOW
SEIZURE-LIKE / INTERMEDIATE
DEATH / HIGH

SUPPLEMENTARY FIGURE S1

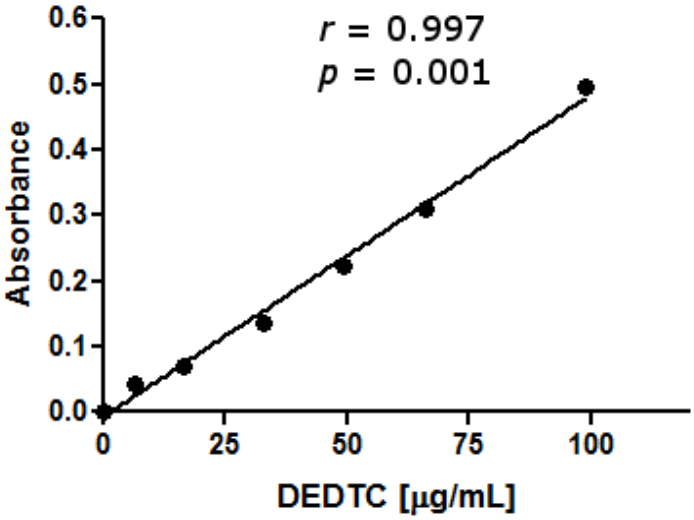

CAPÍTULO IV

Evaluation of spontaneous recovery of behavioral and brain injury profiles in zebrafish after hypoxia

Artigo publicado no periódico *Behavioural Brain Research*

Behavioural Brain Research 253 (2013) 145–151

Contents lists available at SciVerse ScienceDirect

Behavioural Brain Research

journal homepage: www.elsevier.com/locate/bbr

Research report

Evaluation of spontaneous recovery of behavioral and brain injury profiles in zebrafish after hypoxia

Marcos M. Braga[a,b,*], Eduardo P. Rico[a,b], Sandro D. Córdova[a], Charles B. Pinto[a], Rachel E. Blaser[c], Renato D. Dias[a,b], Denis B. Rosemberg[b,d,e], Diogo L. Oliveira[a,b,e], Diogo O. Souza[a,b,e]

[a] Programa de Pós-graduação em Bioquímica, Departamento de Bioquímica, Instituto de Ciências Básicas da Saúde, Universidade Federal do Rio Grande do Sul, Rua Ramiro Barcelos 2600-Anexo, 90035-003 Porto Alegre, RS, Brazil
[b] Instituto Nacional de Ciência e Tecnologia em Excitotoxicidade e Neuroproteção (INCT-EN), 90035-003 Porto Alegre, RS, Brazil
[c] Department of Psychology, University of San Diego, 5998 Alcala Park, San Diego, CA 92110, USA
[d] Laboratório de Genética e Ecotoxicologia Molecular, Programa de Pós-graduação em Ciências Ambientais, Área de Ciências Exatas e Ambientais, Universidade Comunitária da Região de Chapecó, Avenida Senador Attílio Fontana, 591E, 89809-000 Chapecó, SC, Brazil
[e] Zebrafish Neuroscience Research Consortium (ZNRC), USA

HIGHLIGHTS

- Short-term hypoxia produced four distinct behavioral stages in adult zebrafish.
- Brain damage and behavioral impairments were observed in zebrafish after hypoxia.
- Effects induced by hypoxia were reversed after recovery under normoxic conditions.
- Behavioral impairments recovered more quickly than brain damage following a return to normoxic conditions.

ARTICLE INFO

Article history:
Received 4 May 2013
Received in revised form 3 July 2013
Accepted 9 July 2013
Available online 16 July 2013

Keywords:
Zebrafish
Hypoxia
Spontaneous recovery
Brain
Behavior

ABSTRACT

Cerebral hypoxia–ischemia can lead to motor and sensory impairments which can be dependent on the extent of infarcted regions. Since a better understanding of the neurochemical mechanisms involved in this injury is needed, the use of zebrafish as a cerebral hypoxia model has become quite promising because it could improve the knowledge about hypoxia–ischemia. In the current study, we aimed to investigate the spontaneous recovery of brain and behavioral impairments induced by hypoxia in adult zebrafish. Brain injury levels were analyzed by spectrophotometric measurement of mitochondrial dehydrogenase activity by staining with 2,3,5-triphenyltetrazolium chloride, and behavioral profiles were assessed by the open tank test. The induction of hypoxia substantially decreased mitochondrial activity in the brain and impaired behavior. The spontaneous recovery of fish subjected to hypoxia was assessed after 1, 3, 6, 24, and 48 h under normoxia. The quantification of brain injury levels showed a significant increase until 24 h after hypoxia, but after 48 h this effect was completely reversed. Regarding behavioral parameters, we verified that locomotor activity and vertical exploration were impaired by hypoxia and these effects were reversed after 3 h under normoxia. Taken together, these results show that zebrafish exhibited transient cerebral and behavioral impairments when submitted to hypoxia, and 1 h under normoxic conditions was insufficient to reverse both effects. Therefore, our data help to elucidate the time window of spontaneous recovery in zebrafish after hypoxia and also the behavioral phenotypes involved in this phenomenon.

1. Introduction

Hypoxia–ischemia is a phenomenon that develops in vascular pathology and metabolic disruptions, which can trigger tissue infarctions, mainly in the brain due to its high oxygen (O_2) consumption [1]. Cerebral hypoxia–ischemia has affected the human population worldwide, leading to death or chronic adult disability by debilitating neurological conditions. It is well known that

* Corresponding author at: Departamento de Bioquímica, Instituto de Ciências Básicas da Saúde, Universidade Federal do Rio Grande do Sul, Rua Ramiro Barcelos, 2600-Anexo, Zip code: 90035-003 Porto Alegre, RS, Brazil. Tel.: +55 51 33085555; fax: +55 51 33085540.
E-mail address: marcosmbraga@gmail.com (M.M. Braga).

0166-4328/$ – see front matter © 2013 Elsevier B.V. All rights reserved.
http://dx.doi.org/10.1016/j.bbr.2013.07.019

during an ischemic episode, the neurons subjected to O_2 and energy deprivation exhibit structural damage after few minutes [2], resulting in cell apoptosis and necrosis [3,4] followed by the impairment of motor and sensory function [3,5]. Indeed, brain damage produced by hypoxia–ischemia can be devastating, but many individuals survive the initial event and experience some spontaneous recovery, which can be enhanced by neuroprotective therapies. However, even with the advances in research, additional strategies are required in order to better understand the mechanisms underlying hypoxia–ischemia as well as neurochemical actions of therapies.

The zebrafish (*Danio rerio*) is a prominent model used in neuroscience studies [6–9]. The genome of this species shares a high degree of similarity with mammalian genes [10], in addition to other advantageous features such as low-cost, easy maintenance, and abundant offspring [7,11]. Due to its valuable characteristics as an alternative and complementary vertebrate model, the use of zebrafish could be attractive to investigate parameters related to hypoxia–ischemia. Although it belongs to the Cyprinidae family, a group of fish known to be hypoxia-tolerant [12,13], a zebrafish brain hypoxic model has recently been described, showing that it was quite sensitive to severe O_2 deprivation [14]. In addition to its non-invasive properties, this model is highly sensitive to cerebral infarction similar to that observed in ischemic rodents [15,16]. However, as an important model for investigating cerebral hypoxia, a profile of the spontaneous recovery should be evaluated from behavioral and neurochemical perspectives. The complex behavioral repertoire of zebrafish has been evaluated in tests, such as the open tank paradigm, also known as novel tank diving test [7,17–22]. In general, this task evaluates locomotor and vertical exploratory activity in a novel apparatus, since this species initially dives to the bottom and gradually swims to upper areas of the tank [23]. Several reports have already pharmacologically validated the open tank as a test able to assess behavioral changes in zebrafish, such as anxiogenic and anxiolytic manipulations [9,23–30], Thus, the use of this task could be an interesting strategy to examine the spontaneous recovery of behavior in animals subjected to hypoxia.

Therefore, the goal of the present study was to investigate the capacity for spontaneous recovery in zebrafish injured by hypoxia. To address this issue, we subjected the animals to hypoxia and then immediately transferred them to aquariums under normoxic conditions. After different recovery periods, the behavior was assessed using the open tank test to evaluate locomotor and exploratory activity. Additionally, we performed a measurement of formazan produced from 2,3,5-triphenyltetrazolium chloride (TTC) to quantify cerebral damage during the hypoxia episode and after recovery.

2. Materials and methods

2.1. Animals

A hundred and twenty male and female wild-type adult zebrafish (4–7 months) of short-fin phenotype from heterogeneous stock were obtained from a commercial distributor (Delphis, RS, Brazil). Fish were kept in 50 L aquariums (80–100 fish per tank) for at least 2 weeks prior to the experiments in order to acclimate to the laboratory facility. All experiments were performed in tanks filled with conditioned tap water (reverse osmosis water supplemented with Instant Ocean® salt solution) and maintained under mechanical-chemical filtration at 26 ± 2 °C with a light/dark cycle of 14/10 h (lights on at 7:00 am). At these conditions, the normoxic water was 7.5 mg L^{-1} O_2, 500 μS/cm^2 of conductivity and pH 7.2. All animals were fed twice a day with a commercial flake fish food (alcon BASIC®, Alcon, Brazil). They were maintained according to the National Institute of Health Guide for Care and Use of Laboratory Animals. The protocols of the experiments were approved by the Ethics Committee of Universidade Federal do Rio Grande do Sul (number 20121 – CEUA).

2.2. Hypoxia chamber and hypoxic conditions

The hypoxic condition was performed in an 8-L clear glass apparatus containing 1.5 L of conditioned tap water at 26 ± 2 °C (Fig. 1A). An oximeter (Instrutherm, São Paulo, SP, Brazil) was constantly used to measure the levels of dissolved O_2 into the water. As reported in a previous study, the chamber had two openings, one of which was connected to a nitrogen cylinder and the other kept in contact with air space [14]. The hypoxic condition was produced by perfusing pure N_2 into the chamber until the water achieved 1.5–1.7 mg L^{-1} dissolved O_2, a range previously reported for short-term severe hypoxia in zebrafish [31]. Afterwards, four fish were immediately transferred to the chamber and the tank was hermetically sealed, providing a closed air tight system to induce hypoxia. The O_2 levels were measured during hypoxia and were kept constant during the trials. All hypoxia trials were recorded using a video-camera (Sony Handycam SD DCR-SX22) and further analyzed by two independent trained observers (inter rater reliability ≥ 0.85). Animals showed a reliable sequence of behaviors, consisting of four distinct stages of hypoxia (see Table 1 and Supplementary Video 1). The phenotypes were categorized as follows: 1st stage, swimming at the top; 2nd stage, loss of posture; 3rd stage, maintenance of opercular beats with brief movements; and 4th stage, death. Since animals displayed negligible behavioral variations within each stage, the use of four fish per trial allowed us to evaluate the hypoxia conditions in a large scale manner.

Table 1
Behavioral repertoire during hypoxia.

Behavior sequence	Description
1st	Swimming at the top
2nd	Loss of posture
3rd	Maintenance of opercular beats with brief movements
4th	Death

Representative behaviors were obtained by analysis of seven independent experiments each with four animals.

See Supplementary Video 1 as supplementary file. Supplementary material related to this article can be found, in the online version, at http://dx.doi.org/10.1016/j.bbr.2013.07.019.

2.3. Recovery conditions after hypoxia

The recovery of zebrafish under normoxic conditions was measured after they reached the third stage of hypoxia, characterized by a critical but non-lethal condition (average time to the animals reaching 3rd stage was 9′39″ ± 0′29″). Thus, after the hypoxia, the animals were immediately transferred from the hypoxia chamber to aquariums containing 2 L of conditioned tap water with normoxic O_2 levels (experimental design represented in Fig. 1A). After 1, 3, 6, 24 and 48 h of normoxia, brain injury levels were assessed by TTC (Sigma–Aldrich, St. Louis, MO, USA) staining. Importantly, none of the animals died during the recovery period. Behavior was also tested after different periods of recovery and, therefore, matched controls were run in similar conditions to the hypoxia groups except that no N_2 was added to the chamber. This experimental design was important because housing and handling conditions have been observed to affect behavioral responses of zebrafish [32].

2.4. TTC staining and measurement of tissue formazan

As previously described, the brain damage was evaluated by TTC staining that quantifies the level of formazan produced by mitochondrial dehydrogenase activities in living tissues [33]. Briefly, after each hypoxia trial, the animals were cryoanesthetized and euthanatized by decapitation to remove the brain. The whole brains were immediately immersed in vials containing 1 mL of 2% TTC solution in PBS (pH 7.4) at 37 °C for 40 min. The vials were covered with foil due to the light sensitive property of TTC and they were checked during incubation to ensure that the tissues did not adhere to the vial walls. Afterwards, the TTC was removed and 10% formalin in PBS (pH 7.4) was added to terminate the enzymatic reaction. The brains were dried at 40 °C for 2 h and the tissues were weighed. Next, the brains were transferred to 96 wells plates and incubated with 200 μL of dimethylsulfoxide (DMSO). The plates were protected from light and kept under constant agitation for 4 h to solubilize the formazan produced from the TTC reaction. These conditions were sufficient to dissolve and redistribute the brain formazan throughout the contents of the well (pink-to-red eluate). The absorbance of the supernatant was read at 490 ηm in a microplate reader. Results were expressed in absorbance per tissue dry weight (g), which were normalized as a percentage in relation to the control.

2.5. Open tank test

To evaluate the behavior of zebrafish after recovery from hypoxia, the open tank test was performed as previously described [9]. The apparatus was a trapezoidal plastic tank (23.9 cm along the bottom × 28.9 cm at the top × 15.1 cm high) virtually divided into three equal horizontal areas (bottom, middle, and top) and with five sections per area. The open tank was filled with 1.5 L water and the experimental procedures were executed on a stable surface with all environmental interferences kept to a minimum. After each recovery interval, the animals were individually removed from their aquariums to the open tank and the behavioral activity was recorded in a single session lasting 6 min. To evaluate the location and swimming activity of the zebrafish, a webcam (Microsoft® LifeCam 1.1 with Auto-Focus)

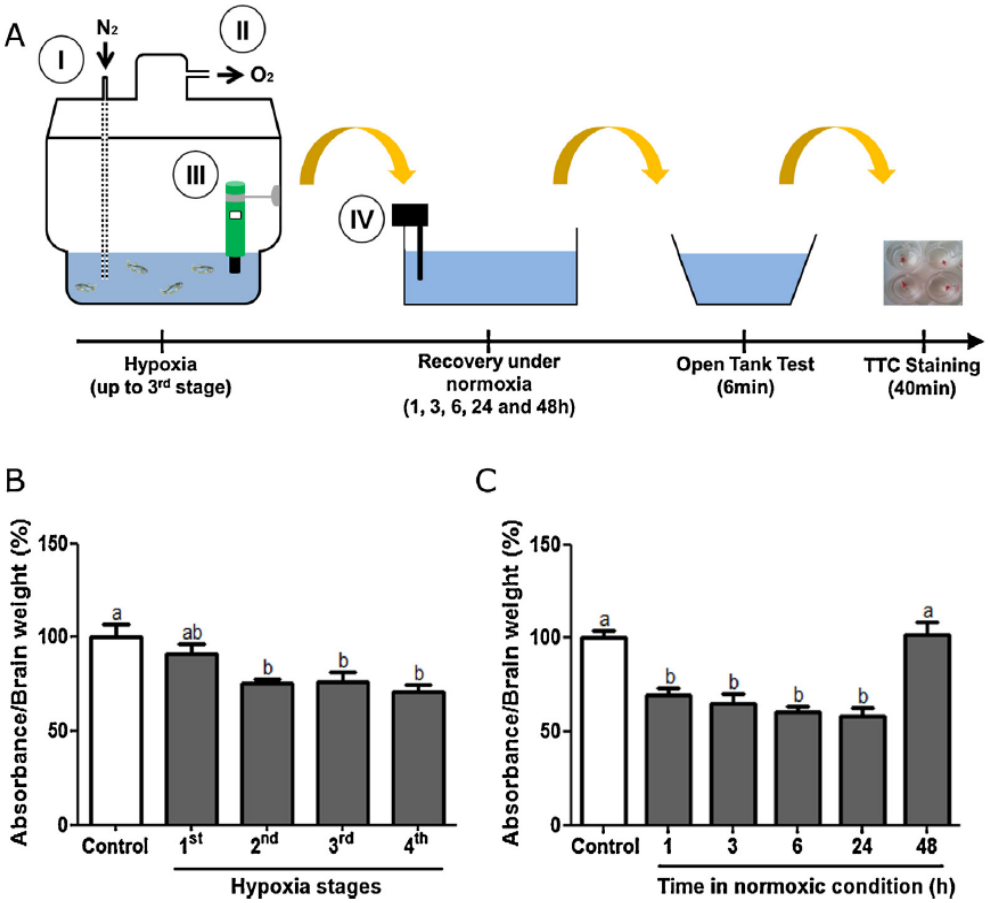

Fig. 1. Schematic representation of the hypoxia chamber, experimental design and brain damage induced during and after hypoxia. (A) The experimental protocol involved a single hypoxia episode (1.5–1.7 mg L^{-1} of dissolved O_2) followed by 1, 3, 6, 24 and 48 h under normoxic conditions. After recovery periods, the behaviors were evaluated by the open tank test and brain injuries were assessed by TTC staining. (I) Nitrogen input, (II) oxygen output, (III) oximeter, and (IV) water filtration and aeration system. (B) Brain damage induced during hypoxia stages. The whole brains of zebrafish were immersed in TTC solution for production of formazan by mitochondria in healthy tissues (n = 7–10). (C) Brain damage in animals at different recovery periods after hypoxia. After a hypoxia episode, the animals were immediately transferred to aquariums under normoxic conditions for 1, 3, 6, 24 and 48 h (n = 12–20). Data represent means ± S.E.M. Distinct letters indicate statistical differences at $p < 0.05$ level (one-way ANOVA followed by Tukey's post hoc test).

connected to a laptop was placed in front of the tank for recording the videos. The behavioral parameters were automatically measured at a rate of 30 frames/s by appropriate video-tracking software (ANY-maze®, Stoelting CO, USA). The behavioral test was performed during the same time frame each day (between 10:00 am and 4:00 pm) and hypoxia recovery times were established within a period of tolerance (±3 min) in order to perform the open tank test individually for the four animals after each hypoxia trial. All precautions were taken to ensure representative behavioral results and the tank water was replaced every session.

2.5.1. Exploratory profile, locomotor parameters and vertical exploration

As previously described [17], an analysis of the exploratory profile of the fish was performed by representative track and occupancy plots in order to represent the overall activity in both horizontal and vertical regions.

The locomotor activity of the zebrafish was assessed by measuring the total time mobile, distance traveled, turn angle (which represents the variations in direction of the center point of the animal) and meandering (absolute turn angle divided by the total distance traveled).

The vertical exploration measure represents the tendency of zebrafish to gradually explore top areas when subjected to novel apparatuses, which suggests habituation to novelty [17,24]. To analyze the vertical activity of fish, the total number of transitions and the duration in top and bottom areas were evaluated by endpoint analysis and 1-min intervals of the 6 min test.

2.6. Statistical analysis

The results of TTC staining were analyzed by one-way analysis of variance (ANOVA). Behavior endpoints were analyzed by two-way ANOVA, while the temporal analysis of behavior was evaluated by repeated-measures ANOVA, using hypoxia and 1-min intervals (across the 6-min trial) as factors. Post hoc comparisons were performed using Tukey's test. Data were expressed as means ± standard error of mean (S.E.M.) and the significance was set at $p < 0.05$.

3. Results

3.1. Brain damage during hypoxia stages

Cerebral injury was examined across the four hypoxia stages by TTC staining (Fig. 1B). A tendency toward a reduction in formazan was observed after the first stage (91% of control). However, a significant reduction was detected after the second, third, and fourth stages (75.5, 76.1, and 70.7% of the absorbance of the control group, respectively).

3.2. Brain damage after hypoxia recovery

After submitting animals to hypoxia until they reached the third stage, hypoxia-induced brain damage was investigated following several recovery times (Fig. 1C). According to the results, recovery under normoxic conditions produced a gradual reduction in cerebral mitochondrial activity after 1, 3, 6 and 24 h, which were significantly reduced in comparison to control (69.1, 65.2, 60.4 and 58.3% of the control activity, respectively). Interestingly, these groups did not significantly differ from animals that were not subjected to recovery (third stage in Fig. 1B). However, after 48 h of

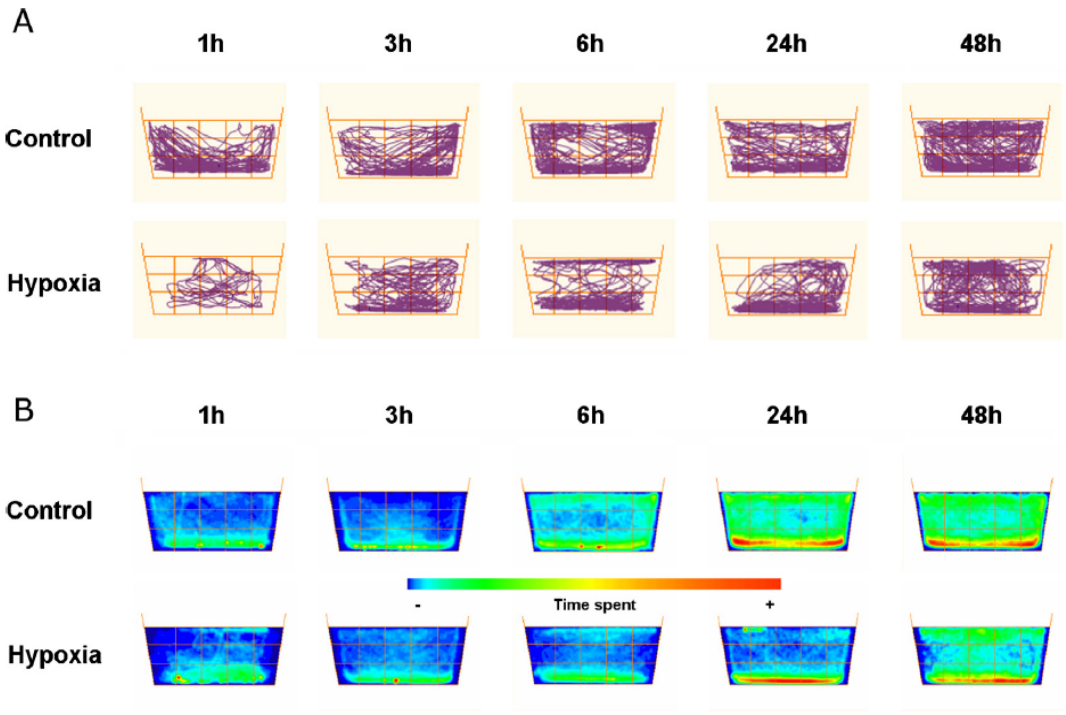

Fig. 2. Exploratory profiles of animals subjected to different recovery times after hypoxia represented by track and occupancy plots. (A) The representative track plots illustrate the path traveled by fish in the apparatus. (B) Representative occupancy plots showing the duration in each area of the open tank.

recovery, the animals showed similar levels of formazan to controls. Thus, the hypoxia-induced brain damage quantified by TTC staining remains for at least 24 h in normoxic conditions, while recovery for 48 h was able to reverse these effects.

3.3. Behavioral repertoire after hypoxia recovery

In order to evaluate the spontaneous recovery of behavior after a hypoxia episode, we performed the open tank test following several recovery intervals (1, 3, 6, 24, and 48 h) to assess both locomotor and exploratory activity.

3.3.1. Exploratory profiles

The influence of hypoxia on the exploratory profiles of the animals was examined using both horizontal and vertical dimensions of the open tank. The representative track plots (Fig. 2A) that illustrate the individual swimming traces of zebrafish in the apparatus showed a marked reduction in exploratory activity caused by hypoxia only in animals subjected to 1 h of recovery, supporting a possible harmful effect of hypoxia on locomotion. In contrast, the occupancy plot of each other hypoxia recovery group (Fig. 2B) suggested exploratory activity spatio-temporally similar to their corresponding controls. Since differences were observed between control and experimental groups, these representative data were further deeply investigated using automated analysis of endpoint data and across 1-min intervals.

3.3.2. Locomotor activity

The endpoint analyses showed that time mobile at all recovery times was similar to matched controls (Fig. 3A). In contrast, the distance traveled and turn angles were reduced after 1 h of hypoxia recovery, while 3, 6, 24, and 48 h did not significantly differ when compared to their control groups. In addition, meandering exhibited a substantial increase only in the 1 h-recovered group.

3.3.3. Vertical exploration

The vertical exploratory behaviors displayed by controls and hypoxia-recovered groups are shown in Fig. 3B. As demonstrated by endpoint analyses, the duration in the top and bottom areas were similar at all recovery times. Furthermore, the transitions to the top area displayed by all recovery groups did not differ as compared to their corresponding controls. However, the number of entries to bottom area was significantly lower after 1 h recovery, while 3, 6, 24, and 48 h under normoxic conditions were able to reverse these changes.

In general, the analysis across 1-min intervals (Fig. 4 and Supplementary Fig. S1) by repeated-measures ANOVA indicated a significant main effect of interval on vertical activity, since duration in the top and the number of entries to the top area increased across intervals in all but the 1 h recovery group: 3 h ($F[5,80] = 3.103$ and $F[5,80] = 6.636$), 6 h ($F[5,85] = 2.401$ and $F[5,85] = 5.304$), 24 h ($F[5,95] = 5.494$ and $F[5,95] = 5.244$) and 48 h ($F[5,85] = 7.164$ and $F[5,85] = 5.976$). We also observed a significant reduction across intervals in duration in the bottom area for all but the 1 h recovery group: 3 h ($F[5,80] = 9.232$), 6 h ($F[5,85] = 2.921$), 24 h ($F[5,95] = 5.531$), and 48 h ($F[5,85] = 8.253$). In contrast, there was an increase in the number of entries to the bottom area across intervals in the 3 h ($F[5,80] = 5.388$) and 6 h ($F[5,85] = 3.686$) groups. The 1 h control group, but not experimental group, also showed an increase in the number of entries to the top ($F[5,85] = 3.700$) and bottom areas ($F[5,85] = 2.446$) as well as an increase in the duration in the top area ($F[5,85] = 3.336$) across intervals.

See Fig. S1 as supplementary file. Supplementary material related to this article can be found, in the online version, at http://dx.doi.org/10.1016/j.bbr.2013.07.019.

There were also significant differences between hypoxia-exposed and control groups. Although the duration in the top area increased across the 6-min trial after 3 h of recovery ($F[1,80] = 5.244$), exposure to hypoxia resulted in a decrease in the number of entries to the top and bottom areas after 1 h ($F[1,85] = 6.144$ and $F[1,85] = 14.98$) and 6 h ($F[1,85] = 5.421$ and

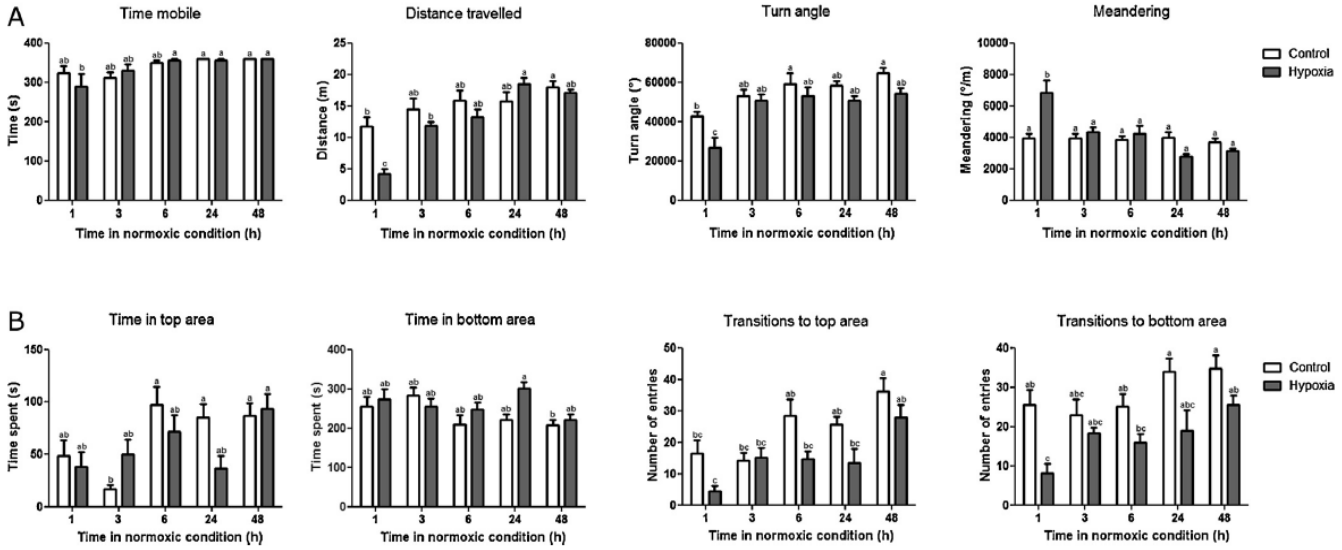

Fig. 3. Locomotor activity and vertical exploration after recovery periods of hypoxia. (A) The figure represents the endpoint analysis of basic locomotor parameters showing the effects on time mobile, distance traveled, turn angle, and meandering (n = 8–11). (B) Effects of a hypoxia episode on vertical exploration after recovery times under normoxia (n = 8–11). Data represent means ± S.E.M. Different letters indicate statistical differences at $p < 0.05$ level (two-way ANOVA followed by Tukey's post hoc test).

$F[1,85] = 5.174$) of recovery. Moreover, a significant interaction of 1-min intervals and hypoxia factors was observed. The significant interaction is due to a substantial effect in the 1 h hypoxia-recovered group, in which fish differed from the control group in entries to top ($F[5,85] = 3.869$) and bottom areas ($F[5,85] = 3.578$) as well as duration in the bottom ($F[5,85] = 3.336$) during the trial.

4. Discussion

The use of alternative models has been increasingly adopted to investigate several parameters of brain injuries. In particular, special attention has been given to studies involving cerebral hypoxia–ischemia [34]. Since many studies have failed to develop new treatments against ischemia, many researchers have attempted to circumvent this issue through alternative animal models of hypoxia. Based on this approach, the zebrafish has been used to assess the underlying neurobiological, molecular mechanisms of hypoxia [14,35]. Nevertheless, a better understanding of the spontaneous recovery following the hypoxia in adult zebrafish still needs to be investigated. The assessment of behavioral and brain injury profiles of zebrafish under different periods of normoxia after hypoxia is particularly relevant in order to determine the spontaneous recovery ability of zebrafish relative to other hypoxic models [36]. This becomes even more important because

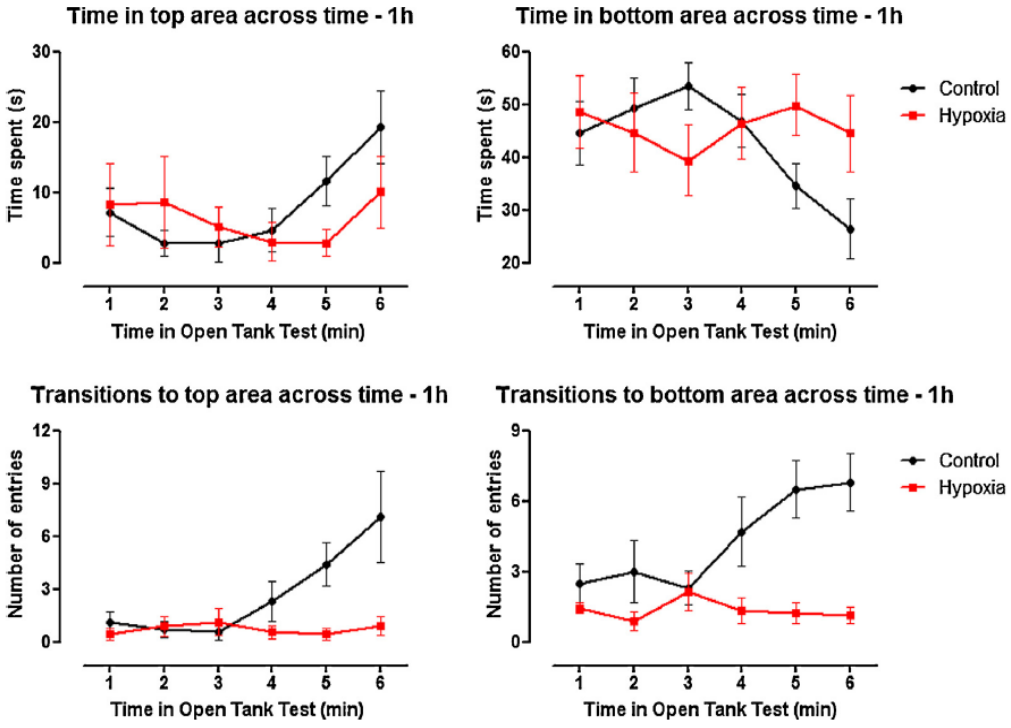

Fig. 4. Effects of hypoxia on vertical exploration across intervals of the open tank test after 1 h under recovery. Data represent means ± S.E.M. for n = 8–11 (repeated measures ANOVA followed by Tukey's post hoc test).

zebrafish is related to a group of aquatic vertebrates resistant to low O_2 levels [12,13].

In the current report, we first attempted to understand the spontaneous recovery that zebrafish could achieve following brain damage induced by hypoxia. Animals showed a cerebral sensitivity to hypoxia, presenting a reduction of approximately 25% in the activity of mitochondrial dehydrogenases. As Preston and Webster previously described [33], the major impact of these data is that mitochondrial inhibition is related to the presence of infarcted brain areas, which have already been observed in zebrafish under hypoxic conditions [14]. Given this approach, our results indicate that hypoxia-induced brain damage directly correlates with the first and second stages. Although this parameter alone has shown that mitochondrial activities were sensitive to O_2 deprivation up to the second hypoxia stage, it is reasonable to suggest that maintaining this detrimental effect on subsequent stages could result in more persistent sequelae, which could delay the spontaneous recovery of neurochemical and behavioral parameters.

Next, we chose the third stage of hypoxia to assess spontaneous recovery of zebrafish under normoxic conditions. Animals were unable to reverse the brain injury caused by hypoxia at least for 24 h. During this period, fish exhibited a slight increase in the levels of brain injury even under normoxic conditions, making this result comparable to the effect triggered by reperfusion in ischemic models. It is well known that brain injury caused by hypoxia can be further intensified by the subsequent reperfusion due to formation of free radicals triggered by brain reoxygenation [37]. Although the levels of reactive oxygen species (ROS) has not been assessed in the zebrafish brain under recovery, a previous study has reported that cerebral reoxygenation after hypoxia led these animals to increase the amount of heat shock factor 1, which is expressed in adverse conditions such as hypoxia and oxidative stress [38]. In this regard, if the production of ROS contributes to the reduction of mitochondrial activity, this effect could be completely reversed after 48 h under normoxic conditions. Indeed, in other models, a reversible effect of brain injury caused by hypoxia–ischemia is due to an decrease of ROS to the control level in a time-dependent manner [39,40], which could be responsible for the recovery of the activity of mitochondrial dehydrogenases following 48 h under normoxia. Although our results possibly reflect those effects reported in traditional models of hypoxia–ischemia, the prominent effect of cellular oxidative balance on mitochondrial functions of zebrafish still requires further investigation.

The decrease of mitochondrial activity related to infarcted brain areas supports the hypothesis that these animals could develop motor and sensory disorders, impairing their performance on behavioral tasks. In fact, locomotor dysfunctions are reported by studies that evaluate the behavioral effects of hypoxia–ischemia in rodents [41,42]. Our data demonstrate that zebrafish kept under normoxic conditions for 1 h following hypoxia also present a locomotor deficit revealed by the shortest distance traveled. Moreover, they showed a substantial increase in meandering suggesting a more sinuous path during testing. In contrast, the impairments caused by hypoxia in fish locomotion were reversed after 3 h under normoxic conditions. These data show the remarkable ability of the zebrafish to quickly recover locomotor skills even after being subjected to an episode of hypoxia that could lead to death. An important question that arises is whether the improvement of locomotor parameters is due to a true recovery or compensatory behaviors. There is an extensive debate that supports the difficulty in observing a true recovery, which can occur because some of the brain tissue that is crucial for function is spared [36]. The absence of a kinematic assessment makes it difficult to affirm whether the recovery of fish locomotion has been achieved through adjustments in movement. However, since our data demonstrated that the brain injury induced by hypoxia was transient, we suggest the occurrence of true recovery in this model.

The spatio-temporal analysis of behavior showed that when zebrafish presented a locomotor impairment, they failed to show the typical change in the number of entries to the top or bottom areas across 1-min intervals, resulting in an overall reduction in transition frequency compared to controls. According to previous studies, a gradual increase in the number of transitions and duration in the upper areas is expected during the trial since it reflects a common habituation of zebrafish to novelty [17,24]. Based on this, after 1 h of hypoxia recovery, the analysis of vertical exploratory parameters during the open tank trial showed that injured fish were significantly impaired on their normal habituation to the apparatus. Although they maintained a clear preference for the bottom area, which has been reported through occupancy plot analysis [9,17], our data support that 1 h under normoxic conditions was insufficient for spontaneous recovery of locomotor and exploratory behaviors. However, after 3 h of recovery, the effects caused by hypoxia were largely reversed. This result reinforces the recovery of the exploratory strategies simultaneously with locomotor parameters, suggesting that impairment on locomotion could be responsible for changes on exploratory profile.

Our analysis also indicates that the brain and locomotor-exploratory behavioral damage caused by hypoxia can be recovered at different times. In regard to brain damage, the level of mitochondrial activity was reestablished in 48 h, while the behavioral effects were apparently normal after 3 h under normoxia. Although the fish present significant behavioral recovery after a short period this fact does not mean that other effects caused by hypoxia are not maintained in the longer term. For example, cognitive decline is often observed in individuals who have suffered hypoxia–ischemia [43,44]. It would be useful to study the effects of hypoxia on more complex learning and memory tasks in zebrafish, and our results suggest that such studies should only be conducted after locomotor activity has recovered, more than 1 h after hypoxia exposure. Furthermore, the fast recovery by zebrafish on the parameters evaluated after a strong episode of hypoxia is not surprising, since cyprinids are resistant to prolonged periods at moderate levels of O_2. In this condition fish showed adaptive capacities such as increase gill surface area [45] and enhanced expression of the monocarboxylate transporter and of the oxygen transporter myoglobin [46]. In the present study it is difficult to assert that these effects take part in the recovery of the zebrafish, since the animals were exposed to short periods at lower levels of oxygen. Thus, future studies focusing on this model could reveal new mechanisms of hypoxia related to cerebral and behavioral recovery, which could have important clinical implications due to its particular features.

In summary, this study showed that zebrafish brain physiology and behavior are affected by decreased levels of O_2, similarly to traditional hypoxia–ischemia models. These effects were transient since they were reversed after periods of spontaneous recovery. Thus, our data complement existing approaches in the zebrafish hypoxia model due to the elucidation of a time window of spontaneous recovery, which brings new insights related to the search of other experimental questions that might be addressed.

Conflict of interest

The authors have declared that no competing interests exist.

Acknowledgements

This work was supported by Coordenação de Aperfeiçoamento de Pessoal de Nível Superior (CAPES), Conselho Nacional de Desenvolvimento Científico e Tecnológico (CNPq), INCT-Excitoxicidade

e Neuroproteção and by FINEP research grant "Rede Instituto Brasileiro de Neurociência (IBN-Net)" # 01.06.0842-00.

References

[1] Magistretti PJ. Brain energy metabolism. In: Zigmond MJ, Bloom FE, Landis SC, Roberts JL, Squire LR, editors. Fundamental neuroscience. San Diego: Academic Press; 1999. p. 389–413.

[2] Murphy TH, Li P, Betts K, Liu R. Two-photon imaging of stroke onset in vivo reveals that NMDAreceptor independent ischemic depolarization is the major cause of rapid reversible damage to dendritesand spines. Journal of Neuroscience 2008;28:1756–72.

[3] Hossmann KA. Pathophysiology and therapy of experimental stroke. Cellular and Molecular Neurobiology 2006;26:1057–83.

[4] Besancon E, Guo S, Lok J, Tymianski M, Lo EH. Beyond NMDA and AMPA glutamate receptors: emerging mechanisms for ionic imbalance and cell death in stroke. Trends in Pharmacological Sciences 2008;29:268–75.

[5] Zhang S, Murphy TH. Imaging the impact of cortical microcirculation on synaptic structure and sensory-evoked hemodynamic responses in vivo. PLoS Biology 2007;5:e119.

[6] Senger MR, Rosemberg DB, Rico EP, de Bem Arizi M, Dias RD, Bogo MR, et al. In vitro effect of zinc and cadmium on acetylcholinesterase and ectonucleotidase activities in zebrafish (*Danio rerio*) brain. Toxicology in Vitro 2006;20:954–8.

[7] Egan RJ, Bergner CL, Hart PC, Cachat JM, Canavello PR, Elegante MF, et al. Understanding behavioral and physiological phenotypes of stress and anxiety in zebrafish. Behavioural Brain Research 2009;205:38–44.

[8] Gerlai R. Using zebrafish to unravel the genetics of complex brain disorders. Current Topics in Behavioral Neurosciences 2012;12:3–24.

[9] Rosemberg DB, Braga MM, Rico EP, Loss CM, Córdova SD, Mussulini BH, et al. Behavioral effects of taurine pretreatment in zebrafish acutely exposed to ethanol. Neuropharmacology 2012;63:613–23.

[10] Barbazuk WB, Korf I, Kadavi C, Heyen J, Tate S, Wun E, et al. The synthetic relationship of the zebrafish and human genomes. Genome Research 2000;10:1351–8.

[11] Gerlai R, Lee V, Blaser R. Effects of acute and chronic ethanol exposure on the behavior of adult zebrafish (*Danio rerio*). Pharmacology Biochemistry and Behavior 2006;85:752–61.

[12] Roesner A, Hankeln T, Burmester T. Hypoxia induces a complex response of globin expression in zebrafish (*Danio rerio*). Journal of Experimental Biology 2006;209(Pt 11):2129–37.

[13] Roesner A, Mitz SA, Hankeln T, Burmester T. Globins and hypoxia adaptation in the goldfish, *Carassius auratus*. FEBS Journal 2008;275(14):3633–43.

[14] Yu X, Li YV. Zebrafish as an alternative model for hypoxic–ischemic brain damage. International Journal of Physiology, Pathophysiology & Pharmacology 2011;3(2):88–96.

[15] Suna C, Menga Q, Zhanga L, Wanga H, Quirionb R, Zheng W. Glutamate attenuates IGF-1 receptor tyrosine phosphorylation in mouse brain: possible significance in ischemic brain damage. Neuroscience Research 2012;74:290–7.

[16] Connell BJ, Di Iorio P, Sayeed I, Ballerini P, Saleh MC, Giuliani P, et al. Guanosine protects against reperfusion injury in rat brains after ischemic stroke. Journal of Neuroscience Research 2013;91(2):262–72.

[17] Rosemberg DB, Rico EP, Mussulini BH, Piato AL, Calcagnotto ME, Bonan CD, et al. Differences in spatiotemporal behavior of zebrafish in the open tank paradigm after a short-period confinement into dark and bright environments. PLoS ONE 2012;6(5):e19397.

[18] Blaser RE, Peñalosa YM. Stimuli affecting zebrafish (*Danio rerio*) behavior in the light/dark preference test. Physiology & Behavior 2011;104(5):831–7.

[19] Gebauer DL, Pagnussat N, Piato AL, Schaefer IC, Bonan CD, Lara DR. Effects of anxiolytics in zebrafish: similarities and differences between benzodiazepines, buspirone and ethanol. Pharmacology Biochemistry and Behavior 2011;99(3):480–6.

[20] Mathur P, Lau B, Guo S. Conditioned place preference behavior in zebrafish. Nature Protocols 2011;6(3):338–45.

[21] Mathur P, Guo S. Differences of acute versus chronic ethanol exposure on anxiety-like behavioral responses in zebrafish. Behavioural Brain Research 2011;219(2):234–9.

[22] Maximino C, da Silva AW, Gouveia Jr A, Herculano AM. Pharmacological analysis of zebrafish (*Danio rerio*) scototaxis. Progress in Neuropsychopharmacology & Biological Psychiatry 2011;35(2):624–31.

[23] Levin ED, Bencan Z, Cerutti DT. Anxiolytic effects of nicotine in zebrafish. Physiology & Behavior 2007;90(1):54–8.

[24] Blaser R, Gerlai R. Behavioral phenotyping in zebrafish: comparison of three behavioral quantification methods. Behavior Research Methods 2006;38:456–69.

[25] Wong K, Elegante M, Bartels B, Elkhayat S, Tien D, Roy S, et al. Analyzing habituation responses to novelty in zebrafish (*Danio rerio*). Behavioural Brain Research 2010;208:450–7.

[26] Cachat J, Stewart A, Grossman L, Gaikwad S, Kadri F, Chung KM, et al. Measuring behavioral and endocrine responses to novelty stress in adult zebrafish. Nature Protocols 2010;5(11):1786–99.

[27] Bencan Z, Sledge D, Levin ED. Buspirone, chlordiazepoxide and diazepam effects in a zebrafish model of anxiety. Pharmacology Biochemistry and Behavior 2009;94:75–80.

[28] Grossman L, Utterback E, Stewart A, Gaikwad S, Chung KM, Suciu C, et al. Characterization of behavioral and endocrine effects of LSD on zebrafish. Behavioural Brain Research 2010;214:277–84.

[29] López-Patiño MA, Yu L, Cabral H, Zhdanova IV. Anxiogenic effects of cocaine withdrawal in zebrafish. Physiology & Behavior 2008;93:160–71.

[30] Seibt KJ, Oliveira Rda L, Zimmermann FF, Capiotti KM, Bogo MR, Ghisleni G, et al. Antipsychotic drugs prevent the motor hyperactivity induced by psychotomimetic MK-801 in zebrafish (*Danio rerio*). Behavioural Brain Research 2010;214:417–22.

[31] Ngan AK, Wang YS. Tissue-specific transcriptional regulation of monocarboxylate transporters (MCTs) during short-term hypoxia in zebrafish (*Danio rerio*). Comparative Biochemistry and Physiology Part B, Biochemistry & Molecular Biology 2009;154(4):396–405.

[32] Parker MO, Millington ME, Combe FJ, Brennan CH. Housing conditions differentially affect physiological and behavioural stress responses of zebrafish, as well as the response to anxiolytics. PLoS ONE 2012;7(4):e34992.

[33] Preston P, Webster J. Spectrophotometric measurement of experimental brain injury. Journal of Neuroscience Methods 2000;94:187–92.

[34] Bickler PE. Clinical perspectives: neuroprotection lessons from hypoxia-tolerant organisms. Journal of Experimental Biology 2004;207:3243–9.

[35] Cao Z, Jensen LD, Rouhi P, Hosaka K, Länne T, Steffensen JF, et al. Hypoxia-induced retinopathy model in adult zebrafish. Nature Protocols 2010;5(12):1903–10.

[36] Murphy TH, Corbett D. Plasticity during stroke recovery: from synapse to behaviour. Nature Reviews Neuroscience 2009;10(12):861–72.

[37] Olmez I, Ozyurt H. Reactive oxygen species and ischemic cerebrovascular disease. Neurochemistry International 2012;60:208–12.

[38] Tucker NR, Middleton RC, Le QP, Shelden EA. HSF1 is essential for the resistance of zebrafish eye and brain tissues to hypoxia/reperfusion injury. PLoS ONE 2011;6(7):e22268.

[39] Nelson CW, Wei EP, Povlishock JT, Kontos HA, Moskowitz MA. Oxygen radicals in cerebral ischemia. American Journal of Physiology 1992;263:H1356–62.

[40] Zweier JL, Flaherty JT, Weisfeldt ML. Direct measurement of free radical generation following reperfusion of ischemic myocardium. Proceedings of the National Academy of Sciences of the United States of America 1987;84:1404–7.

[41] Gschanes A, Valousková V, Windisch M. Ameliorative influence of a nootropic drug on motor activity of rats after bilateral carotid artery occlusion. Journal of Neural Transmission 1997;104:1319–27.

[42] Balkaya M, Kröbera J, Gertz K, Peruzzaro S, Endresa M. Characterization of long-term functional outcome in a murine model of mild brain ischemia. Journal of Neuroscience Methods 2013;213:179–87.

[43] Vermeer SE, Prins ND, den Heijer T, Hofman A, Koudstaal PJ, Breteler MM. Silent brain infarcts and the risk of dementia and cognitive decline. New England Journal of Medicine 2003;348:1215–22.

[44] Pluta R, Jolkkonen J, Cuzzocrea S, Pedata F, Cechetto D, Popa-Wagner A. Cognitive impairment with vascular impairment and degeneration. Current Neurovascular Research 2011;8(4):342–50.

[45] Sollid J, De Angelis P, Gundersen K, Nilsson GE. Hypoxia induces adaptive and reversible gross morphological changes in crucian carp gills. Journal of Experimental Biology 2003;206(Pt 20):3667–73.

[46] van der Meer DL, van den Thillart GE, Witte F, de Bakker MA, Besser J, Richardson MK, et al. Gene expression profiling of the long-term adaptive response to hypoxia in the gills of adult zebrafish. American Journal of Physiology Regulatory, Integrative and Comparative Physiology 2005;289(5):R1512–9.

CAPÍTULO V

Behavioral and brain effects of diethyldithiocarbamate in adult zebrafish subjected to severe hypoxia

Artigo a ser submetido ao periódico *PLOS ONE*

Behavioral and brain effects of diethyldithiocarbamate in adult zebrafish subjected to severe hypoxia

Marcos M. Braga [1,2], Emerson S. Silva [1,2], Tarsila B. Moraes [1], Gabriel Henrique Schirmbeck [1], Eduardo P. Rico [1,2], Charles B. Pinto [1], Denis B. Rosemberg [2,3,4], Carlos S. Dutra-Filho [1], Renato D. Dias [1,2], Diogo L. Oliveira [1,2,4], Diogo O. Souza [1,2,4]*

[1] Programa de Pós-graduação em Bioquímica, Departamento de Bioquímica, Instituto de Ciências Básicas da Saúde, Universidade Federal do Rio Grande do Sul, Rua Ramiro Barcelos 2600-Anexo, 90035-003 Porto Alegre, RS, Brazil

[2] Instituto Nacional de Ciência e Tecnologia em Excitotoxicidade e Neuroproteção (INCT-EN), 90035-003 Porto Alegre, RS, Brazil

[3] Laboratório de Genética e Ecotoxicologia Molecular, Programa de Pós-graduação em Ciências Ambientais, Área de Ciências Exatas e Ambientais, Universidade Comunitária da Região de Chapecó, Avenida Senador Attílio Fontana, 591E, 89809-000 Chapecó, SC, Brazil

[4] Zebrafish Neuroscience Research Consortium (ZNRC), USA

(*) Marcos M. Braga

Departamento de Bioquímica, Instituto de Ciências Básicas da Saúde

Universidade Federal do Rio Grande do Sul

Rua Ramiro Barcelos, 2600-anexo

Zip code: 90035-003

Porto Alegre - RS - Brazil.

Phone: +55 51 33085555

Fax: +55 51 33085540

E-mail address: **marcosmbraga@gmail.com**

Abstract

The change in brain levels of reactive zinc (Zn) observed in hypoxia-ischemia has stimulated its treatment with compounds containing Zn-chelating properties, such as diethyldithiocarbamate (DEDTC). However, agents as DEDTC are redox-actives and should be better evaluated during hypoxic-isquemic injury. Thus, we use ischemic-sensitive zebrafish model in order to evaluate behavioral and neurochemical effects of DEDTC on hypoxia. For this purpose, we induced hypoxia in zebrafish into hypoxic chamber and then animals were kept for 1 h in normoxic water, with or without 0.25mM DEDTC. After treatment, fish behaviors evaluated in the open tank task showed that DEDTC did not reverse the behavioral impairment caused by hypoxia, and it did further increase these alterations. The brain assessment indicated that the increased reactive Zn levels induced by hypoxia were mitigated by DEDTC. However, the reduction in brain mitochondrial dehydrogenase activities caused by hypoxia was further affected by DEDTC. Although DEDTC has reversed the elevation in the superoxide anion level promoted by hypoxia, the compound performed no effect on nitric oxide content generated by hypoxia, and it still caused a pronounced decrease in radical hydroxyl scavenger capacity. Consequently, DEDTC trigger an increase in parameters related to antioxidant responses (sulfhydryl content and superoxide dismutase activity), which were unaltered in zebrafish only subjected to hypoxia. Although DEDTC mitigated the increased reactive Zn, the compound performed an evident pro-oxidant effect that may have led to greater behavioral changes in zebrafish subjected to hypoxia. Therefore, our data discourage the use of DEDTC for neuroprotection in hypoxia-ischemia.

Key words: hypoxia-ischemia; zinc, zebrafish, behavior, oxidative stress, diethyldithiocarbamate

Introduction

Hypoxia-ischemia is a dysfunction in the supply of oxygen (O_2) and energy caused by vascular and metabolic changes, leading to failure of part or whole organs. Specifically, brain hypoxia-ischemia is one of the main causes that triggers strokes, which is the second leading cause of death worldwide (10.64%), accounting for about 6.2 million deaths only in 2011 [1]. However, besides the large number of deaths, many people, after hypoxic-ischemic event, have chronic disability due to impairment of certain neurological conditions. Thus, it is conceivable that a large number of individuals could benefit from the development of potential neuroprotective drugs for cerebral hypoxia-ischemia.

It is well known that after ischemic episode, the neural cells subjected to low levels of O_2 and energy exhibit a sequential disruption in metabolism, consisting of the energy imbalance [2], excitotoxicity [3], inflammation and activation of the immune system [4]. Moreover, the subsequent brain reoxygenation leads to an excessive production of reactive species, including superoxide anion ($O2^{\bullet-}$), hydroxyl radical ($^{\bullet}OH$), hydrogen peroxide (H_2O_2), nitric oxide ($NO^{\bullet}$) and peroxynitrite ($ONOO^-$) [5]. Consequently, this results in apoptosis and cell necrosis [6], generating infarcted brain regions [7], followed by loss of motor and sensory functions [8]. However, the observation that ischemia trigger brain zinc dyshomeostais, has recently led to suggestion that this metal may be a novel contributor to ischemic neurodegeneration [9].

Zinc (Zn) is typically protein-bound in the central nervous system (CNS) [10,11,12]. However, about 20% of total Zn in the brain is free or loosely bound to biomolecules [13], both corresponding to the reactive Zn pool susceptible to chelation. In the brain, reactive Zn presents function important to sinaptophysiology [14]. It is a neuromodulator on several molecular targets, including synaptic

receptors and glutamate transporter [14]. However, its functional role only is maintained through the Zn transporters [15]. In fact, neuropathological accumulations of reactive Zn (e.g., in ischemia) are able to cause oxidative stress due to swelling and release of reactive species from mitochondria [16,17,18]. For this reason, the use of Zn chelators has been considered to mitigate the increased Zn levels induced by hypoxia-ischemia [19,20].

In particular, the diethyldithiocarbamate (DEDTC) is a chelator highly selective for Zn [21,22], and it has the ability to cross the blood-brain barrier [23]. In fact, it has been shown that DEDTC is beneficial against several disorders [24,25]. Because Zn-binding properties, it is postulated that this compound could have also neuroprotective action on hypoxia-ischemia. However, a care must be taken in the protective application of DEDTC, since it can cause behavioral changes [26,27,28] and an inhibitory action on superoxide dismutase (SOD) activity [29]. Moreover, DEDTC is a redox-active compound that can induce antioxidant responses [30,31], or promote the production of reactive species [32,33]. Therefore, due to the multiple actions DEDTC, the evaluation of neuroprotective effect on hypoxia-ischemia must consider not only its action on the levels of reactive Zn but also all these parameters.

The use of the recent model of severe hypoxia in adult zebrafish [34] could be useful for better understanding of the effects caused by DEDTC on cerebral hypoxia-ischemia. As advantages, zebrafish under hypoxic condition allows the investigation of drugs on a large scale manner in a non-invasive model. Importantly, recent studies have shown that this model causes brain damage similar to those triggered by hypoxia-ischemia in mammals [21,34]. Behavioral and brain impairments were also observed in fish 1 h after the hypoxic episode [21], which enables a quick evaluation of compounds-related hypoxia-ischemia. Indeed, zebrafish subjected to this model has been used to evaluate the effect of DEDTC on hypoxia [35]. In this

study it was reported that hypoxia model is able to increase the levels of brain reactive Zn [35], which it has been topographically described throughout zebrafish brain [36]. Thus, based on this initial study, additional investigations using this model could further clarify the effects promoted by DEDTC about cerebral hypoxia-ischemia.

In the present study, we evaluated the behavioral and brain effects of DEDTC on zebrafish subjected of severe hypoxia model. After treatment, with or without DEDTC, the behavioral activity of hypoxic animals was evaluated on open tank test. Next, the brain reactive Zn level of the animals was measured by the Neo-Timm method. To evaluate the DEDTC effect on brain damage induced by hypoxia, we access the activities of mitochondrial dehydrogenases by 2,3,5-triphenyltetrazolium chloride (TTC) staining. To investigate the brain oxidative balance of the experimental groups, we measured the levels of reactive species ($NO^{\bullet}$, $O2^{\bullet-}$, and $^{\bullet}OH$ scavenger capacity), the total content of sulfhydryl (-SH), and SOD activity.

Materials and methods

Animals

Male and female wild-type adult zebrafish (4-7 months-old) were obtained from commercial distributor (Delphis, RS, Brazil). The animals were kept in an aquarium rack system (Zebtec, Tecniplast, Italy) under a density of 5 fish/L and light/dark cycle of 14/10 h (lights on at 7:00 am). Fish were fed twice a day with commercial flake fish food (alcon BASIC®, Alcon, Brazil) and once a day with *Arthemia sp*. In these conditions the zebrafish were kept for at least 2 weeks prior to the experiments. The experiments were performed in reverse osmosis water supplemented with 0.018g.L^{-1} Instant Ocean® salt, which it present 7.5 mg.L^{-1} O_2, 500 µS/cm^2 of conductivity and pH 7.2 under normoxic condition. All experiments were conducted

in accordance with National Institute of Health Guide for Care and Use of Laboratory Animals. Experimental protocols were approved by the Ethics Committee of Universidade Federal do Rio Grande do Sul (number 24471 – CEUA).

Hypoxic conditions

To obtain hypoxic conditions, a hypoxia chamber was used as previously described [21,34]. Briefly, pure N_2 was perfused into the chamber until the water achieve 1.5-1.7 $mg.L^{-1}$ dissolved O_2, a concentration used to induce short-term severe hypoxia in zebrafish. Next, four fish were immediatelly transferred to the hypoxia chamber and the apparatus was hermetically sealed in order to provide a closed air tight system to cause hypoxia. The O_2 levels were kept constant during the hypoxia trials, as measurement with oxymeter (Instrutherm, São Paulo, SP, Brazil). Importantly, a hypoxia trial was considered when fish indifferently reached the third stage of hypoxia, characterized by a critical but non-lethal condition [21].

Treatment conditions after hypoxia

After hypoxia trial, each animal was individually kept in beckers containing 400 mL of normoxic water (7.5 $mg.L^{-1}$ O_2), with or without 0.2 mM DEDTC, for 1h. This DEDTC concentration was used due to potential neuroprotective effect performed in zebrafish [35]. Furthermore, we chose a treatment period of 1h, because in this period the zebrafish still have known behavioral and neurochemical changes caused by hypoxia [21].Thus, animals were divided in four groups: CONTROL, animals kept under normoxia for 1h; DEDTC, animals kept under normoxia and DEDTC for 1h; HYP1, animals subjected to hypoxia and kept under normoxia for 1h; and HYP1 + DEDTC, animals subjected to hypoxia and kept under normoxia and DEDTC for 1h. Because housing and handling have been observed to affect behavioral responses

of zebrafish [37], all animals were handled by similar conditions in order to evaluate the specific effects caused by treatment.

Open tank test

After treatment for 1h (± 3 min), some fish were behaviorally evaluate by the open tank as previously described [38]. The open tank was represented by trapezoidal plastic tank (23.9 cm along the bottom x 28.9 cm at the top x 15.1 cm high) virtually divided into three horizontal areas (bottom, middle, and top) and with five sections per area. To perform the behavioral test, the apparatus was filled with 1.5 L of normoxic water and put on a stable surface with all environmental interferences kept to a minimum. The animals were individually removed from their beckers to the open tank and the behavior was recorded for 6 min. The location and swimming activity was acquired by a webcam (Microsoft® LifeCam 1.1 with Auto-Focus) in front of the tank. The behavioral parameters were measured by video tracking software at 30 frames/s (ANY-maze®, Stoelting CO, USA). All tests were performed during the same time frame each day (between 10:00 am and 4:00 pm), and the tank water was replaced every session. After tests, fish were cryoanesthetized and euthanatized by decapitation to remove the brain.

The locomotor activity was assessed by measuring the total time mobile, distance travelled, turn angle (the variations in direction of the center point of the animal), and meandering (turn angle divided by the distance trevelled). Since it has been described a tendency of zebrafish to gradually explore top areas when subjected to open tank test [39], the vertical exploration was also evaluated by the measurement of number of transitions in top and bottom areas.

Histochemical quantification of brain reactive Zn

The reactive Zn was histochemically stained by Neo-Timm method as performed in zebrafish brain [36]. After each recovery treatment of hypoxia, the animals were euthanatized by decapitation, and the whole brain was removed in order to execute all neurochemical endpoints. To perform Neo-Tim method the brains were immediately immersed in 3% glutaraldehyde in 0.1 M phosphate buffer (pH 7.4) for 24 h, and then transferred to sodium sulfide solution (1% Na_2S) in 0.12 M Millonig's buffer for 24 h. Slices (30-µm-thick) were produced in a vibroslicer (VTS-1000;Leica), and mounted on slides. The histochemical staining was performed by incubation of slices in a solution containing silver. The reaction was conducted in the dark, and only ultrapure and metal-free solutions were used. The NIS Elements AR 2.30 software (Nikon) was used to capture the images from a light microscope (Nikon Eclipse E-600) coupled with a camera (Nikon DXM1200C CCD). To quantify reactive Zn stained by Neo-Timm, it was performed an analysis of the optic density of the total area of the periventricular gray zone of zebrafish under 10x magnification. The optic density was quantified from 8-bit gray scale images using ImageJ 1.37v software. The results were expressed in arbitrary units (a.u.), which were normalized as a percentage in relation to the control.

Measurement of brain mitochondrial activities from TTC staining

The brain mitochondrial dehydrogenases activities were evaluated by the level of formazan produced from TTC staining [21]. As previously published [40], this technique measures mitochondrial dehydrogenase activities, which are affected in episodes of hypoxia-ischemia. Briefly, the whole brains were incubated in 1 mL of phosphate buffer solution (PBS, pH 7.4) containing 2% TTC (Sigma–Aldrich, St. Louis, MO, USA) at 37ºC for 40 min in dark room. Next, the TTC was removed and 10% formalin in PBS (pH 7.4) was added in order to terminate the reaction of

mitochondrial dehydrogenases. The brains were weighed after tissues were dried at 40ºC for 2 h. Then, the brains were incubated with 200 µL of dimethylsulfoxide (DMSO) (Sigma–Aldrich, St. Louis, MO, USA) in 96 wells plates protected from light. The plates were kept under constant agitation for 4 h to solubilize the formazan produced from the TTC staining. The pink-to-red eluate of formazan was read at 490 ηm in a microplate reader. The data were expressed in absorbance per tissue dry weight (g).

Oxidative stress analyses

To measure the content of $NO^{\bullet}$, $O_2^{\bullet-}$, $^{\bullet}OH$ and SH, and to evaluate SOD activity each independent sample was performed using biological preparations from a pool of four brains. The samples were immediately kept on ice and were freshly used and homogenized (1:10, w/v) in 20 mM sodium phosphate buffer, pH 7.4 containing 140 mM KCl. The homogenates were centrifuged at 800 g for 10 min at 4°C to separate nuclei and cell debris. Protein content was measured with bovine albumin standard according to Lowry et al [41].

Reactive species evaluation

The $O_2^{\bullet-}$ levels were detected by measuring the chemiluminescence of lucigenin based on Gupte et al [42]. The supernatant (50 µL) were added in medium reaction (100 µL) with Krebs HEPES buffer (pH 8.6) in the presence of lucigenin (20 µmol/L). The samples luminescences were counting for 10 min and background (buffer and lucigenin without samples) for 5 min. The data expressed in RLU (relative luminescence unit)/min/mg tissue. Luminescence Counter (Perkin Elmer, MicroBeta TriLux) and a spectrophotometer (SpectraMax® M5) were used for the measurements.

Nitric oxide content was assessed from Griess reaction method according to Green et al. [43]. The incubation was performed at room temperature and protected from light in 96-well plates for 10 min with 50 µL of supernatant and 50 µL of Griess reagent (1:1 mixture of 1% sulfanilamide in 5% phosphoric acid and 0.1% dihydrochloride naphthylethylenediamine in water). The absorbance was measured in at 543 ηm. Nitrite concentration was represented as µmol of nitrite / mg of protein.

As previously described by Gutteridge [44], the deoxyribose assay was used to evaluate the $^{\bullet}OH$ production from the auto-reduction of ferric citrate complex. The pentose sugar is attacked by $^{\bullet}OH$ with releasing thiobarbituric acid (TBA) reactive substances. Firstly, samples were incubated at 37°C for 1 h in dark room with a medium reaction containing 3 mM 2-deoxy-D-ribose; 20 µM $FeCl_3$; 100 µM EDTA; 500 µM H_2O_2 and 100 µM ascorbate. After, 10% TCA and 0.67% TBA were added, stirred and incubated for 1 h in a boiling water bath. The absorbance determined at 532 ηm and 1,1,3,3-tetra-methoxypropane (TMP) was used as standard. Results expressed as µmol TMP/mg of protein.

Antioxidant analyses

Sulfhydryl content assay was based on the reduction of 5,5'-dithio-bis(2-nitrobenzoic acid) (DTNB) by thiols [45]. Briefly, 14 µL of homogenate were added to 270 µL of PBS buffer pH 7.4 containing 1 mM EDTA. Then 16 µL of 10 mM DTNB, prepared in a 0.2 M potassium phosphate solution pH 8.0, were added. Subsequently, 30 min incubation at room temperature in a dark room was performed. Absorption was measured at 412 ηm and results were represented as ηmol TNB/mg protein.

Superoxide dismutase activity was analyzed by Marklund [46] method based on pyrogallol autoxidation capacity. Inhibition of pyrogallol autoxidation occurs by SOD

activity which is analyzed at 420 ηm from a mix containing 15 µL samples and 235 µL of a medium reaction (50 mM Tris-HCl 1mM EDTA pH 8.2 buffer, 30 µM catalase, and 24 mM pyrogallol). A 50% inhibition of the pyrogallol autoxidation was defined as one unit of SOD and the specific activity is represented as units per mg of protein.

Statistical analysis

The values were described as means ± SEM. Behavioral and neurochemical paramaters were analyzed by two-way ANOVA, using hypoxia and DEDTC treatment as independent factors. Post hoc comparisons were performed by Tukey's test. Statistical significance was set at $p < 0.05$ level.

Results

Behavioral activity

As illustrated by representative track plots of behavioral profiles (**Figure 1A**), animals kept only on normoxia showed normal exploratory activity when exposed to open tank (NOR1). Moreover, the individual swimming traces in the apparatus showed a marked reduction in the exploratory activity of fish subjected to hypoxia (HYP1), as previously observed by us [21]. However, fish subjected to hypoxia followed by exposure to DEDTC exhibited a more intense decline in exploratory activity (HYP1 + DEDTC), and this result was similar to that shown by animals treated only with DEDTC. Regarding the occupancy plots of each experimental group (**Figure 1B**), it is suggested exploratory activity spatio-temporally similar among all groups, though there was a trend to lower exploration in apparatus top areas in DEDTC treated groups. Because differences were observed among groups, these data were further investigated using analysis of behavior endpoints.

The analyses by two-way ANOVA of parameters related to locomotion (**Figure 2**) indicated a significant effect of hypoxia on distance travelled (F[3,39] = 4.576) and turn angles (F[3,39] = 4.126). In contrast, DEDTC caused significant alterations on all locomotors parameters as observed in time mobile (F[3,39] = 11.286), distance travelled (F[3,39] = 33.898), turn angles (F[3,39] = 18.266), and meandering (F[3,39] = 21.623). The post hoc comparisons showed that the time mobile (**Figure 2A**) was not altered by hypoxia (HYP1) and in hypoxic animals treated with DEDTC (HYP1 + DEDTC), but exposure only to DEDTC caused a significant decrease in time mobile of the animals during the test. There were significant reductions in the distance travelled (**Figure 2B**) and turn angles (**Figure 2C**) in animals subjected hypoxia (HYP1). However, the administration of DEDTC in hypoxic animals (HYP1 + DEDTC) did not reverse these effects and it did further decrease the distance travelled, such as observed in group only exposure to DEDTC. In addition, the hypoxia episode (HYP1) caused no changes on meandering (**Figure 2D**), while normal (DEDTC) or hypoxic animals treated with DEDTC (HYP + DEDTC) had an increase in this parameter.

The vertical exploratory behavior showed that the time spent in bottom and top areas were not altered in hypoxia and DEDTC-treated groups (data not shown). Furthermore, transitions to top (**Figure 2E**) and bottom areas (**Figure 2F**) were observed unaltered after hypoxia, with or without DEDTC, while animals treated only with DEDTC did significantly perform less entries in both areas. Therefore, after the behavioral analysis, we performed an investigation of the neurochemical effects of hypoxia and DEDTC in order to examine an association between these data.

Brain reactive Zn

The analyses of the levels of brain reactive Zn by two-way ANOVA showed a significant effect of hypoxia (*F*[3,9] = 16.723) and DEDTC (F[3,9] = 5.281) on this endpoint. The comparison among groups (**Figure 3**) demonstrated that hypoxia caused a significant increase in reactive Zn content of zebrafish periventricular gray zone (HYP1). However, hypoxic animals treated with DEDTC (HYP1 + DEDTC) showed a mitigatory effect on the increased reactive Zn induced by hypoxia, exhibiting metal content similar to control group. Moreover, normal animals exposure to DEDTC showed no change on reactive Zn content.

Mitochondrial dehydrogenase activities in the brain

The statistical analyses indicated a significant effect of hypoxia (*F*[3,27] =33.799) and DEDTC (*F*[3,27] = 18.817) on the mitochondrial dehydrogenase activities. Indeed, animals subjected to hypoxia (HYP1) had a reduction in mitochondrial activities (**Figure 4A**) and hypoxic fish treated with DEDTC (HYP1 + DEDTC) did further decrease this parameter. The treatment with DEDTC in normal animals caused also a significant decline in mitochondrial activities.

Cerebral reactive species

The analyses by two-way ANOVA showed a significant effect of hypoxia on all reactive species, as indicated in the levels of $NO^{\bullet}$ (*F*[3,12] = 24.121), $O2^{\bullet-}$ (*F*[3,13] = 5.880), and $^{\bullet}OH$ scavenger capacity (*F*[3,13] = 56.502). The DEDTC also performed substantial effect on levels of $O2^{\bullet-}$ (*F*[3,13] = 17.617), while there was a significant interaction effect on $^{\bullet}OH$ scavenger capacity (*F*[3,13] = 11.239). The comparison among groups showed that the levels of NO• (**Figure 4B**) were increased in animals subjected to hypoxia (HYP1), but hypoxic fish treated with DEDTC (HYP1 + DEDTC) did not alter this effect. Regarding the $O2^{\bullet-}$ levels (**Figure 4C**), the hypoxic episode

induced an increase in this reactive specie (HYP1), while the hypoxic fish exposure to DEDTC (HYP1 + DEDTC) presented $O2^{\bullet-}$ content similar to the control group. The measure of $^{\bullet}OH$ scavenger capacity (**Figure 4D**) on each group demonstrated that animals had an elevated content of $^{\bullet}OH$ after hypoxia (HYP1), but treatment with DEDTC (HYP1 + DEDTC) caused a pronounced increase of this effect.

Brain antioxidant responses

The statistical evaluation of antioxidant responses indicated a significant effect of DEDTC on -SH content (F[3,14] = 53.519) and SOD activity (F[3,12] = 23.644). The hypoxia also presented a significant effect on SOD activity (F[3,12] = 5.433). The post hoc analyses on each experimental group showed that animals subjected to hypoxia did not alter -SH content (HYP1) (**Figure 4E**), while DEDTC administration to animals subjected to hypoxia caused an increase in the thiol levels (HYP1 + DEDTC). Also, the -SH content was substantially elevated in animals only treated with DEDTC. This same analysis on SOD (**Figure 4F**) showed that hypoxia caused no change in the enzyme activity (HYP1), but treatment with DEDTC in zebrafish subjected to hypoxia resulted in a significant increase in this parameter.

Discussion

The investigation of new drugs in the hypoxia-ischemia is stimulated due to the increased number of people affected by this injury. In this sense, the participation of reactive Zn content in the pathology of hypoxia-ischemia has attracted the attention of many researchers. During this brain dysfunction the exacerbated levels of reactive zinc can induce neurotoxic events culminating in neuronal death in hypoxia-ischemia [47]. Therefore, agents with Zn chelating properties, such as DEDTC, have been designed as drug candidates for the treatment of ischemia. However, in the

investigation of DEDTC effects on a model of hypoxia in zebrafish, we listed results (**Table 1**) that discourage the use of the compound to exert neuroprotection in hypoxia-ischemia, though it has exerted Zn chelating action on the increased brain Zn content.

Regarding cerebral reactive Zn we showed that hypoxia induces an increase in the levels of metal in the periventricular gray region of the zebrafish brain. Interestingly, a previous study has also reported an increase in brain reactive Zn of zebrafish after hypoxia [35]. Furthermore, exposure to DEDTC was able to decrease the content of reactive Zn close to control levels. Similarly, this result has been obtained in other studies about ischemia after Zn chelator administration [48,49]. Although Zn chelators can act directly on the metal, there is a possibility of these compounds promote this attenuating effect indirectly on pathways that induce brain reactive Zn release. In hypoxia-ischemia, it is known that the increased levels of reactive Zn are mainly induced by $NO^{\bullet}$, which is widely produced in this condition [50,51]. Thus, considering this role of $NO^{\bullet}$, our data demonstrated that the action of DEDTC was more related to direct reactive Zn chelating intervention, since the $NO^{\bullet}$ levels were unchanged by the compound.

As the production of reactive species is a major cause of cellular injury that occurs in hypoxia-ischemia, we did measure the levels of $NO^{\bullet}$, $O2^{\bullet-}$, $^{\bullet}OH$ scavenger capacity and mitochondrial dehydrogenase activities. Our data showed that brain reactive species were elevated after 1 h of hypoxia, which the animals did also show significant damage on mitochondrial activities. In fact, mitochondrial injury is an eminent effect caused by brain hypoxia-ischemia [52], leading to increased levels of these reactive species [5]. In order to reverse these effects we expose the hypoxic animals to DEDTC and as a result we observe a decrease of $O2^{\bullet-}$ levels and no change on the levels of $NO^{\bullet}$. In contrast, hypoxic fish treated with DEDTC did further

enhance mitochondrial injury. Consequently, this may have led to substantial smaller $^{\bullet}OH$ scavenger capacity in animals treated with DEDTC, indicating that the compound may have performed a pro-oxidant effect on its neural cells. Indeed, the decrease in the levels of $O2^{\bullet-}$ contrary this hypothesis. However, as $O2^{\bullet-}$ can serve as a substrate for the formation of highly reactive $^{\bullet}OH$ in Haber-Weiss reactions [53], it is reasonable to think that these effects are simultaneously provoked in animals of this group. Therefore, based on all these results it is supported that DEDTC failed to exert protection of brain mitochondrial damage, and it still did more increase this effect caused by hypoxia, probably by the $^{\bullet}OH$ formation.

Since the SOD plays a key role in maintaining of fine-tuning regulation of $O2^{\bullet-}$ [54] and the total sulfhydryl refer mainly to the level of non-oxidized proteins [45], these two parameters are related to the cellular antioxidant defenses. In this sense, despite high levels of reactive species we observed that the animals showed no changes on these brain parameters after 1h of hypoxia episode. In fact, it has been reported that the increase in several brain antioxidant enzymes (e.g., SOD) occur 72h after ischemic event [55]. Furthermore, we have previously observed that the brain mitochondrial damage generated by hypoxia in zebrafish begins to be reversed after 24h, which we suppose is due to induction of antioxidant responses [21]. Therefore, these results seem indicate a non-activation of antioxidant more than a redox balance adaptation after 1h of hypoxia. In contrast, administration of DEDTC did induce SOD activity and an increase of the reduced thiol content in brain of animals subjected to hypoxia. Although these data indicate an induction of antioxidant response, these effects are consistent with a possible pro-oxidant state generated by the compound. In accordance with this, Rahden-Staroń et al. [32] have shown that the *per se* administration of DEDTC on cell culture generates oxidative damage to proteins and lipids along with the induction of antioxidant enzymes

activities and production of glutathione, which is an SH-containing molecule. Thus, the hypothesis that DEDTC may have presented a pro-oxidant effect in the brain of hypoxic animals is also reinforced by alterations in these parameters. Nevertheless, the induction of SOD in this group shows that neurotoxic effects generated by DEDTC were not caused by an inhibition of the enzyme.

Behavioral changes are a common effect observed after a hypoxic-ischemic event. For example, it is known that hypoxia-ischemia causes locomotor changes [56,57] and cognitive decline in rodents [58,59], while hypoxia induces behavioral changes related to exploratory activity in zebrafish [21]. Here, we confirmed this alteration caused by hypoxia in zebrafish that did show significant reduction on the distance travelled and turn angles. However, DEDTC did not reverse these effects and it did still increase behavioral changes. Indeed, other studies have shown that administration of DEDTC can lead behavioral disorders such as locomotor alterations [22,60] and damages to the memory in rodents [26,27,28]. Overall, our data showed only a main effect of DEDTC on the behavioral parameters of zebrafish, suggesting that these locomotor and cognitive disturbances may have also occurred in hypoxic-fish treated with DEDTC.

Based on our results, DEDTC did mitigate the brain levels of reactive Zn induced by hypoxia. However, hypoxic animals treated with DEDTC showed an increase in brain mitochondrial damage and a decrease $^{\bullet}OH$ scavengers, which may have contributed to trigger greater behavioral alterations. This leads us to postulate that the compound may have performed a pro-oxidant role, which was further reinforced by the fact that *per se* administration of DEDTC (DEDTC group) also caused impairments on mitochondrial and behavioral parameters. Indeed, there is a range of studies showing that DEDTC has pro-oxidative properties, which may lead to cellular apoptosis and necrosis [32,61,62]. Despite these effects, a previous study

has shown that exposure of zebrafish to 0.25mM DEDTC, after hypoxia episode, results in neuroprotection of brain mitochondrial changes and induces no change on behavior [35]. However, these authors obtained these effects through a shorter exposure time of DEDTC (30min), and no behavioral task was tested, making it difficult to compare these results. Therefore, though DEDTC has mitigated the increased cerebral reactive Zn our data demonstrated that it failed to protect zebrafish of the hypoxia-induced effects, which was a similar result obtained in a traumatic brain injury model [63].

In summary, in the present study we have observed a detrimental effect of DEDTC on brain hypoxia. However, along with this finding, our data demonstrated that the hypoxia model in zebrafish is a promising tool for studies involving parameters related to ischemia. Although the fish are commonly resistant to hypoxia, the zebrafish has been reported as a less tolerant species to low O_2 levels [64]. Indeed, many effects caused by brain ischemia in other vertebrates have extended to the zebrafish subjected to hypoxic chamber. Thus, given their advantageous characteristics, the use of this model may help in future pre-clinical trials of other potential drugs related to brain hypoxia-ischemia.

Acknowledgements

This work was supported by Coordenação de Aperfeiçoamento de Pessoal de Nível Superior (CAPES), Conselho Nacional de Desenvolvimento Científico e Tecnológico (CNPq), INCT-Excitoxicidade e Neuroproteção and by FINEP research grant “Rede Instituto Brasileiro de Neurociência (IBN-Net)” # 01.06.0842-00. The authors declare no competing financial interests.

References

1. World Health Organiztion (2013) The top 10 causes of death. Available: http://www.who.int/mediacentre/factsheets/fs310/en/. [Accessed 01 February 2014].

2. Obrenovitch TP, Richards DA (1995) Extracellular neurotransmitter changes in cerebral ischaemia. Cerebrovasc Brain Metab Rev 7: 1-54

3. Choi DW, Rothman SM (1990) The role of glutamate neurotoxicity in hypoxic-ischemic neuronal death. Annu Rev Neurosci 13: 171-182.

4. Becker KJ (1998) Inflammation and acute stroke. Curr Opin Neurol 11: 45-49.

5. Collard CD, Gelman S (2001) Pathophysiology, clinical manifestations, and prevention of ischemia-reperfusion injury. Anesthesiology 94: 1133-1138.

6. Besancon E, Guo S, Lok J, Tymianski M, Lo EH (2008) Beyond NMDA and AMPA glutamate receptors: emerging mechanisms for ionic imbalance and cell death in stroke. Trends Pharmacol Sci 29: 268-275.

7. Murphy TH, Li P, Betts K, Liu R (2008) Two-photon imaging of stroke onset in vivo reveals that NMDA receptor independent ischemic depolarization is the major cause of rapid reversible damage to dendrites and spines. J Neurosci 28: 1756-1772.

8. Hossmann KA (2006) Pathophysiology and therapy of experimental stroke. Cell Mol Neurobiol 26: 1057-1083.

9. Shuttleworth CW, Weiss JH (2011) Zinc: new clues to diverse roles in brain ischemia. Trends Pharmacol Sci 32: 480-486.

10. Frederickson CJ, Klitenick MA, Manton WI, Kirkpatrick JB (1983) Cytoarchitectonic distribution of zinc in the hippocampus of man and the rat. Brain Res 273: 335-339.

11. Frederickson CJ, Rampy BA, Reamy-Rampy S, Howell GA (1992) Distribution of histochemically reactive zinc in the forebrain of the rat. J Chem Neuroanat 5: 521-530.

12. Klitenick MA, Frederickson CJ, Manton WI (1983) Acid-vapor decomposition for determination of zinc in brain tissue by isotope dilution mass spectrometry. Anal Chem 55: 921-923.

13. Cole TB, Robbins CA, Wenzel HJ, Schwartzkroin PA, Palmiter RD (2000) Seizures and neuronal damage in mice lacking vesicular zinc. Epilepsy Res 39: 153-169.

14. Paoletti P, Vergnano AM, Barbour B, Casado M (2009) Zinc at glutamatergic synapses. Neuroscience 158: 126-136.

15. Lichten LA, Cousins RJ (2009) Mammalian zinc transporters: nutritional and physiologic regulation. Annu Rev Nutr 29: 153-176.

16. Dineley KE, Richards LL, Votyakova TV, Reynolds IJ (2005) Zinc causes loss of membrane potential and elevates reactive oxygen species in rat brain mitochondria. Mitochondrion 5: 55-65.

17. Jiang D, Sullivan PG, Sensi SL, Steward O, Weiss JH (2001) Zn(2+) induces permeability transition pore opening and release of pro-apoptotic peptides from neuronal motochondria. J Biol Chem 276:47524-47529.

18. Weiss JH, Sensi SL, Koh JY (2000) Zn (2+): a novel ionic mediator of neural injury in brain disease. Trends Pharmacol Sci 21:395-401.

19. Carter RE, Weiss JH, Shuttleworth CW (2010) Zn^{2}+ chelation improves recovery by delying spreading depression-like events. Neuroreport 21: 1060-1064.

20. Grabrucker AM, Rowan M, Garner CC (2011) Brain-delivery of zinc-ions as potential treatment for neurological diseases: mini review. Drug Deliv Lett 1: 13-23.

21. Braga MM, Rico EP, Córdova SD, Pinto CB, Blaser RE, Dias RD, Rosemberg DB, Oliveira DL, Souza DO (2013) Evaluation of spontaneous recovery of behavioral and brain injury profiles in zebrafish after hypoxia. Behav Brain Res 253: 145-151.

22. Foresti ML, Arisi GM, Fernandes A, Tilelli CQ, Garcia-Cairasco N (2008) Chelatable zinc modulates excitability and seizure duration in the amygdale rapid kindling model. Epilepsy Res 79: 166-172.

23. Guillaumin JM, Lepape A, Renoux G (1986) Fate and distribution of radioactive sodium diethyldithiocarbamate (imuthiol) in the mouse. Int J Immunopharmacol 8: 859-865.

24. Biagini G, Sala D, Zini I (1995) Diethyldithiocarbamate, a superoxide dismutase inhibitor, counteracts the maturation of ischemic-like lesions caused by endothelin-1 intrastriatal injection. Neurosci Lett 190: 212-216.

25. Daocheng W, Mingxi W (2010) Preparation of the core-shell structure adriamycin lipiodol microemulsions and their synergistic anti-tumor effects with diethyldithiocarbamate in vivo. Biomed Pharmacother 64: 615-623.

26. Daumas S, Halley H, Lassalle JM (2004) Disruption of hippocampal CA3 network: effects on episodic-like memory processing in C57BL/6J mice. Eur. J Neurosci 20: 597-600.

27. Frederickson RE, Frederickson CJ, Danscher G (1990) In situ binding of bouton zinc reversibly disrupts performance on a spatial memory task. Behav Brain Res 38: 25-33.

28. Lassalle JM, Bataille T, Halley H (2000) Reversible in activation of the hippocampal mossy fiber synapses in mice impairs spatial learning, but neither consolidation nor memory retrieval, in the Morris navigation task. Neurobiol Learn Mem 73: 243-257.

29. Heikkila RE, Cabbat FS, Cohen G (1976) In vivo inhibition of superoxide dismutase in mice by diethyldithiocarbamate. J Biol Chem 251: 2182-2185.

30. Koster JF, van Berkel TJ (1983) The effect of diethyldithiocarbamate on the lipid peroxidation of rat-liver microsomes and intact hepatocytes. Biochem Pharmacol 32: 3307–3310.

31. Liu J, Shigenaga MK, Yan LJ, Mori A, Ames BN (1996) Antioxidant activity of diethyldithiocarbamate. Free Radic Res 24: 461–472.

32. Rahden-Staroń I, Grosicka-Maciąg E, Kurpios-Piec D, Czeczot H, Grzela T, Szumiło M (2012) The effects of sodium diethyldithiocarbamate in fibroblasts V79 cells in relation to cytotoxicity, antioxidative enzymes, glutathione, and apoptosis. Arch Toxicol 86: 1841-1850.

33. Viquez OM, Lai B, Ahn JH, Does MD, Valentine HL, Valentine WM (2009) N,N-diethyldithiocarbamate promotes oxidative stress prior to myelin structural changes and increases myelin copper content. Toxicol Appl Pharmacol 239: 71-79.

34. Yu X, Li YV (2011) Zebrafish as an alternative model for hypoxic–ischemic brain damage. Zebrafish 3: 88-96.

35. Yu X, Li YV (2013) Neuroprotective effect of zinc chelator DEDTC in a zebrafish (Danio rerio) Model of Hypoxic Brain Injury. Zebrafish 10: 30-35.

36. Braga MM, Rosemberg DB, de Oliveira DL, Loss CM, Córdova SD, Rico EP, Silva ES, Dias RD, Souza DO, Calcagnotto ME (2013) Topographical analysis of reactive zinc in the central nervous system of adult zebrafish (Danio rerio). Zebrafish 10: 376-388.

37. Parker MO, Millington ME, Combe FJ, Brennan CH (2012) Housing conditions differ-entially affect physiological and behavioural stress responses of zebrafish, aswell as the response to anxiolytics. PLoS ONE 7: e34992.

38. Rosemberg DB, Rico EP, Mussulini BH, Piato AL, Calcagnotto ME, Bonan CD, Dias RD, Blaser RE, Souza DO, de Oliveira DL (2012) Differences in spatiotemporal behavior of zebrafish in the open tank paradigmafter a short-period confinement into dark and bright environments. PLoS ONE 6: e19397.

39. Blaser R, Gerlai R (2006) Behavioral phenotyping in zebrafish: comparisonof three behavioral quantification methods. Behavior Research Methods 38: 456-469.

40. Preston P, Webster J (2000) Spectrophotometric measurement of experimental brain injury. J Neurosci Methods 94: 187-192.

41. Lowry OH, Rosebrough NJ, Lewis Farr A, Randall RJ (1951) Protein measurement with Folin phenol reagent. J Biol Chem 193: 265-275.

42. Gupte SA, Levine RJ, Gupte RS, Young ME, Lionetti V, Labinskyy V, Floyd BC, Ojaimi C, Bellomo M, Wolin MS, Recchia FA (2006) Glucose-6-phosphate dehydrogenase-derived NADPH fuels superoxide production in the failing heart. J Moll Cell Cardiol 41: 340-349.

43. Green LC, Wagner DA, Glogowski J, Skipper PL, Wishnok JS, Tannenbaum SR (1982) Analysis of nitrate, nitrite and nitrate in biological fluids. Anal Biochem 126: 131-138.

44. Gutteridge JMC (1991) Hydroxyl radical formation from the auto-reduction of a ferric citrate complex. Free Rad Biol Med 11: 401-406.

45. Aksenov MY, Markesbery WR (2001) Changes in thiol content and expression glutathione redox system genes in the hippocampus and cerebellum in Alzheimer’s disease. Neurosci Lett 302, 141-145.

46. Marklund SL (1985) Pyrogallol autoxidation. In: Greenwald RA (ed) CRC Handbook of Methods for Oxygen Radical Research. CRC Press, Boca Raton, pp 243-247.

47. Choi DW, Koh JY (1998) Zinc and brain injury. Annu Rev Neurosci 21: 347-375.

48. Koh JY, Suh SW, Gwag BJ, He YY, Hsu CY, Choi DW (1996) The role of zinc in selective neuronal death after transient global cerebral ischemia. Science 272: 1013-1016.

49. Suh SW, Chen JW, Motamedi M, Bell B, Listiak K, Pons NF, Danscher G, Frederickson CJ (2000) Evidence that synaptically-released zinc contributes to neuronal injury after traumatic brain injury. Brain Res 852: 268-273.

50. Cuajungco MP, Lees GJ (1998) Nitric oxide generators produce accumulation of chelatable zinc in hippocampal neuronal perikarya. Brain Res 799: 118-129.

51. Frederickson CJ, Cuajungco MP, LaBuda CJ, Suh SW (2002) Nitric oxide causes apparent release of zinc from presynaptic boutons. Neuroscience 115: 471-474.

52. Dirnagl U, Iadecola C, Moskowitz MA (1999) Pathobiology of ischaemic stroke: an integrated view. Trends Neurosci 22: 391-397.

53. Halliwell B, Gutteridge JMC (2007) Free radicals in biology and medicine. Ed 4. Clarendon Press, Oxford.

54. Halliwell B (2006) Reactive species and antioxidants. Redox biology is a fundamental theme of aerobic life. Plant Physiol 141: 312-322.

55. Mahadik SP, Makar TK, Murthy JN, Ortiz A, Wakade CG, Karpiak SE (1993) Temporal changes in superoxide dismutase, glutathione peroxidase, and

catalase levels in primary and peri-ischemic tissue. Monosialoganglioside (GM1) treatment effects. Mol Chem Neuropathol 18: 1-14.

56. Balkaya M, Kröbera J, Gertz K, Peruzzaro S, Endresa M (2013) Characterization of long-term functional outcome in a murine model of mild brain ischemia. J Neurosci Methods 213: 179-187.

57. Gschanes A, Valousková V, Windisch M (1997) Ameliorative influence of a nootropicdrug on motor activity of rats after bilateral carotid artery occlusion. J Neural Transm 104: 1319-1327.

58. Pluta R, Jolkkonen J, Cuzzocrea S, Pedata F, Cechetto D, Popa-Wagner A (2011) Cognitive impairment with vascular impairment and degeneration. Curr Neurovasc Res 8: 342-350.

59. Vermeer SE, Prins ND, den Heijer T, Hofman A, Koudstaal PJ, Breteler MM (2003) Silent brain infarcts and the risk of dementia and cognitive decline. N Engl J Med 348: 1215-1222.

60. Dominguez MI, Blasco-Ibanez JM, Crespo C, Marques-Mari AI, Martinez-Guijarro FJ (2003) Zinc chelation during non-lesioning overexcitation results in neuronal death in the mouse hippocampus. Neuroscience 116: 791-806.

61. Kimoto-Kinoshita S, Nishida S, Tomura TT (2004) Diethyldithiocarbamate can induce two different type of death: apoptosis and necrosis mediating the differential MAP kinase activation and redox regulation in HL60 cells. Mol Cell Biochem 265: 123-132.

62. Zucconi GG, Laurenzi MA, Semprevivo M, Torni F, Lindgren JA, Marinucci E (2002) Microglia activation and cell death in response to diethyl-dithiocarbamate acute administration. J Comp Neurol 446: 135-150.

63. Doering P, Stoltenberg M, Penkowa M, Rungby J, Larsen A, Danscher G (2010) Chemical blocking of zinc ions in CNS increases neuronal damage following traumatic brain injury (TBI) in mice. PLoS ONE 5: e10131.

64. Roesner A, Mitz SA, Hankeln T, Burmester T (2008) Globins and hypoxia adaptation in the goldfish, Carassius auratus. FEBS J 275: 3633-3643.

Figure Legends

Figure 1. Exploratory profiles of zebrafish after hypoxia followed by normoxic treatment, with or without DEDTC. (A) Representative track plots illustrating the path travelled by fish in the apparatus. (B) Occupancy plots of each experimental group showing the duration in each area of the open tank. CONTROL, animals under normoxia for 1h; DEDTC, animals kept under normoxia and DEDTC for 1h; HYP1, animals subjected to hypoxia and kept under normoxia for 1h; and HYP1 + DEDTC, animals subjected to hypoxia and kept under normoxia and DEDTC for 1h.

Figure 2. Locomotory activity and vertical exploration after hypoxia followed by normoxic treatment, with or without DEDTC. The figure represents the analysis of basic locomotor paramaters, such as time mobile (A), distance travelled (B), turn angle (C), and meandering (D). The spacial exploration of the animals was represented in transitions to top (E) and bottom areas (F) of the open tank. CONTROL, animals under normoxia for 1h; DEDTC, animals kept under normoxia and DEDTC for 1h; HYP1, animals subjected to hypoxia and kept under normoxia for 1h; and HYP1 + DEDTC, animals subjected to hypoxia and kept under normoxia and DEDTC for 1h. Data represent means ± SEM (n = 9). Different letters indicate statistical differences at $p < 0.05$ level (two-way ANOVA followed by Tukey's post hoc test).

Figure 3. Reactive Zn in the optic tectum of zebrafish brain stained with Neo-Timm after hypoxia followed by normoxic treatment, with or without DEDTC. The higher reactive Zn content is indicated by the presence of the darker granules. The figures in (E-H) represent higher magnification of the area delimited by red square in (A-D). Optic densities of periventricular gray zone is showed in I. CONTROL, animals under normoxia for 1h; DEDTC, animals kept under normoxia and DEDTC

for 1h; HYP1, animals subjected to hypoxia and kept under normoxia for 1h; and HYP1 + DEDTC, animals subjected to hypoxia and kept under normoxia and DEDTC for 1h. Bars represent 200 µm in A-D panels, and 400 µm in E-H panels. In I the values are presented as the mean ± SEM (*n* = 3-4). Different letters indicate statistical differences at $p < 0.05$ level (two-way ANOVA followed by Tukey's post hoc test).

Figure 4. Brain effect of hypoxia followed by normoxia, with or without DEDTC, on mitochondrial dehydrogenase activities, reactive species and antioxidant responses. In (A) is showed mitochondrial activities (*n* = 7-9). The lowest values indicate greater inhibition of mitochondrial enzymes. The levels of $NO^{\bullet}$, $O_2^{\bullet-}$ and $^{\bullet}OH$ scavenger capacities are demonstrated in (B), (C) and (D), respectively. The SH contents are showed in (E) and SOD activities are represented in (F) (*n* = 4-5). CONTROL, animals under normoxia for 1h; DEDTC, animals kept under normoxia and DEDTC for 1h; HYP1, animals subjected to hypoxia and kept under normoxia for 1h; and HYP1 + DEDTC, animals subjected to hypoxia and kept under normoxia and DEDTC for 1h. Data are presented as the means ± SEM. Distinct letters indicate statistical differences at $p < 0.05$ level (two-way ANOVA followed by Tukey's post hoc test).

Table 1. Behavioral and neurochemical effects on each experimental group in comparison to control.

TYPE	PARAMETER	DEDTC	HYP1	HYP1 + DEDTC
BEHAVIORAL	Time mobile	-	0	0
	Distance travelled	- -	-	- -
	Turn angle	-	-	-
	Meandering	+	0	+
	Entries to top area	-	0	0
	Entries to bottom area	-	0	0
NEUROCHEMICAL	Reactive Zn	0	+	0
	Mitochondrial actvities	-	-	- -
	Nitric oxide	0	+	+
	Superoxide anion	0	+	0
	Scavenger capacity ($^{\bullet}OH$)	0	+	+ +
	Total sulfhydryl	+	0	+
	SOD activity	0	0	+

DEDTC: animals kept under normoxia and DEDTC for 1h; HYP1: animals subjected to hypoxia and kept under normoxia for 1h; HYP1 + DEDTC: animals subjected to hypoxia and kept under normoxia and DEDTC for 1h. (0), no change in relation to control (-), reduction in relation to control; (+) elevation in relation to control.

FIGURE 1

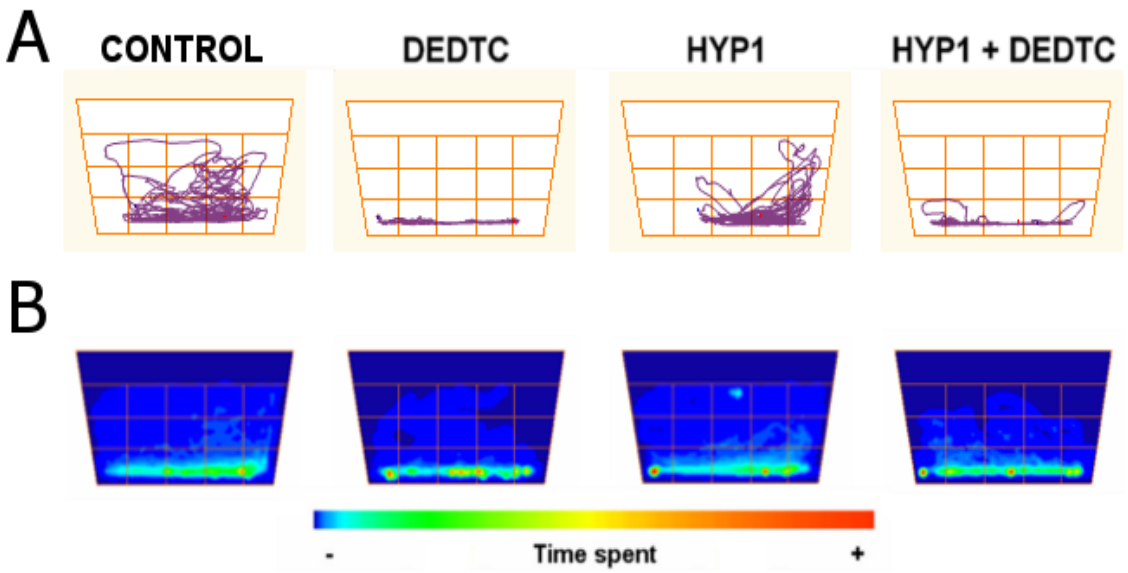

FIGURE 2

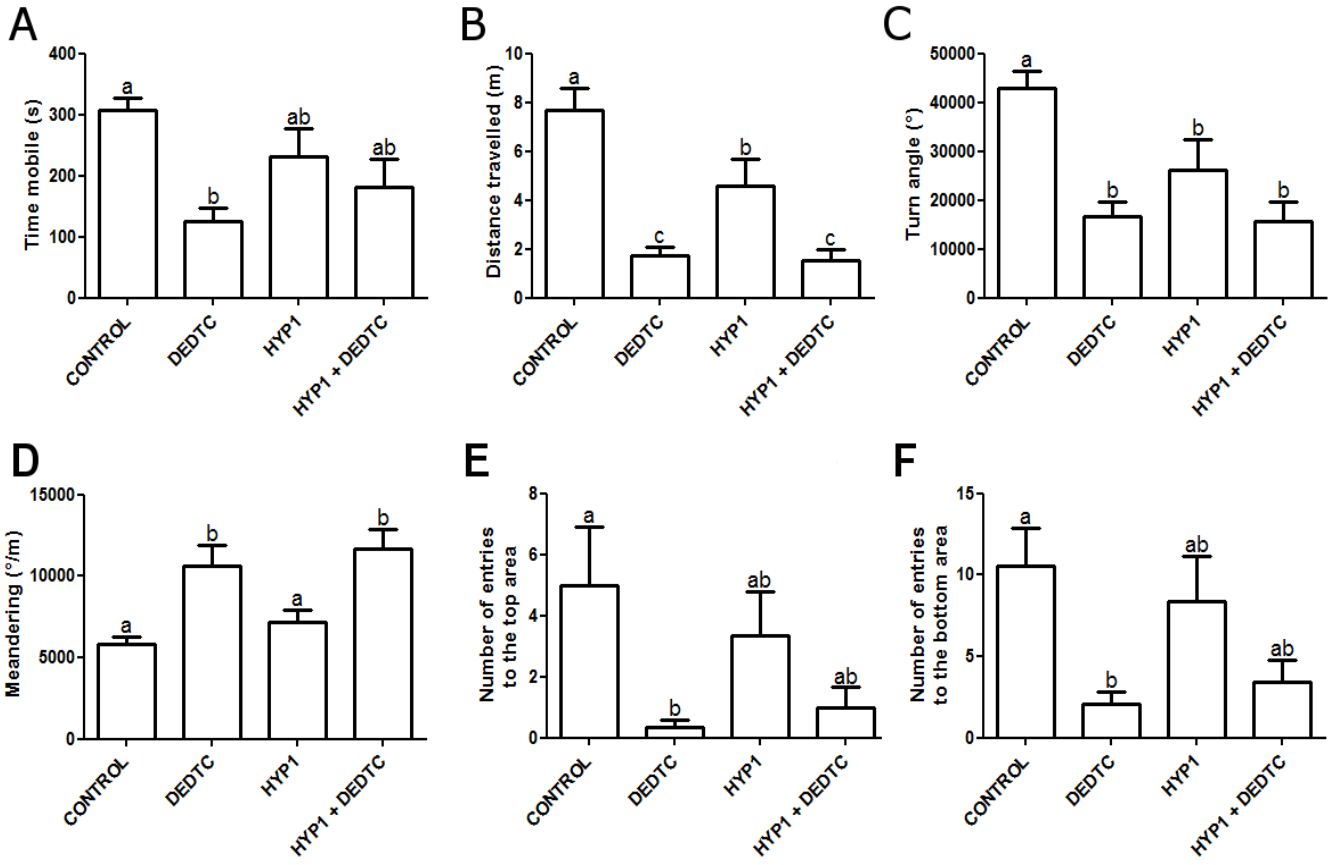
A
Time mobile (s)
400
300
200
100
0
a
b
ab
ab
CONTROL
DEDTC
HYP1
HYP1 + DEDTC
B
Distance travelled (m)
10
8
6
4
2
0
a
c
b
c
CONTROL
DEDTC
HYP1
HYP1 + DEDTC
C
Turn angle (°)
50000
40000
30000
20000
10000
0
a
b
b
b
CONTROL
DEDTC
HYP1
HYP1 + DEDTC
D
Meandering (°/m)
15000
10000
5000
0
a
b
a
b
CONTROL
DEDTC
HYP1
HYP1 + DEDTC
E
Number of entries to the top area
8
6
4
2
0
a
b
ab
ab
CONTROL
DEDTC
HYP1
HYP1 + DEDTC
F
Number of entries to the bottom area
15
10
5
0
a
b
ab
ab
CONTROL
DEDTC
HYP1
HYP1 + DEDTC

FIGURE 3

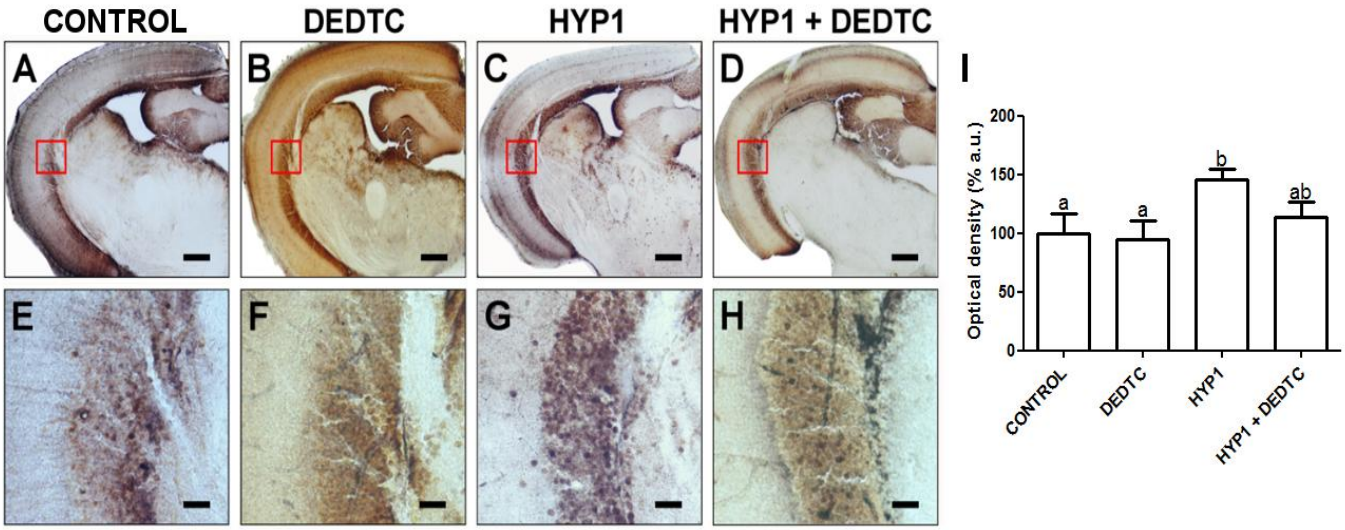
CONTROL
DEDTC
HYP1
HYP1 + DEDTC
A
B
C
D
E
F
G
H
I
Optical density (% a.u.)
200
150
100
50
0
a
a
b
ab
CONTROL
DEDTC
HYP1
HYP1 + DEDTC

FIGURE 4

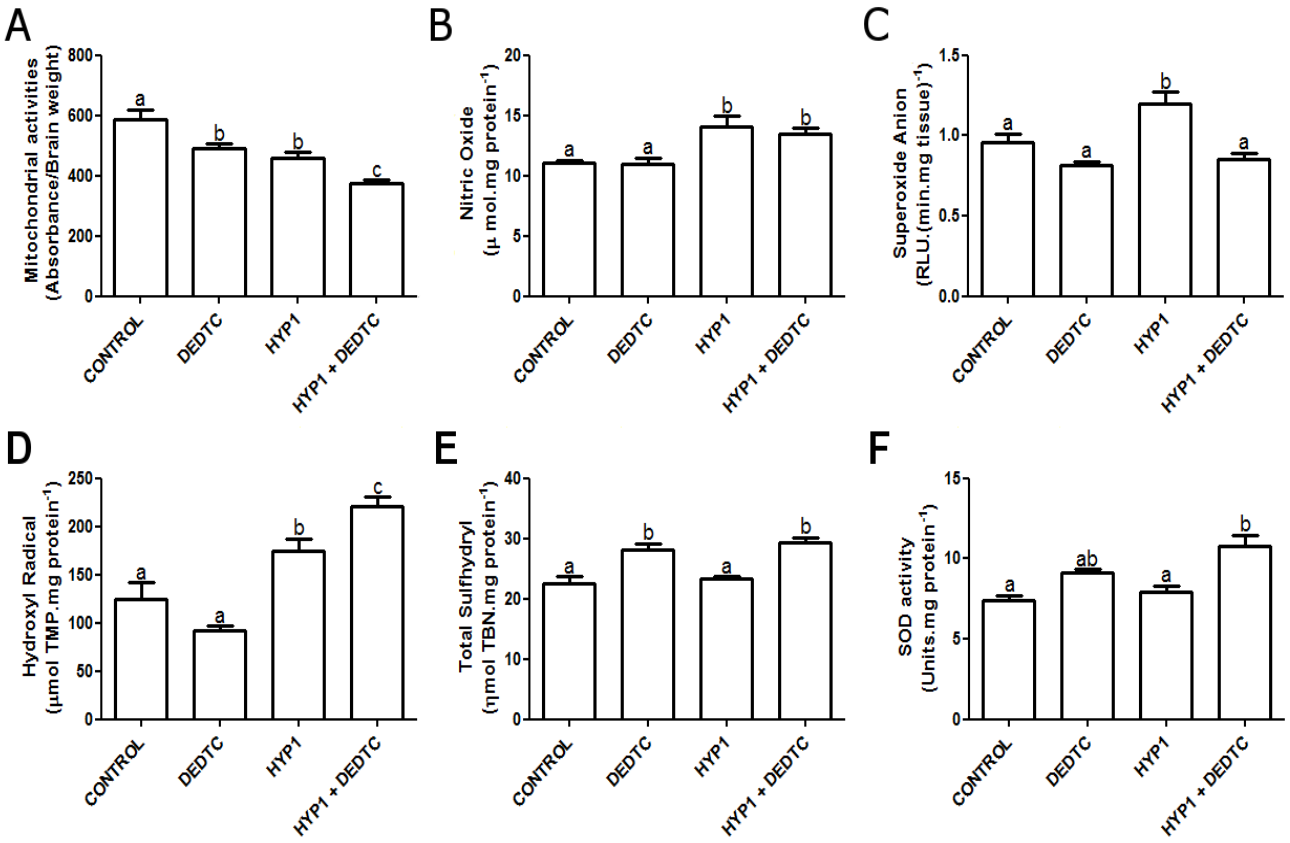
A
Mitochondrial activities (Absorbance/Brain weight)
800
600
400
200
0
a
b
b
c
CONTROL
DEDTC
HYP1
HYP1 + DEDTC
B
Nitric Oxide (µ mol.mg protein-1)
20
15
10
5
0
a
a
b
b
CONTROL
DEDTC
HYP1
HYP1 + DEDTC
C
Superoxide Anion (RLU.(min.mg tissue)-1)
1.5
1.0
0.5
0.0
a
a
b
a
CONTROL
DEDTC
HYP1
HYP1 + DEDTC
D
Hydroxyl Radical (µmol TMP.mg protein-1)
250
200
150
100
50
0
a
a
b
c
CONTROL
DEDTC
HYP1
HYP1 + DEDTC
E
Total Sulfhydryl (ηmol TBN.mg protein-1)
40
30
20
10
0
a
b
a
b
CONTROL
DEDTC
HYP1
HYP1 + DEDTC
F
SOD activity (Units.mg protein-1)
15
10
5
0
a
ab
a
b
CONTROL
DEDTC
HYP1
HYP1 + DEDTC

PARTE III

1. DISCUSSÃO

1.1 Zn reativo no cérebro de peixe-zebra

1.1.1 Especificidade do método Neo-Timm para marcar Zn reativo em peixe-zebra

No presente estudo, nós mostramos que o cérebro de peixe-zebra contém Zn reativo, agregando-o ao grupo de modelos animais com conhecida distribuição cerebral do metal revelado por Neo-Timm. Contudo, isto só pôde ser confirmado através do uso de diferentes abordagens metodológicas, dado que a técnica de Neo-Timm poderia marcar outros metais como ferro e cobre (Danscher, 1981).

O teste com compostos para quelar Zn reativo é uma estratégia metodológica bastante utilizada para comprovar a especificidade do método de Neo-Timm sobre novos modelos experimentais. Embora estas substâncias possam se ligar a outros íons divalentes, a escolha de TPEN e DEDTC para este propósito é considerada adequada, pois ambos são classificados como fortes quelantes de Zn reativo (Paoletti, 2009). Na prática, a administração intraperitoneal (i.p.) de TPEN e DEDTC causa uma diminuição na marcação desenvolvida por Neo-Timm, em regiões cerebrais com conhecido conteúdo de Zn reativo (Foresti et al., 2008; Lees et al, 1998). Aqui, nós mostramos que a exposição *in vitro* de cérebros de peixe-zebra a 5 mM de TPEN fez diminuir parcialmente os níveis de marcação, colocando em dúvida se a marcação histoquímica remanescente era devida a aplicação de concentrações não-saturáveis do quelante, ou mesmo, a indicação da presença de outros metais no conteúdo revelado por Neo-Timm. Conforme já fora reportado uma diminuição na marcação de Zn reativo em função da dose de DEDTC em roedores (Foresti et al., 2008), a concentração de TPEN pode ter sido insuficiente para

mobilizar todo o Zn reativo cerebral de peixe-zebra. Baseado neste estudo, nós administramos nos peixes, uma dose de DEDTC capaz de quelar todo o Zn reativo de roedores, e, de fato, isto preveniu totalmente a marcação, indicando que o método revela regiões contendo Zn reativo no cérebro do peixe-zebra. Além disso, o uso de soluções degradantes de sulfeto de Zn fez, substancialmente, diminuir a marcação de Neo-Timm (principalmente com HCl), indicando uma contribuição negligível de outros metais.

Mesmo tendo comprovado a especificidade da marcação de Neo-Timm no cérebro dos peixes, nós conduzimos ainda uma marcação alternativa de Zn reativo através de sonda fluorescente. Estas sondas possuem um caráter mais específico para marcar Zn reativo do que Neo-Timm, sendo adotado o uso delas para fins de comparação entre ambas as técnicas (Frederickson et al., 2004a; Ketterman & Li, 2008). Portanto, com a aplicação de ZP1 nós mostramos regiões cerebrais de peixe-zebra com elevada concentração de Zn reativo, as quais foram coincidentes com as demonstradas por Neo-Timm.

Em conclusão, todos estes testes demonstram a alta especificidade de Neo-Timm para marcar Zn reativo cerebral de peixe-zebra. Assim, através da densidade óptica de sua marcação, este método pode ser utilizado para quantificar o conteúdo de Zn reativo de regiões cerebrais específicas do peixe.

1.1.2 Distribuição topográfica e citoarquitectônica do Zn reativo em cérebro de peixe-zebra

Desde que o Neo-Timm foi instituído como técnica para a determinação dos níveis de Zn reativo, o conteúdo do metal no cérebro de diferentes espécies de vertebrados tem sido predominantemente localizado em estruturas telencefálicas como córtex, amígdala e, principalmente, hipocampo (Paoletti et al., 2009). Além

disso, um trabalho mostrou que o tálamo de roedores também possui conteúdo de Zn reativo (Mengual et al., 2001). Comparado a este último achado, nós temos encontrado elevado conteúdo de Zn reativo em estruturas talâmicas de peixe-zebra. Contudo, a maior parte do conteúdo de Zn reativo do peixe-zebra está concentrada em estruturas do rombencéfalo, enquanto que o telencéfalo, em geral, apresentou um baixo nível de Zn reativo. Em conformidade com este resultado, Piñuela e colaboradores (1992) mostraram que uma espécie de truta também contém um nível inferior de Zn reativo no telencéfalo quando comparado com outras partes do seu cérebro. Assim, a união dos resultados obtidos nestas duas espécies suporta a hipótese de que este grupo de animais possui uma distribuição bastante distinta do metal em relação a outros vertebrados.

A constatação de que, o telencéfalo desses animais apresenta um conteúdo bastante reduzido de Zn reativo, faz refletir sobre as razões que teriam protagonizado esta característica exclusiva entre os vertebrados. Ao menos em peixe-zebra, isto poderia ser explicado por distintas organizações neurobiológicas que ocorrem na formação do telencéfalo desses animais, resultando em estruturas bastante rudimentares, tal como o córtex e o hipocampo (Mueller et al., 2011). De fato, em mamíferos é mostrado que o rico conteúdo hipocampal de Zn reativo é concentrado dentro de terminais sinápticos inervados por células pertencentes a complexas vias cerebrocorticais (Frederickson et al., 2005). Desta forma, os circuitos mais simples destas duas estruturas podem ter sido determinantes para que o peixe-zebra apresente um nível reduzido de Zn reativo no telencéfalo.

Em relação à localização citoarquitectônica, através da co-marcação com as técnicas de Nissl e Neo-Timm foi possível mostrar que o peixe-zebra contém Zn reativo em regiões “neuropilares” e em regiões limítrofes a corpos celulares de neurônios. Além disso, a localização de Zn reativo no neuropilo foi mais comumente

encontrada em estruturas do rombencéfalo dos peixes, enquanto o telencéfalo mostrou apenas o segundo tipo de localização. A detecção no neuropilo indica que o peixe-zebra compartilha pelo menos em parte com a localização de Zn reativo dos roedores (Frederickson et al., 1992). Contudo, o Zn reativo situado próximo ao corpo celular de neurônios tem sido, exclusivamente, observado em truta (Piñuela et al., 1992), e agora também em peixe-zebra. Embora seja necessário um estudo de microscopia eletrônica para identificar a localização precisa deste conteúdo de Zn reativo, é esperado que nestas regiões do peixe-zebra ele esteja predominantemente acima dos neurônios, dado que todo o conteúdo cerebral de Zn reativo marcado por ZP1 foi detectado fora dos corpos celulares. Se isto for confirmado, a presença de Zn reativo nestas regiões poderia indicar a presença de sinapses axo-somáticas contendo Zn, tal como tem sido especulado para o cérebro de truta (Piñuela et al., 1992).

1.2 Células neurais contendo Zn reativo no cérebro de peixe-zebra

1.2.1 Especificidade do método para identificar e quantificar células neurais contendo Zn reativo no cérebro de peixe-zebra

Em razão da detecção de Zn reativo em peixe-zebra, em um passo seguinte nós buscamos identificar as células neurais que contêm Zn reativo no cérebro desses animais. Contudo, a inexistência de métodos práticos para esta avaliação nos encorajou a padronizar uma técnica que permitisse a identificação e quantificação cerebral de células neurais, contendo ou não, Zn reativo, assim como o conteúdo intracelular do metal nestas células.

Desta maneira, usando peixe-zebra como amostra, uma medida rigorosa destas células foi alcançada através da aplicação de 1% de PFA. De fato, as

amostras fixadas não tiveram nenhuma perda de neurônios glutamatérgicos, ao contrário das preparações de células neurais não-fixadas. Outro aspecto importante, é que o nosso método preveniu qualquer acréscimo artificial, que poderia ocorrer sobre o conteúdo intracelular de Zn reativo, ao manter, constantemente, as células neurais fixadas sob soluções com Ca-EDTA. Como um cuidado adicional, a suplementação de Ca-EDTA em soluções fisiológicas é recomendada para estudos envolvendo Zn reativo, pois ele é um quelante impermeável a membranas biológicas e com alta afinidade para metais divalentes (Smith & Martell, 2003), sendo capaz de minimizar possíveis contaminações experimentais de Zn (Kay, 2004). Portanto, após a padronização do protocolo, a nossa técnica permitiu obter, de forma rápida, a porcentagem de células neurais contendo Zn reativo em toda uma amostra de cérebro. Em combinação com o número total de células neurais obtido pelo método de quantificação de núcleos neurais (Herculano-Houzel & Lent, 2005), estes dados possibilitaram a determinação do número de células contendo Zn reativo em todo o cérebro.

1.2.2 Quantificação de astrócitos e neurônios glutamatérgicos contendo Zn reativo em cérebro de peixe-zebra

A aplicação do nosso método sobre peixe-zebra adulto mostrou que o cérebro desses animais tem ~50% de astrócitos (~400.000 células) e ~30% de neurônios glutamatérgicos (~250.000 células), enquanto que o número de astrócitos e neurônios glutamatérgicos contendo Zn foi bastante semelhante (respectivamente, ~55.000 e ~70.000 células). Conforme nossos dados, nós estimamos que 2 a cada 15 astrócitos e 2 a cada 7 neurônios glutamatérgicos têm Zn reativo no cérebro do peixe-zebra, indicando que apenas um subgrupo da sua população de neurônios glutamatérgicos contêm Zn reativo, tal como observado em outros vertebrados

(Sindreu et al., 2003). Entretanto, um trabalho recente mostrou que Zn reativo também é encontrado em astrócitos de outros modelos, o que suportaria a participação das células gliais na homeostasia do Zn reativo cerebral (Sekler & Silverman, 2012). Em acordo com estes trabalhos, nós encontramos um considerável número de astrócitos contendo Zn no cérebro de peixe-zebra. Além disso, nós conseguimos observar que ~4% de todas as células contendo Zn não foram identificadas como astrócitos ou neurônios glutamatérgicos. Assim, outras células neurais no cérebro de peixe-zebra podem conter Zn reativo, tal como neurônios GABAérgicos e glicinérgicos, que no cordão espinal de lampreia são células que contêm Zn (Birinyi et al., 2001).

1.2.3 Níveis intracelulares de Zn reativo em astrócitos e neurônios glutamatérgicos de peixe zebra

Pela análise dos níveis intracelulares de Zn reativo nós observamos que o conteúdo de Zn reativo é mais abundante em neurônios glutamatérgicos do que em astrócitos. Interessantemente, no estudo anterior nós descrevemos altos níveis de Zn reativo localizados em regiões cerebrais de peixe-zebra, que contêm conhecida população de neurônios glutamatérgicos (Braga et al., 2013a). Contudo, aqui, nós mostramos pela primeira vez a co-localização entre os neurônios glutamatérgicos e o elevado conteúdo de Zn reativo de peixe-zebra. Conforme mencionado, anteriormente, outros vertebrados também contêm altos níveis de Zn reativo em neurônios glutamatérgicos, dentro de suas vesículas sinápticas (Paoletti et al., 2009). Realmente, no presente estudo, nós não conseguimos determinar a exata localização subcelular de Zn reativo nestes neurônios, mas a aplicação do nosso protocolo sobre distintas frações celulares (por exemplo, sinaptossomas) poderia atingir este objetivo.

1.3 Localização subcelular de Zn reativo no cérebro de peixe-zebra

Ao demonstrar que os maiores níveis cerebrais de Zn reativo estão concentrados dentro dos mesmos neurônios, nós buscamos determinar o compartimento subcelular onde estaria este conteúdo do metal no peixe-zebra. Entretanto, conforme demonstrado nos APÊNDICES A e B, as análises das marcações histoquímicas por microscopia eletrônica de transmissão não nos permitiram obter uma localização precisa do Zn reativo nestas células do peixe-zebra. Na verdade, em outra espécie de peixe teleósteo já foi descrita a presença de terminais sinápticos contendo Zn reativo na região do telencéfalo (Yamane et al., 1996). Embora ainda tenha que ser demonstrada a presença de Zn reativo dentro de vesículas glutamatérgicas de peixe-zebra, a descoberta de que esses animais contêm Zn reativo no cérebro acaba ao menos subsidiando o uso deste modelo em triagem pré-clínica de substâncias com potencial ação sobre o conteúdo cerebral de Zn reativo.

1.4 Efeitos neuro-comportamentais de DEDTC relacionados ao conteúdo de Zn cerebral

O DEDTC está entre os compostos com potencial ação quelante de metais, o qual tem sido usado no tratamento de diversas doenças. Contudo, a aplicação terapêutica de DEDTC, em geral, requer altas doses de DEDTC, a qual pode resultar em efeitos adversos sobre o conteúdo cerebral de Zn. De fato, ao expor o peixe-zebra sob estes níveis de DEDTC, nós observamos mudanças, dependentes da concentração, sobre o comportamento e nos níveis de Zn cerebral.

1.4.1 Efeitos comportamentais de DEDTC

É notável que somente poucos estudos têm focado a atenção para avaliar os efeitos comportamentais causados por altas concentrações de DEDTC. Aqui, nós mostramos que a exposição a 5 mM de DEDTC resultou em perda de postura e morte, enquanto 1 mM de DEDTC causou nado acelerado (*"burst swimming"*) e comportamentos tipo-crise. Em roedores, outros trabalhos reportaram uma diminuição na locomoção (Domínguez et al., 2003; Foresti et al., 2008) e comportamentos tipo-crise (Blasco-Ibáñez et al., 2004), sugerindo que altas concentrações de DEDTC podem agir como um pró-convulsivante (Domínguez et al., 2003; Mitchell & Barnes, 1993). Ainda, Haycock e colaboradores (1978) demonstraram um registro eletro-encefalográfico de crises induzidas por alta concentração de DEDTC em ratos, o qual sugere um efeito convulsivo do composto. Desta forma, como nós observamos comportamentos tipo-crise, tal como àqueles induzidos em peixe-zebra por clássicos agentes convulsivantes (Alfaro et al., 2011; Baraban et al., 2005; Mussulini et al., 2013), um maior cuidado deveria ser tomado com o uso de altas concentrações de DEDTC.

1.4.2 Acúmulo cerebral de DEDTC e o efeito quelante de Zn reativo

A indução de comportamento anormal é uma eminente consequência da exposição ao DEDTC. Neste sentido, nós mostramos pela primeira vez que as mudanças comportamentais causadas pela exposição a altas concentrações de DEDTC foram relacionadas com o acúmulo cerebral do composto. Além disso, a análise por marcação histoquímica e por citometria de fluxo revelou que estes efeitos foram acompanhados por uma redução de Zn reativo cerebral (~40%). Em relação a isto, a diminuição nos níveis de Zn reativo por DEDTC vem sendo associada com prejuízos comportamentais em roedores, resultando em um efeito pró-convulsivo nesses animais (Blasco-Ibáñez et al., 2004; Domínguez et al., 2003;

Mitchell & Barnes, 1993). Concordando com estes trabalhos, nossos resultados também mostraram que DEDTC teve efeito quelante de Zn somente naquelas concentrações que induziram alterações comportamentais, tal como o comportamento tipo-crise.

1.4.3 Efeitos de DEDTC sobre o conteúdo de Zn reativo de neurônios glutamatérgicos e astrócitos

De acordo com a análise citométrica, os neurônios glutamatérgicos mostraram uma redução do conteúdo de Zn reativo (~35%) depois da exposição 1 e 5 mM de DEDTC. A diminuição nos níveis de Zn reativo dessas células é associada a uma suscetibilidade a convulsões em ratos tratados com dieta deficiente em Zn (Takeda et al., 2003) e em camundongos “knockout” para o transportador vesicular ZnT-3 (Cole et al., 2000). Isto fortalece a hipótese de que o conteúdo de Zn desses neurônios tem importante função sobre as manifestações comportamentais induzidas por altas concentrações de DEDTC. Assim, é possível que a ação de DEDTC tenha implicação sobre homeostasia da rede neural, dado que o Zn reativo liberado de neurônios glutamatérgicos pode modular células neurais vizinhas, incluindo astrócitos (Paoletti et al., 2009). Embora os astrócitos tenham uma quantidade de Zn reativo, substancialmente, inferior aos neurônios glutamatérgicos (Sekler and Silverman, 2012), nós temos observado que as células gliais tiveram uma redução no conteúdo do metal (~35%) após a exposição a 0,2 e 5 mM de DEDTC, tal como demonstrado em um estudo prévio (Sekler & Silverman, 2012). Entretanto, após exposição a 1 mM de DEDTC, o conteúdo astrocitário de Zn reativo foi similar ao controle. De fato, a captação astrocitária de Zn advindo de outras fontes (p. ex., neurônios glutamatérgicos) poderia ser a razão para o aumento nas células gliais tratadas com 1 mM de DEDTC, conforme já fora

demonstrado durante crises induzidas pelo ácido caínico (Revuelta et al., 2005). Portanto, reunindo todos estes dados, é possível afirmar que altas concentrações de DEDTC causam distintos efeitos neurotóxicos sobre conteúdo de Zn reativo de neurônios glutamatérgicos e astrócitos.

1.4.4 Ação de DEDTC sobre a atividade da δ-ALA-D

Como o DEDTC alterou o conteúdo de Zn reativo, outras frações de Zn cerebral poderiam também ser afetadas. Por exemplo, a δ-ALA-D é uma enzima que contém Zn, rigidamente ligado à estrutura molecular, mas altas concentrações de quelante de Zn podem inibir sua atividade (Emanuelli et al., 1998). Embora os efeitos de DEDTC sobre a atividade cerebral da δ-ALA-D sejam ainda desconhecidos, nossos dados indicaram nenhuma mudança na atividade da enzima dos peixes expostos ao DEDTC. A administração de DEDTC em ratos também resultou em nenhuma alteração sobre a atividade da δ-ALA-D hepática e sanguínea (Khandelwal et al., 1987). Certamente, a investigação sobre outras biomoléculas contendo Zn ligado à sua estrutura poderia esclarecer se altas concentrações de DEDTC são incapazes de mobilizar esta fração de Zn cerebral. Mesmo assim, é razoável afirmar que os efeitos neurotóxicos de DEDTC descritos aqui foram mais relacionados à sua ação quelante sobre o Zn reativo do que sobre a fração do metal fortemente associado a biomoléculas.

1.4.5 DEDTC: toxicidade x neuroproteção

Em resumo, os resultados deste trabalho fornecem uma base para o entendimento maior do mecanismo neurotóxico causado por altas concentrações de DEDTC, considerando sua potencial ação quelante de Zn cerebral. Como DEDTC pode prejudicar a função de outros alvos-moleculares, futuros estudos poderiam

esclarecer ainda mais seus efeitos neurotóxicos. Contudo, nossos dados reforçam o cuidado com o uso de DEDTC como fármaco protetor devido à sua propriedade quelante. Prestando atenção nisto, Qazi e colegas (1988) determinaram, em um estudo clínico, a dose de 150 mg/kg como limitante para os efeitos tóxicos de DEDTC. Aqui, DEDTC mostrou ter poucos efeitos neurotóxicos somente em 0.2 mM (ou < 100 mg/kg de tecido cerebral). Nesta mesma linha, estudos prévios demonstraram que nestas concentrações de DEDTC são obtidos efeitos benéficos contra várias desordens (Daocheng & Mingxi, 2010; Pang et al., 2007). Além disso, Yu & Li (2013) reportaram uma ação neuroprotetora com 0,25 mM de DEDTC em um modelo experimental de hipóxia em peixe-zebra. Assim, através de todos estes dados, é plausível que nesta concentração os efeitos protetores de DEDTC se sobreponham a sua ação tóxica.

1.5 Avaliação da recuperação espontânea das alterações comportamentais e cerebrais de peixes-zebra submetido a um modelo de hipóxia cerebral severa

A fim de avaliar o possível efeito neuroprotetor de DEDTC sobre as alterações comportamentais e cerebrais induzidos por hipóxia-isquemia, nós selecionamos um modelo de hipóxia severa recentemente descrito para peixe-zebra adulto (Yu & Li, 2011). Entretanto, por ser um modelo novo ainda era necessário saber se os danos induzidos por hipóxia em peixe-zebra eram permanentes ou se eram recuperados de forma espontânea em condições de normóxia. Por esta razão, neste estudo, nós nos detemos somente a este último objetivo.

1.5.1 Dano cerebral durante o episódio de hipóxia

Primeiramente, nós mostramos que os animais apresentaram uma sensibilidade cerebral ao modelo de hipóxia, reduzindo ~25% a atividade das desidrogenases mitocondriais. Conforme Preston & Webster (2000) demonstraram, o principal impacto desses dados é que eles estão relacionados à presença de áreas cerebrais infartadas, as quais já foram observadas em peixes-zebra submetidos à hipóxia (Yu & Li, 2011). Assim, os nossos resultados indicam que os danos cerebrais induzidos pelo modelo de hipóxia estariam, diretamente, correlacionados com o 1º e 2º estágios (Braga et al., 2013b). Embora este parâmetro isolado tenha mostrado que as atividades mitocondriais foram sensíveis à privação de O_2 até o segundo estágio da hipóxia, é razoável sugerir que a manutenção deste efeito no estágio subsequente poderia resultar em sequelas mais persistentes. Por esta razão nós escolhemos o 3º estágio de hipóxia para avaliar a recuperação espontânea de peixe-zebra sob condições de normóxia.

1.5.2 Dano cerebral durante a recuperação do episódio de hipóxia

Através dos nossos dados foi observado que o dano cerebral causado por hipóxia persisitu até 24 h após o episódio hipóxico. Durante este período, os peixes exibiram um pequeno aumento nos danos cerebrais, tornando este resultado comparável ao efeito desencadeado pela reperfusão em modelos de isquemia. Nestes modelos se sabe bem que o dano cerebral é intensificado devido à formação de radicais livres, induzida pela reoxigenação cerebral (Olmez & Ozyurt, 2012). Se a produção de espécies reativas contribui para a redução da atividade mitocondrial, no presente estudo, este efeito poderia ser completamente revertido depois de 48 h da hipóxia. Realmente, em outros modelos, o dano cerebral causado por hipóxia-isquemia é revertido devido a uma diminuição tempo-dependente de espécies reativas a níveis normais (Nelson et al., 1992; Zweier et al., 1987),

podendo este fato ser o responsável pela recuperação das atividades das desidrogenases mitocondriais após os animais ficarem 48 h sob normóxia.

1.5.3 Dano locomotor durante a recuperação do episódio de hipóxia

A diminuição das atividades mitocondriais, refletindo em áreas cerebrais infartadas, indica que estes animais poderiam desenvolver desordens motoras e sensoriais, prejudicando suas performances sobre tarefas comportamentais. Neste sentido, alguns estudos já observaram disfunções locomotoras em roedores após a isquemia (Balkaya et al., 2013; Gschanes et al., 1997). Com relação aos nossos dados, é demonstrado que os peixes, 1 h após a hipóxia, também apresentam um déficit locomotor. Entretanto, os prejuízos causados na locomoção dos animais foram revertidos 3 h após a hipóxia. Estes resultados mostram a elevada capacidade do peixe-zebra para recuperar as funções locomotoras, mesmo depois de episódio de hipóxia, capaz de conduzir a morte. Em vista disto, uma importante questão que surge é se a melhora dos seus parâmetros locomotores é devido à recuperação verdadeira ou a comportamentos compensatórios. Existe uma grande dificuldade na detecção de uma verdadeira recuperação, da qual pode ocorrer quando é poupada parte do tecido cerebral, que é crucial para determinada função (Murphy & Corbett, 2009). Todavia, como o dano cerebral induzido por hipóxia foi transiente, nossos dados sugerem a ocorrência de uma recuperação verdadeira neste modelo.

1.5.4 Dano sobre a atividade exploratória durante a recuperação do episódio de hipóxia

A análise espaço-temporal do comportamento mostrou que, quando o peixe-zebra teve um prejuízo locomotor, os animais não apresentaram o típico aumento

no número de entradas no topo e no fundo do “open tank”. De acordo com estudos prévios, é esperado, durante o teste, um aumento gradual no número de transições e na duração do tempo na área do topo do aparato, refletindo uma habituação comum do peixe-zebra a novidade (Blaser & Gerlai, 2006; Rosemberg et al., 2012). Baseado nisto, a análise dos parâmetros exploratórios verticais, mostrou que os peixes, 1h após a hipóxia, apresentaram prejuízos quanto à habituação ao aparato, indicando que este tempo é insuficiente para a recuperação espontânea dos comportamentos relacionados à locomoção e exploração. Em contraste, depois de 3h de recuperação foi observado que estes efeitos causados por hipóxia foram amplamente revertidos. Portanto, estes resultados demonstram a recuperação das estratégias exploratórias, simultaneamente, com os parâmetros locomotores, sugerindo que os prejuízos sobre a locomoção poderiam ser responsáveis pela mudança no perfil exploratório destes peixes.

1.5.5 Potencialidade do uso do modelo

Nossa análise também mostra que os danos cerebrais e comportamentais causados por hipóxia são recuperados em tempos distintos. Em relação ao dano cerebral, o nível das atividades mitocondriais foi restabelecido em 48h, enquanto que os comportamentos foram, aparentemente, normais depois de 3h. O fato dos peixes apresentarem recuperação comportamental em um curto período não significa que outros efeitos causados por hipóxia não são mantidos em um prazo mais longo, como, por exemplo, declínio cognitivo, que é freqüentemente observado em indivíduos que têm sofrido hipóxia-isquemia (Pluta et al., 2011; Vermeer et al., 2013). Desta maneira, futuros estudos, com foco neste modelo, poderão revelar novos mecanismos de hipóxia relacionados à recuperação comportamental e

cerebral, que poderiam ter importantes implicações clínicas devido a suas características particulares.

Em resumo, este trabalho mostrou que o comportamento e a fisiologia cerebral de peixe-zebra são afetados por níveis baixos de O_2, similarmente, a tradicionais modelos de hipóxia-isquemia. Contudo, estes efeitos foram transientes, sendo revertidos depois de períodos de recuperação espontânea. Apesar disto, nossos dados mostraram pela primeira vez a janela de tempo da recuperação espontânea dos animais que sofreram hipóxia. Portanto, isto permite o uso do modelo para a avaliação de fármacos candidatos a neuroproteção em hipóxia-isquemia (por exemplo, DEDTC), uma vez que se torna viável a distinção entre a recuperação espontânea e o efeito destes compostos em futuras triagens.

1.6 Avaliação do efeito de DEDTC sobre as alterações comportamentais e cerebrais causadas por hipóxia cerebral severa em peixe-zebra

A investigação de fármacos com ação sobre a hipóxia-isquemia é estimulada devido ao enorme número de pessoas afetadas por esta disfunção. Neste sentido, a participação do conteúdo de Zn reativo na patologia da hipóxia-isquemia tem atraído a atenção de muitos pesquisadores. Durante esta disfunção cerebral os níveis aumentados de Zn reativo podem induzir eventos neurotóxicos, culminando na morte de neurônios (Choi & Koh, 1998). Portanto, agentes químicos com propriedades quelantes de Zn, tal como o DEDTC, têm sido designados como fármacos candidatos para o tratamento da isquemia. Entretanto, na investigação dos efeitos de DEDTC, sobre o modelo de hipóxia em peixe-zebra, nós listamos resultados que desencorajam o seu uso como composto neuroprotetor em hipóxia-isquemia.

1.6.1 Ação de DEDTC no elevado conteúdo de Zn reativo induzido por hipóxia

Em relação ao Zn reativo cerebral, nós mostramos que a hipóxia induz um aumento nos níveis do metal na região periventricular do cérebro de peixe-zebra. Interessantemente, um estudo prévio também reportou um aumento no Zn reativo no cérebro de peixe-zebra após a hipóxia (Yu & Li, 2013). Além disso, a exposição ao DEDTC foi capaz de diminuir o conteúdo de Zn reativo próximo aos níveis do controle. Interessantemente, este resultado foi similar ao obtido em outros estudos sobre a administração de quelante de Zn após isquemia (Koh et al., 1996; Suh et al., 2000). Embora quelantes de Zn possam agir diretamente sobre o metal, existe a possibilidade destes compostos afetarem vias neuroquímicas que induzem a liberação de Zn reativo. Em hipóxia-isquemia, se sabe que o aumento nos níveis de Zn reativo é induzido principalmente por NO•, o qual é amplamente produzido nesta condição (Cuajungco & Lees, 1998; Frederickson et al., 2002). Desta maneira, conforme os níveis de NO• foram inalterados pela ação de DEDTC, os nossos dados demonstraram que, provavelmente, o composto causou uma direta ação quelante de Zn reativo.

1.6.2 Ação de DEDTC sobre as alterações induzidas por hipóxia nas atividades das desidrogenases mitocondriais e nos níveis de espécies reativas

Os nossos dados demonstraram que a produção de espécies reativas cerebrais ($NO^{\bullet}$, $O2^{\bullet-}$ e $^{\bullet}OH$) foram elevadas após 1 h do evento hipóxico, e este resultado foi acompanhado por uma significante diminuição das atividades mitocondriais. De fato, o dano mitocondrial é um eminente efeito causado por hipóxia-isquemia cerebral (Dirnagl et al., 1999), conduzindo ao aumento destas espécies reativas (Collard & Gelman, 2001). A fim de reverter estes efeitos os animais hipóxicos foram expostos ao DEDTC e como resultado nós observamos

uma diminuição de $O2^{\bullet-}$ e nenhuma mudança sobre $NO^{\bullet}$. Em contraste, os peixes hipóxicos tratados com DEDTC apresentaram uma diminuição ainda maior sobre as atividades mitocondriais. Consequentemente, isto pode ter sido a razão para estes animais apresentarem uma diminuição mais acentuada em *"scavengers"* de $^{\bullet}OH$, indicando que o composto pode ter causado um efeito pró-oxidante sobre suas células neurais. Realmente, a diminuição nos níveis $O2^{\bullet-}$ contraria esta hipótese. Contudo, como $O2^{\bullet-}$ é um substrato para a formação de $^{\bullet}OH$ em reações de Haber-Weiss (Halliwell & Gutteridge, 2007), é razoável supor que estes efeitos foram provocados simultaneamente nos peixes deste grupo. Portanto, baseado nestes resultados é suportado que o DEDTC não reverteu o dano mitocondrial, aumentando ainda mais o efeito nocivo causado pela hipóxia, provavelmente pela formação de $^{\bullet}OH$.

1.6.3 Ação de DEDTC sobre parâmetros relacionados à resposta antioxidante em animais submetidos à hipóxia

Apesar dos altos níveis de espécies reativas, nós observamos que, após 1 h da hipóxia, os animais não apresentaram mudanças sobre parâmetros relacionados a defesas celulares antioxidantes (sulfidrilas totais e atividade da SOD). De fato, o aumento em várias enzimas antioxidantes cerebrais (por exemplo, SOD) pode ocorrer após 72 h do evento isquêmico (Mahadik et al., 1993). Além disso, previamente, nós temos observado que o dano mitocondrial gerado pela hipóxia começa a ser revertido após 24 h em cérebro de peixe-zebra, quando nós supomos ocorrer a indução de respostas antioxidantes (Braga et al., 2013b). Portanto, estes resultados parecem indicar mais uma falta de ativação de respostas antioxidantes do que uma adaptação do balanço redox celular após 1 h da hipóxia. Em contraste, o DEDTC aumentou a atividade da SOD e o conteúdo de tióis reduzidos no cérebro

dos animais submetidos à hipóxia. Embora estes dados indiquem uma indução neural de respostas antioxidantes, estes efeitos são consistentes com um possível estado pró-oxidante gerado pelo composto. Em acordo com esta hipótese, Rahden-Staroń e colaboradores (2012) mostraram que o tratamento *per se* de DEDTC, em cultura de células, gera danos oxidativos a proteínas e lipídios juntamente com a indução de enzimas antioxidantes e a produção de glutationa. Assim, a hipótese de que o DEDTC pode ter apresentado um efeito pró-oxidante nos animais hipóxicos é reforçada pelas alterações nestes parâmetros. Contudo, o aumento da atividade da SOD nestes mesmos animais mostra que os efeitos neurotóxicos gerados por DEDTC não foram causados pela inibição da enzima.

1.6.4 Efeito de DEDTC sobre prejuízos comportamentais induzidos por hipóxia

As mudanças comportamentais são comumente observadas após eventos hipóxico-isquêmicos. Por exemplo, se sabe que, em roedores, a hipóxia-isquemia causa mudanças locomotoras (Balkaya et al., 2013; Gschanes et al., 1997) e declínio congnitivo (Pluta et al., 2011; Vermeer et al., 2013), enquanto em peixe-zebra são observadas mudanças relacionadas à atividade exploratória no “open tank” até 1 h após a hipóxia (Braga et al., 2013b). Aqui, nós confirmamos estas alterações causadas pela hipóxia em peixe-zebra, tendo estes animais apresentado uma redução sobre a distância percorrida e em ângulo de giros. Entretanto, DEDTC não reverteu estes efeitos e ele ainda causou um aumento nas alterações comportamentais induzidas por hipóxia. Outros estudos têm mostrado que a administração de DEDTC pode conduzir a desordens comportamentais, tais como, alterações locomotoras (Domínguez et al., 2003; Foresti et al., 2008) e danos a memória de roedores (Daumas et al., 2004; Frederickson et al., 1990; Lassalle et al., 2000). Conforme nossos dados mostraram, principalmente, um efeito de DEDTC

nos parâmetros comportamentais, é presumível que estes distúrbios locomotores e cognitivos tenham ocorrido também em peixes hipóxicos tratados com DEDTC.

1.6.5 Efeito pró-oxidante de DEDTC sobre animais hipóxicos e o uso do modelo para a triagem de outros fármacos candidatos à neuroproteção em isquemia

Baseado em nossos resultados, o DEDTC atenuou os níveis cerebrais de Zn reativo induzidos pela hipóxia. Entretanto, animais hipóxicos tratados com DEDTC mostraram um aumento no dano mitocondrial e uma diminuição na capacidade redutora de $^{\bullet}OH$, da qual podem ter contribuído para desencadear maiores alterações comportamentais. Isto nos fez postular que o composto executou um provável papel pró-oxidante, o qual foi reforçado pelo fato da exposição *per se* de DEDTC ter também causado um prejuízo sobre os parâmetros comportamentais e mitocondriais. Existem inúmeros estudos mostrando que o DEDTC tem propriedades pró-oxidantes, as quais podem levar a apoptose e necrose celular (Kimoto-Kinoshita et al., 2004; Rahden-Staroń et al., 2012; Zucconi et al., 2002). Apesar destes efeitos, um estudo prévio mostrou que, após a hipóxia, a exposição de peixes-zebra a 0.25 mM de DEDTC resulta em neuroproteção das alterações mitocondriais e em nenhuma alteração comportamental (Yu & Li, 2013). Todavia, os autores obtiveram estes efeitos em um tempo mais curto de exposição ao DEDTC (30 min), e nenhuma tarefa comportamental foi testada nesses animais, o que dificulta a comparação destes resultados. Desta maneira, mesmo que o DEDTC tenha atenuado o aumento de Zn reativo cerebral, o composto falhou em proteger o peixe-zebra dos efeitos induzidos pela hipóxia, sendo este resultado similar ao obtido em um modelo de trauma encefálico (Doering et al., 2010).

2. CONCLUSÕES GERAIS

Devido as suas vantagens intrínsecas como um modelo vertebrado mais simples, o peixe-zebra tem sido usado em diversas áreas da neurociência. Até o presente momento estes estudos iniciais têm provado que esses peixes respondem a conhecidos fármacos psicoativos, de forma bastante próxima a mamíferos, indicando que eles conservam a base neurofisiológica de vertebrados superiores. Contudo, jamais havia sido investigada a presença e função de Zn reativo no cérebro desses animais, embora a importância desta fração do metal sobre a neuropatologia de eventos hipóxicos-isquêmicos. Portanto, os nossos resultados conseguiram mostrar pela primeira vez a distribuição topográfica de Zn reativo através de todo o cérebro do peixe-zebra, o qual apresenta neurônios glutamatérgicos como as células que contêm a maior porção do conteúdo do metal. Nós também mostramos que o uso de quelante de Zn, DEDTC, fez modular o conteúdo do metal em peixe-zebra, desencadeando comportamentos relacionados a crises, tal como ocorre em roedores. Além disso, nós mostramos que a indução de um modelo de hipóxia, que resulta em danos relacionados à isquemia, gerou um aumento no conteúdo de Zn reativo no cérebro desses animais. Conseqüentemente, a investigação do tempo de recuperação espontânea desses animais submetidos ao modelo de câmara hipóxica, nos permitiu fazer uma triagem do efeito do DEDTC neste modelo. Como conclusão, o DEDTC apresentou efeito atenuante sobre o conteúdo cerebral de Zn reativo de peixe-zebra elevado pela hipóxia, mas o composto produziu efeitos colaterais relacionados à ação pró-oxidante. Portanto, apesar do DEDTC ter falhado como substância neuroprotetora da hipóxia, o uso deste modelo em peixe-zebra torna agora possível a triagem de futuros fármacos candidatos para o tratamento dos aumentados níveis de Zn reativo induzidos durante a isquemia.

REFERÊNCIAS

ANDREWS, G. K.; WANG, H.; DEY, S. K.; PALMITER, R. D. Mouse zinc transporter 1 gene 328 provides an essential function during early embryonic development. **Genesis**, v. 40, p. 74-81, 2004.

AGÊNCIA NACIONAL DE VIGILÂNCIA SANITÁRIA. Monografias Autorizadas de Agrotóxicos. Endereço eletrônico: **http://portal.anvisa.gov.br/wps/content/Anvisa+Portal/Anvisa/Inicio/Agrotoxicos+e+Toxicologia/Assuntos+de+Interesse/Monografias+de+Agrotoxicos/Monografias** , 2005. [Acesso em 01 de outubro de 2013].

ALFARO, J. M.; RIPOLL-GÓMEZ, J.; BURGOS, J. S. Kainate administered to adult zebrafish causes seizures similar to those in rodent models. **Eur. J. Neurosci.**, v. 33, p. 1252-1255, 2011.

BALKAYA, M.; KRÖBERA, J.; GERTZ, K.; PERUZZARO, S.; ENDRESA, M. Characterization of long-term functional outcome in a murine model of mild brain ischemia. **J. Neurosci. Methods**, v. 213, p. 179-187, 2013.

BARABAN, S. C.; TAYLOR, M. R.; CASTRO, P. A.; BAIER, H. Pentylenetetrazole induced changes in zebrafish behavior, neural activity and c-fos expression. **Neuroscience**, v. 131, p. 759-768, 2005.

BARBAZUK, W. B.; KORF, I.; KADAVI, C.; HEYEN, J.; TATE, S.; WUN, E.; BEDELL, J. A.; MCPHERSON, J. D.; JOHNSON, S. L. The syntenic relationship of the zebrafish and human genomes. **Genome Res.**, v. 10, p. 1351-1358, 2000.

BECKER, K. J. Inflammation and acute stroke. **Curr. Opin. Neurol.**, v. 11, p. 45-49, 1998.

BECKER, T. S.; RINKWITZ, S. Zebrafish as a genomics model for human neurological and polygenic disorders. **Dev. Neurobiol.**, v. 72, p. 415-428, 2012.

BEYERSMANN, D.; HAASE, H. Functions of zinc in signaling, proliferation and differentiation of mammalian cells. **Biometals**, v. 14, p. 331-341, 2001.

BESANCON, E.; GUO, S.; LOK, J.; TYMIANSKI, M.; LO, E. H. Beyond NMDA and AMPA glutamate receptors: emerging mechanisms for ionic imbalance and cell death in stroke. **Trends Pharmacol. Sci.**, v. 29, p. 268-275, 2008.

BIAGINI, G.; SALA, D.; ZINI, I. Diethyldithiocarbamate, a superoxide dismutase inhibitor, counteracts the maturation of ischemic-like lesions caused by endothelin-1 intrastriatal injection. **Neurosci. Lett.**, v. 190, p. 212-216, 1995.

BIRINYI, A.; PARKER, D.; ANTAL, M.; SHUPLIAKOV, O. Zinc co-localizes with GABA and glycine in synapses in the lamprey spinal cord. **J. Comp. Neurol.**, v. 433, p. 208-221, 2001.

BLASCO-IBÁÑEZ, J. M.; POZA-AZNAR, J.; CRESPO, C.; MARQUES-MARI, A. I.; GRACIA-LLANES, F. J.; MARTINEZ-GUIJARRO, F. J. Chelation of synaptic zinc induces overexcitation in the hilar mossy cells of the rat hippocampus. **Neurosci. Lett.**, v. 355, p. 101-104, 2004.

BLASER, R.; GERLAI, R. Behavioral phenotyping in zebrafish: comparison of three behavioral quantification methods. **Behav. Res. Methods**, v. 38, p. 456-469, 2006.

BRAGA, M. M.; ROSEMBERG, D. B.; DE OLIVEIRA, D. L.; LOSS, C. M.; CÓRDOVA, S. D.; RICO, E. P.; SILVA, E. S.; DIAS, R. D.; SOUZA, D. O.; CALCAGNOTTO, M. E. Topographical analysis of reactive zinc in the central nervous system of adult zebrafish (Danio rerio). **Zebrafish**, v. 10, p. 376-388, 2013a.

BRAGA, M. M.; RICO, E. P.; CÓRDOVA, S. D.; PINTO, C. B.; BLASER, R. E.; DIAS, R. D.; ROSEMBERG, D. B.; OLIVEIRA, D. L.; SOUZA, D. O. Evaluation of spontaneous recovery of behavioral and brain injury profiles in zebrafish after hypoxia. **Behav. Brain Res.**, v. 253, p. 145-151, 2013b.

BROOKS-KAYAL, A. R.; SHUMATE, M. D.; JIN, H.; RIKHTER, T. Y.; KELLY, M. E.;

CHAKRAVARTY, D. N.; BABB, T. L.; CHUNG, C. K.; MIKUNI, N. Bilateral kainic acid lesions in the rat hilus induce non-linear additive mossy fiber neoinnervation. **Neurosci. Lett.**, v. 230, p. 175-178, 1997.

CHEN, Y-C.; ZHAO, D.; QING, D.; CHENG, D-L.; MAO, J-Y.; WANG, B. Zebrafish embryonic brain cell apoptosis and c-fos gene expression after hypoxia reperfusion. **Chin. J. Tissue Eng. Res.**, v. 17, p. 6613-6619, 2013.

CHOI, D. W.; KOH, J. Y. Zinc and brain injury. **Annu. Rev. Neurosci.**, v. 21, p. 347-375, 1998.

CHOI, D. W.; ROTHMAN, S. M. The role of glutamate neurotoxicity in hypoxic-ischemic neuronal death. **Annu. Rev. Neurosci.**, v. 13, p. 171-182, 1990.

COLE, T. B.; WENZEL, H. J.; KAFER, K. E.; SCHWARTZKROIN, P. A.; PALMITER, R. D. Elimination of zinc from synaptic vesicles in the intact mouse brain by disruption of the ZnT3 gene. **Proc. Natl. Acad. Sci. USA**, v. 96, p. 1716-1721, 1999.

COLE, T. B.; ROBBINS, C. A.; WENZEL, H. J.; SCHWARTZKROIN, P. A.; PALMITER, R. D. Seizures and neuronal damage in mice lacking vesicular zinc. **Epilepsy Res.**, v. 39, p. 153-169, 2000.

COLEMAN, J. E. Zinc proteins: enzymes, storage proteins, transcriptions factors, and replication proteins. **Annu. Rev. Biochem.**, v. 61, p. 897-946, 1992.

COLLARD, C. D.; GELMAN, S. Pathophysiology, clinical manifestations, and prevention of ischemia-reperfusion injury. **Anesthesiology**, v. 94, p. 1133-1138, 2001.

COOPER, R. L.; GOLDMAN, J. M.; STOKER, T. E. Neuroendocrine and reproductive effects of contemporary-use pesticides. **Toxicol. Ind. Health**, v. 15, p. 26-36, 1999.

COUSINS, R. J. Metal elements and gene expression. **Annu. Rev. Nutr.**, v. 14, p. 449-469, 1994.

COULTER, D. A. γ-Aminobutyric acid A receptor subunit expression predicts functional changes in hippocampal dentate granule cells during postnatal development. **J. Neurochem.**, v. 77, p. 1266-1278, 2001.

CUAJUNGCO, M. P.; LEES, G. J. Nitric oxide generators produce accumulation of chelatable zinc in hippocampal neuronal perikarya. **Brain Res.**, v. 799, p. 118-129, 1998.

CVEK, B.; DVORAK, Z. Targeting of nuclear factor-kappaB and proteasome by dithiocarbamate complexes with metals. **Curr. Pharm. Des.**, v. 13, p. 3155-3167, 2007.

DALTON, T. P.; BITTEL, D.; ANDREWS, G. K. Reversible activation of mouse metal response element-binding transcription factor 1 DNA binding involves zinc interaction with the zinc finger domain. **Mol. Cell Biol.**, v. 17, p. 2781-2789, 1997.

DANSCHER, G. Histochemical demonstration of heavy metals. A revised version of the sulphide silver method suitable for both light and electron microscopy. **Histochemistry**, v. 71, p. 1-16, 1981.

DANSCHER, G.; HOWELL, G.; PEREZ-CLAUSELL, J.; HERTEL, N. The dithizone, Timm's sulphide silver and the selenium methods demonstrate a chelatable pool of zinc in CNS. A proton activation (PIXE) analysis of carbon tetrachloride extracts from rat brains and spinal cords intravitally treated with dithizone. **Histochemistry**, v. 83, p. 419-422, 1985.

DANSCHER, G. The autometallographic zinc-sulphide method. A new approach involving in vivo creation of nanometersized zinc sulphide crystal lattices in zinc-enriched synaptic and secretory vesicles. **Histochem. J.**, v. 28, p. 361-373, 1996.

DAOCHENG, W.; MINGXI, W. Preparation of the core-shell structure adriamycin lipiodol microemulsions and their synergistic anti-tumor effects with diethyldithiocarbamate in vivo. **Biomed. Pharmacother.**, v. 64, p. 615-623, 2010.

DAUMAS, S.; HALLEY, H.; LASSALLE, J. M. Disruption of hippocampal CA3 network: effects on episodic-like memory processing in C57BL/6J mice. **Eur. J. Neurosci.**, v. 20, p. 597-600, 2004.

DICHTER, M. A.; AYALA, G. F. Cellular mechanisms of epilepsy: a status report. **Science**, v. 237, p. 157-164, 1987.

DILLMANN, W. H. Heat shock proteins and protection against ischemic injury. **Infect. Dis. Obstet. Gynecol.** v. 7, p. 55-57, 1999.

DI MONTE, D.; IRWIN, I.; KUPSCH, A.; COOPER, S.; DELANNEY, L. E.; LANGSTON, J. W. Diethyldithiocarbamate and disulfiram inhibit MPP+ and dopamine uptake by striatal synaptosomes. **Eur. J. Pharmacol.**, v. 166, p. 23-29, 1989.

DINELEY, K. E.; RICHARDS, L. L.; VOTYAKOVA, T. V.; REYNOLDS, I. J. Zinc causes loss of membrane potential and elevates reactive oxygen species in rat brain mitochondria. **Mitochondrion**, v. 5, p. 55-65, 2005.

DIRNAGL, U.; IADECOLA, C.; MOSKOWITZ, M. A. Pathobiology of ischaemic stroke: an integrated view. **Trends Neurosci.**, v. 22, p. 391-397, 1999.

DITTMER, P. J.; MIRANDA, J. G.; GORSKI, J. A.; PALMER, A. E. Genetically encoded sensors to elucidate spatial distribution of cellular zinc. **J. Biol.Chem.**, v. 284, p. 16289-16297, 2009.

DOERING, P.; STOLTENBERG, M.; PENKOWA, M.; RUNGBY, J.; LARSEN, A.; DANSCHER, G. Chemical blocking of zinc ions in CNS increases neuronal damage following traumatic brain injury (TBI) in mice. **PLoS ONE**, v. 5, p. e10131, 2010.

DOMINGUEZ, M. I.; BLASCO-IBANEZ, J. M.; CRESPO, C.; MARQUES-MARI, A. I.; MARTINEZ-GUIJARRO, F. J. Zinc chelation during non-lesioning overexcitation results in neuronal death in the mouse hippocampus. **Neuroscience**, v. 116, p. 791-806, 2003.

EMANUELLI, T.; ROCHA, J. B.; PEREIRA, M. E.; NASCIMENTO, P. C.; SOUZA, D. O.; BEBER, F. A. delta-Aminolevulinate dehydratase inhibition by 2,3-dimercaptopropanol is mediated by chelation of zinc from a site involved in maintaining cysteinyl residues in a reduced state. **Pharmacol. Toxicol.**, v. 83, p. 95-103, 1998.

ESBAUGH, A. J.; PERRY, S. F.; GILMOUR, K. M. Hypoxia-inducible carbonic anhydrase IX expression is insufficient to alleviate intracellular metabolic acidosis in the muscle of zebrafish, Danio rerio. **Am. J. Physiol. Regul. Integr. Comp. Physiol.**, v. 296, p. R150-160, 2009.

FABER, H.; BRAUN, K.; ZUSCHRATTER, W.; SCHEICH, H. System specific distribution of zinc in the chick brain. A light- and electron microscopic study using the Timm method. **Cell Tissue Res.**, v. 258, p. 247-257, 1989.

FAVIER, M.; HININGER-FAVIER, I. Zinc and pregnancy. **Gynecol. Obstet. Fertil.**, v. 33, p. 253-258, 2005.

FELLER, D. J.; TSO-OLIVAS, D. Y.; SAVAGE, D. D. Hippocampal mossy fiber zinc deficit in mice genetically selected for ethanol withdrawal seizure susceptibility. **Brain Res.**, v. 545, p. 73-79, 1991.

FLYNN, C.; BROWN, C. E.; GALASSO, S. L.; MCINTYRE, D. C.; TESKEY, G. C.; DYCK, R. H. Zincergic innervation of the forebrain distinguishes epilepsy-prone from epilepsy-resistant rat strains. **Neuroscience**, v. 144, p. 1409-1414, 2007.

FORESTI, M. L.; ARISI, G. M.; FERNANDES, A.; TILELLI, C. Q.; GARCIA-CAIRASCO, N. Chelatable zinc modulates excitability and seizure duration in the amygdala rapid kindling model. **Epilepsy Res.**, v. 79, p. 166-172, 2008.

FREDERICKSON, C. J.; KLITENICK, M. A.; MANTON, W. I.; KIRKPATRICK, J. B. Cytoarchitectonic distribution of zinc in the hippocampus of man and the rat. **Brain Res.**, v. 273, p. 335-339, 1983.

FREDERICKSON, R. E.; FREDERICKSON, C. J.; DANSCHER, G. In situ binding of bouton zinc reversibly disrupts performance on a spatial memory task. **Behav. Brain Res.**, v. 38, p. 25-33, 1990.

FREDERICKSON, C. J.; RAMPY, B. A.; REAMY-RAMPY, S.; HOWELL, G. A. Distribution of histochemically reactive zinc in the forebrain of the rat. **J. Chem. Neuroanat.**, v. 5, p. 521-530, 1992.

FREDERICKSON, C. J.; CUAJUNGCO, M. P.; LABUDA, C. J.; SUH, S. W. Nitric oxide causes apparent release of zinc from presynaptic boutons. **Neuroscience**, v. 115, p. 471-474, 2002.

FREDERICKSON, C. J.; BURDETTE, S. C.; FREDERICKSON, C. J.; SENSI, S. L.; WEISS, J. H.; YIN, H. Z.; BALAJI, R. V.; TRUONG-TRAN, A. Q.; BEDELL, E.; PROUGH, D. S.; LIPPARD, S. J. Method for identifying neuronal cells suffering zinc toxicity by use of a novel fluorescent sensor. **J. Neurosci. Methods**, v. 139, p. 79-89, 2004a.

FREDERICKSON, C. J.; MARET, W.; CUAJUNGCO, M. P. Zinc and excitotoxic brain injury: a new model. **Neuroscientist**, v. 10, p. 18-25, 2004b.

FREDERICKSON, C. J.; KOH, J. Y.; BUSH, A. I. The neurobiology of zinc in health and disease. **Nat. Rev. Neurosci.**, v. 6, p. 449-462, 2005.

FUKAHORI, M.; ITOH, M. Effects of dietary zinc status on seizure susceptibility and hippocampal zinc content in the El (epilepsy) mouse. **Brain Res.**, v. 529, 16-22, 1990.

GARCIA-CAIRASCO, N.; WAKAMATSU, H.; OLIVEIRA, J. A.; GOMES, E. L.; DEL BEL, E. A.; MELLO, L. E. Neuroethological and morphological (Neo-Timm staining) correlates of limbic recruitment during the development of audiogenic kindling in seizure susceptible Wistar rats. **Epilepsy Res.**, v. 26, p. 177-192, 1996.

GIBSON, K. D.; NEUBERGER, A.; SCOTT, J. J. The purification and properties of delta-aminolevulinic acid dehydratase. **Biochem. J.**, v. 61, p. 618-629, 1955.

GOLDSMITH, P. Zebrafish as a pharmacological tool: the how, why and when. **Curr. Opin. Pharmacol.**, v. 4, p. 504-512, 2004.

GSCHANES, A.; VALOUSKOVÁ, V.; WINDISCH, M. Ameliorative influence of a nootropic drug on motor activity of rats after bilateral carotid artery occlusion. **J. Neural Transm.**, v. 104, p. 1319-1327, 1997.

GUILLAUMIN, J. M.; LEPAPE, A.; RENOUX, G. Fate and distribution of radioactive sodium diethyldithiocarbamate (imuthiol) in the mouse. **Int. J. Immunopharmacol.**, v. 8, p. 859-865, 1986.

HALLIWELL, B.; GUTTERIDGE, J. M. C.; **Free radicals in biology and medicine**. Ed 4. Clarendon Press, Oxford, 2007.

HARTWIG, A. Role of DNA repair inhibition in lead- and cadmium-induced genotoxicity: a review. **Environ. Health Perspect.**, v. 102, p. 45-50, 1994.

HAUG, F. M. S. Heavy metals in the brain. A light microscope study of the rat with Timm's sulphite silver method. Methodological considerations and cytological and regional staining patterns. **Adv. Anat. Embryol. Cell Biol.**, v. 43, p. 1-71, 1973.

HAYCOCK, J. W.; VAN BUSKIRK, R.; GOLD, P. E.; MCGAUGH, J. L. Effects of diethyldithiocarbamate and fusaric acid upon memory storage processes in rats. **Eur. J. Pharmacol.**, v. 51, p. 261-273, 1978.

HEIKKILA, R. E.; CABBAT, F. S.; COHEN, G. In vivo inhibition of superoxide dismutase in mice by diethyldithiocarbamate. **J. Biol. Chem.**, v. 251, p. 2182-2185, 1976.

HERCULANO-HOUZEL, S.; LENT, R. Isotropic fractionator: a simple, rapid method for the quantification of total cell and neuron numbers in the brain. **J. Neurosci.**, v. 25, p. 2518-2521, 2005.

HO, E.; DUKOVCIC, S.; HOBSON, B.; WONG, C. P.; MILLER, G.; HARDIN, K.; TRABER, M. G.; TANGUAY, R. L. Zinc transporter expression in zebrafish (Danio rerio) during development. Comp. **Biochem. Physiol. C Toxicol. Pharmacol.**, v. 155, p. 26-32, 2012.

HOSSMANN, K. A. Pathophysiology and therapy of experimental stroke. **Cell. Mol. Neurobiol.**, v. 26, p. 1057-1083, 2006.

HOUETO, P.; BINDOULA, G.; HOFFMAN, J. R. Ethylenebisdithiocarbamates and ethylenethiourea: possible human health hazards. **Environ. Health. Perspect.**, v. 103, p. 568-573, 1995.

KALUEFF, A. V.; STEWART, A. M.; GERLAI, R. Zebrafish as an emerging model for studying complex brain disorders. **Trends Pharmacol. Sci.**, v. 35, p. 63-75, 2014.

KHANDELWAL, S.; KACHRU, D. N.; TANDON, S. K. Influence of metal chelators on metalloenzymes. **Toxicol. Lett.**, v. 37, p. 213-219, 1987.

KIMOTO-KINOSHITA, S.; NISHIDA, S.; TOMURA, T. T. Diethyldithiocarbamate can induce two different type of death: apoptosis and necrosis mediating the differential MAP kinase activation and redox regulation in HL60 cells. **Mol. Cell. Biochem.**, v. 265, p. 123-132, 2004.

KAY, A. R. Detecting and minimizing zinc contamination in physiological solutions. **BMC Physiol.**, v. 4, p. 4, 2004.

KELLER, K. A.; CHU, Y.; GRIDER, A.; COFFIELD, J. A. Supplementation with l-histidine during dietary zinc repletion improves short-term memory in zinc-restricted young adult male rats. **J. Nutr.**, v. 130, p. 1633-1640, 2000.

KETTERMAN, J. K.; LI, Y. V. Presynaptic evidence for zinc release at the mossy fiber synapse of rat hippocampus. **J. Neurosci. Res.**, v. 86, p. 422-434, 2008.

KLITENICK, M. A.; FREDERICKSON, C. J.; MANTON, W. I. Acid-vapor decomposition for determination of zinc in brain tissue by isotope dilution mass spectrometry. **Anal. Chem.**, v. 55, p. 921-923, 1983.

KOH, J. Y.; SUH, S. W.; GWAG, B. J.; HE, Y. Y.; HSU, C. Y.; CHOI, D. W. The role of zinc in selective neuronal death after transient global cerebral ischemia. **Science**, v. 272, p. 1013-1016, 1996.

KOZMA, M.; SZERDAHELYI, P.; KASA, P. Histochemical detection of zinc and copper in various neurons of the central nervous system. **Acta Histochem.**, v. 69, p. 12-17, 1981.

LASOŃ, W.; CHLEBICKA, M.; REJDAK, K. Research advances in basic mechanisms of seizures and antiepliptic drug action. **Pharmacol. Rep.**, v. 65, p. 787-801, 2013.

LASSALLE, J. M.; BATAILLE, T.; HALLEY, H. Reversible in activation of the hippocampal mossy fiber synapses in mice impairs spatial learning, but neither consolidation nor memory retrieval ,in the Morris navigation task. **Neurobiol. Learn. Mem.**, v. 73, p. 243-257, 2000.

LEES, G. J.; CUAJUNGCO, M. P.; LEONG, W. Effect of metal chelating agents on the direct and seizure-related neuronal death induced by zinc and kainic acid. **Brain Research.**, v. 799, p. 108-117, 1998.

LICHTEN, L. A.; COUSINS, R. J. Mammalian zinc transporters: nutritional and physiologic regulation. **Annu. Rev. Nutr.**, v. 29, p. 153-176, 2009.

MAGISTRETTI, P. J. Brain energy metabolism. In: Zigmond MJ, Bloom FE, Landis SC, Roberts JL, Squire LR, editors. **Fundamental neuroscience**. San Diego: AcademicPress, p. 389-413, 1999.

MAHADIK, S. P.; MAKAR, T. K.; MURTHY, J. N.; ORTIZ, A.; WAKADE, C. G.; KARPIAK, S. E. Temporal changes in superoxide dismutase, glutathione

peroxidase, and catalase levels in primary and peri-ishemic tissue. Monosialoganglioside (GM1) treatment effects. **Mol. Chem. Neuropathol.**, v. 18, p. 1-14, 1993.

MAURES, T. J.; DUAN, C. Structure, developmental expression, and physiological regulation of zebrafish IGF binding protein-1. **Endocrinology**, v. 143, p. 2722-2731, 2002.

MARTINEZ-GUIJARRO, F. J.; SORIANO, E.; DEL RIO, J. A.; LOPEZ-GARCIA, C. Zinc-positive boutons in the cerebral cortex of lizards show glutamate immunoreactivity. **J. Neurocytol.**, v. 20, 834-843, 1991.

MENGUAL, E.; CASANOVAS-AGUILAR, C.; PEREZ-CLAUSELL, J.; GIMENEZ-AMAYA, J. M. Thalamic distribution of zinc-rich terminal fields and neurons of origin in the rat. **Neuroscience**, v. 102, p. 863-884, 2001.

MILLER, N. Y.; GERLAI, R. Shoaling in zebrafish: what we don't know. **Rev. Neurosci.**, v. 22, p. 17-25, 2011.

MITCHELL, C. L., BARNES, M. I. Proconvulsant action of diethyldithiocarbamate in stimulation of the perforant path. **Neurotoxicol. Teratol.**, v. 15, p. 165-171, 1993.

MORO, E.; VETTORI, A.; PORAZZI, P.; SCHIAVONE, M.; RAMPAZZO, E.; CASARI, A.; EK, O.; FACCHINELLO, N.; ASTONE, M.; ZANCAN, I.; MILANETTO, M.; TISO, N.; ARGENTON, F. Generation and application of signaling pathway reporter lines in zebrafish. **Mol. Genet. Genomics**, v. 288, p. 231-242, 2013.

MOUSSAVI NIK, S. H.; NEWMAN, M.; LARDELLI, M. The response of HMGA1 to changes in oxygen availability is evolutionarily conserved. **Exp. Cell. Res.**, v. 317, p. 1503-1512, 2011.

MUELLER, T.; DONG, Z.; BERBEROGLU, M. A.; GUO, S. The dorsal pallium in zebrafish, Danio rerio (Cyprinidae, Teleostei). **Brain Res.**, v. 1381, p. 95-105, 2011.

MURPHY, T. H.; LI, P.; BETTS, K.; LIU, R. Two-photon imaging of stroke onset in vivo reveals that NMDA receptor independent ischemic depolarization is the major cause of rapid reversible damage to dendrites and spines. **J. Neurosci.**, v. 28, p. 1756-1772, 2008.

MURPHY, T. H.; CORBETT, D. Plasticity during stroke recovery: from synapse to behaviour. **Nat. Rev. Neurosci.**, v. 10, 861-872, 2009.

MUSSULINI, B. H.; LEITE, C. E.; ZENKI, K. C.; MORO, L.; BAGGIO, S.; RICO, E. P.; ROSEMBERG, D. B.; DIAS, R. D.; SOUZA, T. M.; CALCAGNOTTO, M. E.; CAMPOS, M. M.; BATTASTINI, A. M.; DE OLIVEIRA, D. L. Seizures induced by pentylenetetrazole in the adult zebrafish: a detailed behavioral characterization. **PLoS One**, v. 8, p. e54515, 2013.

NELSON, C. W.; WEI, E. P.; POVLISHOCK, J. T.; KONTOS, H. A.; MOSKOWITZ, M. A. Oxygen radicals in cerebral ischemia. **Am. J. Physiol.**, v. 263, H1356-1362, 1992.

NGAN, A. K.; WANG, Y. S. Tissue-specific transcriptional regulation of monocarboxylate transporters (MCTs) during short-term hypoxia in zebrafish (Danio rerio). **Comp. Biochem. Physiol. B Biochem. Mol. Biol.**, v. 154, p. 396-405, 2009.

OBRENOVITCH, T. P.; RICHARDS, D. A. Extracellular neurotransmitter changes in cerebral ischaemia. **Cerebrovasc. Brain Metab. Rev.**, v. 7, p. 1-54, 1995.

OLMEZ, I.; OZYURT, H. Reactive oxygen species and ischemic cerebrovascular disease. **Neurochem. Int.**, v. 60, p. 208-212, 2012.

PALMITER, R. D.; COLE, T. B.; QUAIFE, C. J.; FINDLEY, S. D. ZnT-3, a putative transporter of zinc into synaptic vesicles. **Proc. Natl. Acad. Sci. USA.**, v. 93, p. 14934-14939, 1996.

PANG, H.; CHEN, D.; CUI, Q. C.; DOU, Q. P. Sodium diethyldithiocarbamate, an AIDS progression inhibitor and a copper-binding compound, has proteasome-inhibitory and apoptosis-inducing activities in cancer cells. **Int. J. Mol. Med.**, v. 19, p. 809-816, 2007.

PAOLETTI, P.; ASCHER, P.; NEYTON, J. High-affinity zinc inhibition of NMDA NR1-NR2 receptors. **J. Neurosci.**, v. 17, p. 5711-5725, 1997.

PAOLETTI, P.; VERGNANO, A. M.; BARBOUR, B.; CASADO, M. Zinc at glutamatergic synapses. **Neuroscience**, v. 158, p. 126-136, 2009.

PEI, Y. Q.; KOYAMA, I. Features of seizures and behavioral changes induced by intrahippocampal injection of zinc sulfate in the rabbit: a new experimental model of epilepsy. **Epilepsia**, v. 27, p. 183-188, 1986.

PEREZ-CLAUSELL, J. The organization of zinc-containing terminal fields in the brain of the lizard Podarcis hispanica. A histochemical study. **J. Comp. Neurol.**, v. 267, p. 153-171, 1988.

PIÑUELA, C.; BAATRUP, E.; GENESER, F. A. Histochemical distribution of zinc in the brain of the rainbow trout, Oncorhynchos myciss. I. The telencephalon. **Anat. Embryol.**, v. 185, p. 379-388, 1992.

PLUTA, R.; JOLKKONEN, J.; CUZZOCREA, S.; PEDATA, F.; CECHETTO, D.; POPA-WAGNER, A. Cognitive impairment with vascular impairment and degeneration. **Curr. Neurovasc. Res.**, v. 8, p. 342-350, 2011.

PRESTON, P.; WEBSTER, J. Spectrophotometric measurement of experimental brain injury. **J. Neurosci. Methods**, v. 94, p. 187-192, 2000.

QAZI, R.; CHANG, A. Y.; BORCH, R. F.; MONTINE, T.; DEDON, P.; LOUGHNER, J.; BENNETT, J. M. Phase I clinical and pharmacokinetic study of diethyldithiocarbamate as a chemoprotector from toxic effects of cisplatin. **J. Natl. Cancer Inst.**, v. 80, p. 1486-1488, 1988.

QIAN, J.; NOEBELS, J. L. Exocytosis of vesicular zinc reveals persistent depression of neurotransmitter release during metabotropic glutamate receptor long-term depression at the hippocampal CA3-CA1 synapse. **J. Neurosci.**, v. 26, p. 6089-6095, 2006.

RAHDEN-STAROŃ, I.; GROSICKA-MACIAG, E.; KURPIOS-PIEC, D.; CZECZOT, H.; GRZELA, T.; SZUMILO, M. The effects of sodium diethyldithiocarbamate in fibroblasts V79 cells in relation to cytotoxicity, antioxidativeenzymes, glutathione, and apoptosis. **Arch. Toxicol.**, v. 86, p. 1841-1850, 2012.

RATH, N. C.; RASAPUTRA, K. S.; LIYANAGE, R.; HUFF, G. R.; HUFF, W. E. Dithiocarbamate toxicity-An appraisal. In: Stoytcheva M, editor. **Pesticides in the Modern World-Effects of Pesticides Exposure**, New York: InTech Publishing Online, p. 323-340, 2011.

REDENTI, S.; RIPPS, H.; CHAPPELL, R. L. Zinc release at the synaptic terminals of rod photoreceptors. **Exp. Eye. Res.**, v. 85, p. 580-584, 2007.

REVUELTA, M.; CASTAÑO, A.; MACHADO, A.; CANO, J.; VENERO, J. L. Kainate-induced zinc translocation from presynaptic terminals causes neuronal and astroglial cell death and mRNA loss of BDNF receptors in the hippocampal formation and amygdala. **J. Neurosci. Res.**, v. 82, p. 184-195, 2005.

RICO, E. P.; ROSEMBERG, D. B.; SEIBT, K. J.; CAPIOTTI, K. M.; DA SILVA, R. S.; BONAN, C. D. Zebrafish neurotransmitter systems as potential pharmacological and toxicological targets. **Neurotoxicol. Teratol.**, v. 33, 608-617, 2011.

ROESNER, A.; HANKELN, T.; BURMESTER, T. Hypoxia induces a complex response of globin expression in zebrafish (Danio rerio). **J. Exp. Biol.**, v. 209, p. 2129-2137, 2006.

ROESNER, A.; MITZ, S. A.; HANKELN, T.; BURMESTER, T. Globins and hypoxia adaptation in the goldfish, Carassius auratus. **FEBS J.**, v. 275, p. 3633-3643, 2008.

ROJAS, D. A.; PEREZ-MUNIZAGA, D. A.; CENTANIN, L.; ANTONELLI, M.; WAPPNER, P.; ALLENDE, M. L.; REYES, A. E. Cloning of hif-1alpha and hif-2alpha and mRNA expression pattern during development in zebrafish. **Gene Expr. Patterns**, v. 7, p. 339-3345, 2007.

ROSEMBERG, D. B.; RICO, E. P.; MUSSULINI, B. H.; PIATO, A. L.; CALCAGNOTTO, M. E.; BONAN, C. D.; DIAS, R. D.; BLASER, R. E.; SOUZA, D. O.; DE OLIVEIRA, D. L. Differences in spatiotemporal behavior of zebrafish in the open tank paradigmafter a short-period confinement into dark and bright environments. **PLoS One**, v. 6, p. e19397, 2012.

RUSSELL, R.; BEARD, J. L.; COUSINS, R. J.; DUNN, J. T.; FERLAND, G.; HAMBIDGE, K. M.; LYNCH, S.; PENLAND, J. G.; ROSS, A. C.; STOEKER, B. J.; SUTTIE, J. W.; TURNLUND, J. R.; WEST, K. P.; ZLOTKIN, S. H. Zinc. In: **Dietary reference intakes for vitamin A, vitamin K, arsenic, boron, chromium, copper, iodine, iron manganese, molybdenum, nickel, silicon, vanadium, zinc,** Washington, DC: The National Academies Press, p. 442-501, 2002.

SEKLER, I.; SILVERMAN, W. F. Zinc homeostasis and signaling in glia. **Glia**, v. 60, p. 843-850, 2012.

SENGER, M. R.; ROSEMBERG, D. B.; RICO, E. P.; DE BEM ARIZI, M.; DIAS, R. D.; BOGO, M. R.; BONAN, C. D. In vitro effect of zinc and cadmium on acetylcholinesterase and ectonucleotidase activities in zebrafish (Danio rerio) brain. **Toxicol. In Vitro**, v. 20, p. 954-958, 2006.

SHUTTLEWORTH, C. W.; WEISS, J. H. Zinc: new clues to diverse roles in brain ischemia. **Trends Pharmacol. Sci.**, v. 32, p. 480-486, 2011.

SINDREU, C. B.; VAROQUI, H.; ERICKSON, J. D.; PÉREZ-CLAUSELL, J. Boutons containing vesicular zinc define a subpopulation of synapses with low AMPAR content in rat hippocampus. **Cereb. Cortex**, v. 13, p. 823-829, 2003.

SINDREU, C.; STORM, D. R. Modulation of neuronal signal transduction and memory formation by synaptic zinc. **Front. Behav. Neurosci.**, v. 5, p. 68, 2011.

SMART, T. G.; HOSIE, A. M.; MILLER, P. S. Zn^{2+} ions: modulators of excitatory and inhibitory synaptic activity. **Neuroscientist**, v. 10, p. 432-442, 2004.

SMITH, R. M.; MARTELL, A. E. **NIST Critically Selected Stability Constants of Metal Complexes Database**, 7.0th edition. Gaithersburg, MD, NIST, 2003.

STEVENSON, T. J.; TRINH, T.; KOGELSCHATZ, C.; FUJIMOTO, E.; LUSH M. E.; PIOTROWSKI, T.; BRIMLEY, C. J.; BONKOWSKY, J. L. Hypoxia disruption of vertebrate CNS pathfinding through ephrinB2 Is rescued by magnesium. **PLoS Genet.**, v. 8, p. e1002638, 2012.

SUTULA, T.; CASCINO, G.; CAVAZOS, J.; PARADA, I.; RAMIREZ, L. Mossy fiber synaptic reorganization in the epileptic human temporal lobe. **Ann. Neurol.**, v. 26, p. 321-330, 1989.

SUTULA, T. P.; DUDEK, F. E. Unmasking recurrent excitation generated by mossy fiber sprouting in the epileptic dentate gyrus: an emergent property of a complex system. **Prog. Brain Res.**, v. 163, p. 541-563, 2007.

SUH, S. W.; CHEN, J. W.; MOTAMEDI, M.; BELL, B.; LISTIAK, K.; PONS, N. F.; DANSCHER, G.; FREDERICKSON, C. J. Evidence that synaptically-released zinc contributes to neuronal injury after traumatic brain injury. **Brain Res.**, v. 852, p. 268-273, 2000.

SUWA, H.; SAINT-AMANT, L.; TRILLER, A.; DRAPEAU, P.; LEGENDRE, P. High-affinity zinc potentiation of inhibitory postsynaptic glycinergic currents in the zebrafish hindbrain. **J. Neurophysiol.**, v. 85, p. 912-925, 2001.

SZERDAHELYI, P.; KASA, P. Histochemical demonstration of copper in normal rat brain and spinal cord. Evidence of localization in glial cells. **Histochemistry**, v. 85, p. 341-347, 1986.

TAKEDA, A.; HIRATE, M; TAMANO, H.; NISIBABA, D.; OKU, N. Susceptibility to kainate-induced seizures under dietary zinc deficiency. **J. Neurochem.**, v. 85, p. 1575-1580, 2003.

TAKEDA, A.; TAMANO, H.; KAN, F.; ITOH, H.; OKU, N. Anxiety-like behaviorofyoungratsafter2-week zinc deprivation. **Behav. Brain Res.**, v. 177, p. 1-6, 2007.

TAKEDA, A.; TAMANO, H.; IMANO, S.; OKU, N. Increases in extra- cellular zinc in the amygdale in acquisition and recall of fear experience and their roles in response to fear. **Neuroscience**, v. 168, p. 715-722, 2010.

TASSABEHJI, N. M.; CORNIOLA, R. S.; ALSHINGITI, A.; LEVENSON, C. W. Zinc deficiency induces depression-like symptoms in adult rats. **Physiol. Behav.**, v. 95, p. 365-369, 2008.

TAUCK, D. L.; NADLER, J. V. Evidence of functional mossy fiber sprouting in hippocampal formation of kainic acid-treated rats. **J. Neurosci.**, v. 5, p. 1016-1022, 1985.

TILTON, F.; LA DU, J. K.; VUE, M.; ALZARBAN, N.; TANGUAY, R. L., Dithiocarbamates have a common toxic effect on zebrafish body axis formation. **Toxicol. Appl. Pharmacol.**, v. 216, p. 55-68, 2004.

TONKIN, E. G.; VALENTINE, H. L.; MILATOVIC, D. M.; VALENTINE, W. M. N,N-diethyldithiocarbamate produces copper accumulation, lipid peroxidation, and myelin injury in rat peripheral nerve. **Toxicol. Sci.**, v. 81, p. 160-171, 2004.

TOSCANO-SILVA, M.; GOMES DA SILVA, S.; SCORZA, F. A.; BONVENT, J. J.; CAVALHEIRO, E. A.; ARIDA, R. M. Hippocampal mossy fiber sprouting induced by forced and voluntary physical exercise. **Physiol. Behav.**, v. 101, p. 302-308, 2010.

TUCKER, N. R.; MIDDLETON, R. C.; LE, Q. P.; SHELDEN, E. A. HSF1 is essential for the resistance of zebrafish eye and brain tissues to hypoxia/reperfusion injury. **PLoS One**, v. 6, p. e22268, 2011.

UNITED STATES ENVIRONMENTAL PROTECTION AGENCY. EBDC fungicides mancozeb, maneb, and metiram; notice of receipt of requests to voluntarily cancel, amend, or terminate uses of certain pesticide registrations. Endereço eletrônico: **http://www.epa.gov/fedrgstr/EPA-PEST/2005/June/Day-01/p10577.htm** , 2005. [Acesso em 01 de outubro de 2013].

VANDENBERG, R. J.; MITROVIC, A. D.; JOHNSTON, G. A. Molecular basis for differential inhibition of glutamate transporter subtypes by zinc ions. **Mol. Pharmacol.**, v. 54, p. 189-196, 1998.

VAREA, E.; ALONSO-LLOSA, G.; MOLOWNY, A.; LOPEZ-GARCIA, C.; PONSODA, X. Capture of extracellular zinc ions by astrocytes. **Glia**, v. 54, p. 304-315, 2006.

VARGAS, R.; THORSTEINSSON, H.; KARLSSON, K. A. Spontaneous neural activity of the anterodorsal lobe and entopeduncular nucleus in adult zebrafish: a putative homologue of hippocampal sharp waves. **Behav. Brain Res.**, v. 229, p. 10-20, 2012.

VERMEER, S. E.; PRINS, N. D.; DEN HEIJER, T.; HOFMAN, A.; KOUDSTAAL, P. J.; BRETELER, M. M. Silent brain infarcts and the risk of dementia and cognitive decline. **N. Engl. J. Med.**, v. 348, p. 1215-1222, 2003.

VIQUEZ, O. M.; LAI, B.; AHN, J. H.; DOES, M. D.; VALENTINE, H. L.; VALENTINE, W. M.; N,N-diethyldithiocarbamate promotes oxidative stress prior to myelin structural changes and increases myelin copper content. **Toxicol. Appl. Pharmacol.**, v. 239, p. 71-79, 2009.

WHITTLE, N.; HAUSCHILD, M.; LUBEC, G.; HOLMES, A.; SINGEWALD, N. Rescue of impaired fear extinction and normalization of cortico-amygdala circuit dysfunction in a genetic mouse model by dietary zinc restriction. **J. Neurosci.**, v. 30, p. 13586-13596, 2010.

WILLIAMS, K. Separating dual effects of zinc at recombinant N-methyl-D-aspartate receptors. **Neurosci. Lett.**, v. 215, p. 9-12, 1996.

WOODROOFE, C. C.; MASALHA, R.; BARNES, K. R.; FREDERICKSON, C. J.; LIPPARD, S. J. Membrane -permeable and -impermeable sensors of the Zinpyr family and their application to imaging of hippocampal zinc in vivo. **Chem. Biol.**, v. 11, p. 1659-1666, 2004.

WOODS, I. G.; WILSON, C.; FRIEDLANDER, B.; CHANG, P.; REYES, D. K.; NIX, R.; KELLY, P. D.; CHU, F.; POSTLETHWAIT, J. H.; TALBOT, W. S. The zebrafish gene map defines ancestral vertebrate chromosomes. **Genome Res.**, v. 15, p. 1307-1314, 2005.

WORLD HEALTH ORGANIZATION. The top 10 causes of death. Endereço eletrônico: **http://www.who.int/mediacentre/factsheets/fs310/en/** , 2013. [Acesso em 01 de fevereiro de 2014].

XIE, X. M.; SMART, T. G. A physiological role for endogenous zinc in rat hippocampal synaptic neurotransmission. **Nature**, v. 349, p. 521-524, 1991.

YAMANE, Y.; YOSHIMOTO, M.; ITO, H. Area dorsalis pars lateralis of the telencephalon in a teleost (Sebastiscus marmoratus) can be divided into dorsal and ventral regions. **Brain Behav. Evol.**, v. 48, p. 338-349, 1996.

YU, X.; LI, Y. V. Zebrafish as an alternative model for hypoxic-ischemic brain damage. **Int. J. Physiol. Pathophysiol. Pharmacol.**, v. 3, p. 88-96, 2011.

YU, X.; LI, Y. V. Neuroprotective effect of zinc chelator DEDTC in a zebrafish (Danio rerio) model of hypoxic brain injury. **Zebrafish**, v. 10, p. 30-35, 2013.

ZALEWSKI, P. D.; TRUONG-TRAN, A. Q.; GROSSER, D.; JAYARAM, L.; MURGIA, C.; RUFFIN, R. E. Zinc metabolism in airway epithelium and airway inflammation: basic mechanisms and clinical targets. A review. **Pharmacol. Ther.**, v. 105, p. 127-149, 2005.

ZUCCONI, G. G.; LAURENZI, M. A.; SEMPREVIVO, M.; TORNI, F.; LINDGREN, J. A.; MARINUCCI, E. Microglia activation and cell death in response to diethyl-dithiocarbamate acute administration. **J. Comp. Neurol.**, v. 446, p. 135-150, 2002.

ZWEIER, J. L.; FLAHERTY, J. T.; WEISFELDT, M. L. Direct measurement of free radical generation following reperfusion of ischemic myocardium. **Proc. Natl. Acad. Sci. USA**, v. 84, p. 1404-1407, 1987.

APÊNDICE A

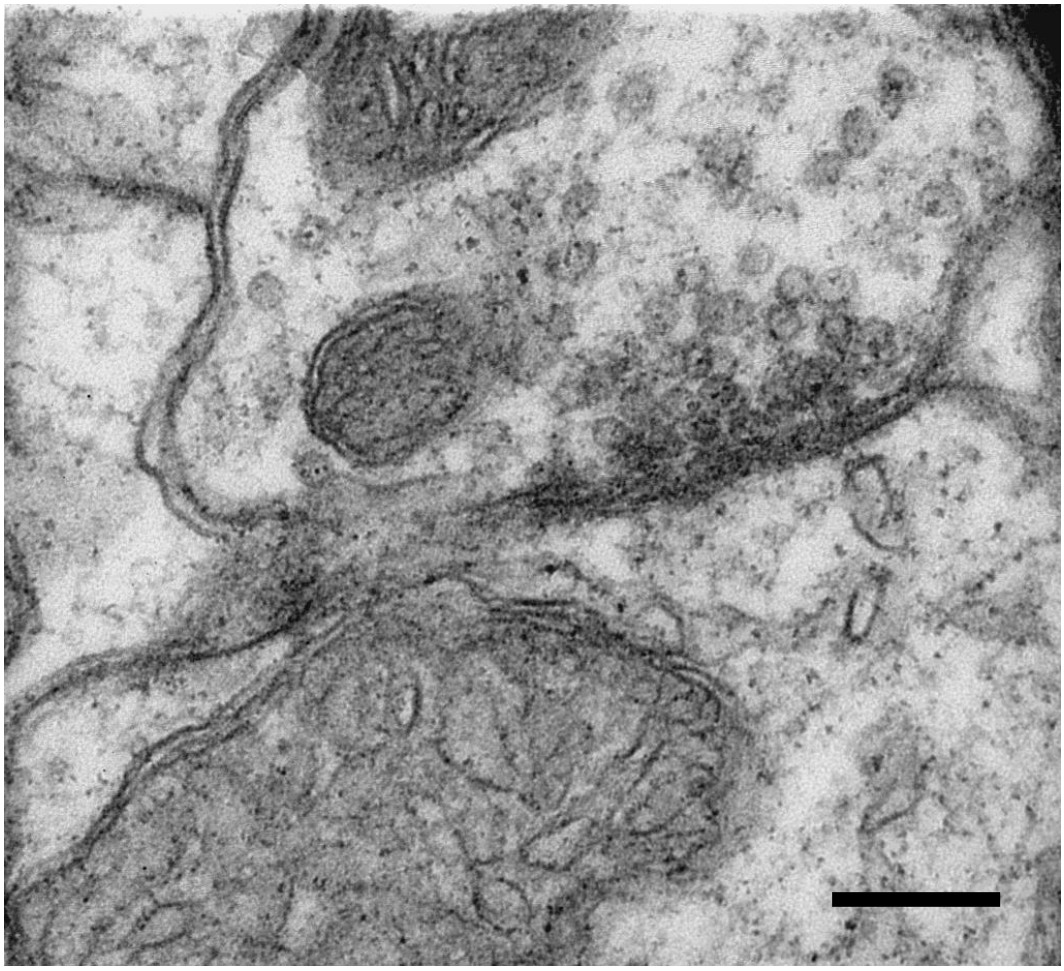

Imagem adquirida em microscópio eletrônico de transmissão de uma fatia de teto óptico de peixe-zebra sem a marcação por Neo-Timm. Barra = 200 ηm.

APÊNDICE B

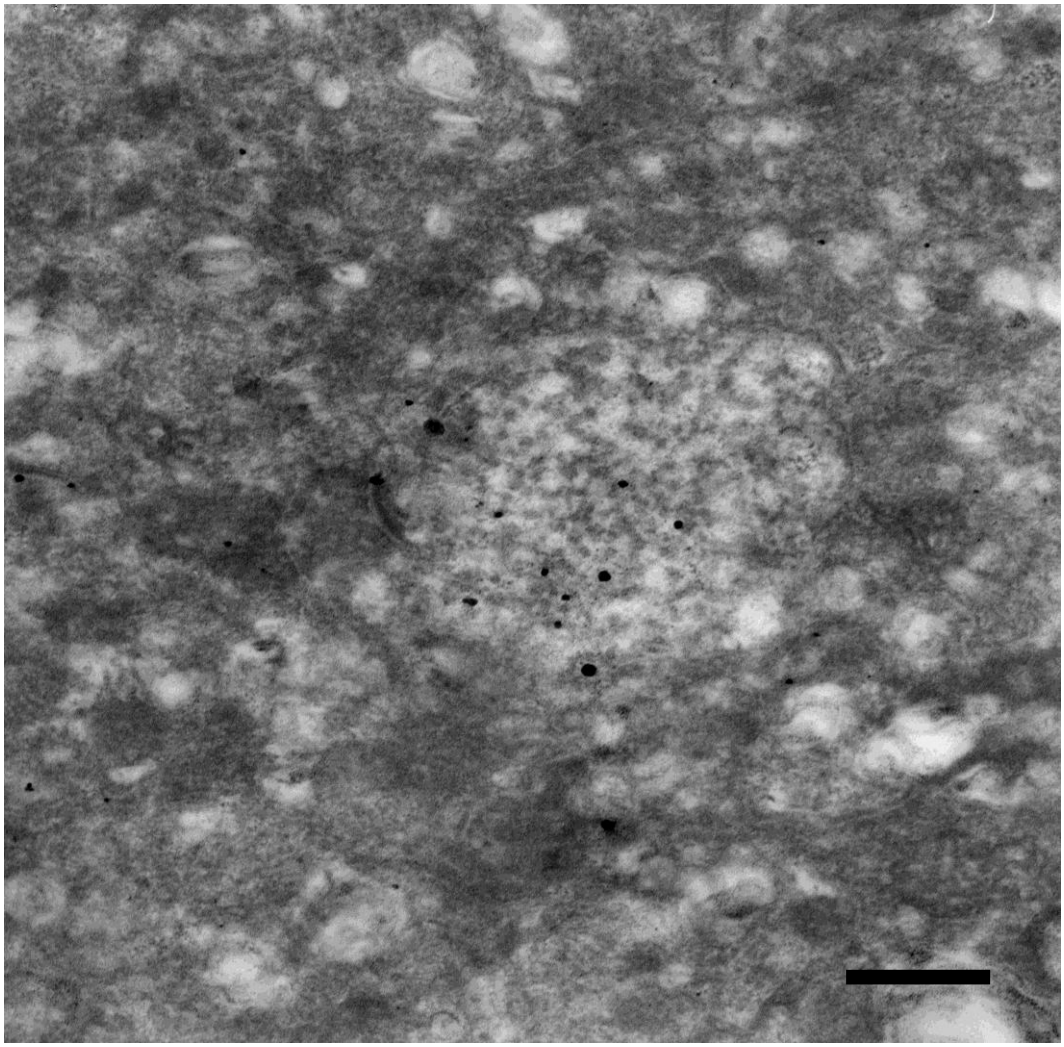

Imagem adquirida em microscópio eletrônico de transmissão de uma fatia de teto óptico de peixe-zebra com marcação por Neo-Timm. Barra = 400 ηm.